Thermo-kinetic Investigation of Polyethylene Terephthalate (PET) Plastic Waste Catalytic Pyrolysis over Biomass Fly Ash (BFA)

By

Ali Raza

(Registration No: 00000362370)

Department of Thermal Energy Engineering

U.S. Pakistan Center for Advanced Studies in Energy

National University of Sciences & Technology (NUST)

Islamabad, Pakistan

(2024)

Thermo-kinetic Investigation of Polyethylene Terephthalate (PET) Plastic Waste Catalytic Pyrolysis over Biomass Fly Ash (BFA)

By

Ali Raza

(Registration No: 00000362370)

A thesis submitted to the National University of Sciences and Technology, Islamabad,

in partial fulfillment of the requirements for the degree of

Master of Science in
Thermal Energy Engineering

Supervisor: Dr. Asif Hussain Khoja

Co Supervisor: Dr. Majid Ali

U.S. Pakistan Center for Advanced Studies in Energy

National University of Sciences & Technology (NUST)

Islamabad, Pakistan

(2024)

THESIS ACCEPTANCE CERTIFICATE

Certified that final copy of MS Thesis written by Mr. Ali Raza (Registration No. 00000362370), of U.S. Pakistan Center for Advanced Studies in Energy has been vetted by undersigned, found complete in all respects as per NUST Statutes/ Regulations/ Masters Policy, is free of plagiarism, errors, and mistakes and is accepted as partial fulfillment for award of Master's degree. It is further certified that necessary amendments as pointed out by GEC members and foreign/ local evaluators of the scholar have also been incorporated in the said thesis.

Signature: ____________________

Name of Supervisor: Dr. Asif Hussain Khoja

Date: 25/09/2024

Signature (HOD): ____________________

Date: 25/09/2024

Signature (Dean/ Principal) ____________________

Date: 27/09/2024

FORM TH-4

National University of Sciences & Technology

MASTER'S THESIS WORK

We hereby recommend that the dissertation be prepared under our supervision by **Ali Raza** (Reg. No: **362370**).

Titled: "Thermo-kinetic investigation of polyethylene terephthalate (PET) plastic waste catalytic pyrolysis over biomass fly ash (BFA)" be accepted in partial fulfillment of the requirements for the award of **MS Thermal Energy Engineering** degree with (A) grade.

Examination Committee Members

1. Name: Dr. Muhammad Hassan — Signature: ____________
2. Name: Dr. Mustafa Anwar — Signature: ____________
3. Name: Dr. Abeera Ayaz Ansari — Signature: ____________

Supervisor's name: Dr. Asif Hussain Khoja — Signature: ____________ Date: 25/09/2024

Co-Supervisor's name: Dr. Majid Ali — Signature: ____________ Date: 25/9/2024

Dr. Asif Hussain Khoja
Head of Department — Signature: ____________ Date: 25/09/2024

COUNTERSIGNED

Date: 27/09/2024 — Principal: ____________

CERTIFICATE OF APPROVAL

This is to certify that the research work presented in this thesis, entitled "Thermo-kinetic investigation of polyethylene terephthalate (PET) plastic waste catalytic pyrolysis over biomass fly ash (BFA)" was conducted by Mr. Ali Raza under the supervision of Dr. Asif Hussain Khoja.

No part of this thesis has been submitted anywhere else for any other degree. This thesis is submitted to the Department of Thermal Energy Engineering in partial fulfillment of the requirements for the degree of Master of Science in Field of Thermal Energy Engineering Department of Thermal Energy Engineering National University of Sciences and Technology, Islamabad.

Student Name: Ali Raza — Signature: ____

Examination Committee:

a) GEC 1: Dr. Muhammad Hassan — Signature: ____
Associate Professor, USPCAS-E, NUST

b) GEC 2: Dr. Mustafa Anwar — Signature: ____
Assistant Professor, USPCAS-E, NUST

b) GEC 3: Dr. Abeera Ayaz Ansari — Signature: ____
Assistant Professor, USPCAS-E, NUST

Supervisor Name: Dr. Asif Hussain Khoja — Signature: ____

Co-Supervisor Name: Dr. Majid Ali — Signature: ____

Name of HOD: Dr. Asif Hussain Khoja — Signature: ____

Name of Principal: Prof. Dr. Adeel Waqas — Signature: ____

AUTHOR’S DECLARATION

I Ali Raza hereby state that my MS thesis titled “Thermo-kinetic investigation of polyethylene terephthalate (PET) plastic waste catalytic pyrolysis over biomass fly ash (BFA)” is my own work and has not been submitted previously by me for taking any degree from National University of Sciences and Technology, Islamabad or anywhere else in the country/world.

At any time if my statement is found to be incorrect even after I graduate, the university has the right to withdraw my MS degree.

Name of Student: Ali Raza

Date: 01/10/2024

PLAGIARISM UNDERTAKING

I solemnly declare that research work presented in the thesis titled “Thermo-kinetic investigation of polyethylene terephthalate (PET) plastic waste catalytic pyrolysis over biomass fly ash (BFA)” is solely my research work with no significant contribution from any other person. Small contribution/ help wherever taken has been duly acknowledged and that complete thesis has been written by me.

I understand the zero-tolerance policy of the HEC and National University of Sciences and Technology (NUST), Islamabad towards plagiarism. Therefore, I as an author of the above titled thesis declare that no portion of my thesis has been plagiarized and any material used as reference is properly referred/cited.

I undertake that if I am found guilty of any formal plagiarism in the above titled thesis even after award of MS degree, the University reserves the rights to withdraw/revoke my MS degree and that HEC and NUST, Islamabad has the right to publish my name on the HEC/University website on which names of students are placed who submitted plagiarized thesis.

Student Signature: ______________

Name: Ali Raza

DEDICATION

This thesis is dedicated to my friend, Usama Akhtar,

who encouraged me to join NUST.

ACKNOWLEDGEMENTS

All praise and thanks to Allah Almighty, who provided me with the power and skills to comprehend, learn, and complete my thesis report.

It gives me great pleasure to express my heartfelt gratitude to my research supervisor, Dr. Asif Hussain Khoja, for allowing me to join the Fossil Fuels Lab study group, USPCAS-E, NUST, Islamabad. I consider myself fortunate to have worked under his supervision. It was a combination of his patience, perseverance, guidance, and inspiration that enabled me to complete my research goals on time. He showed me the approach for conducting research and presenting the findings as clearly as possible.

My heartfelt gratitude goes to my dear Parents, whose unwavering support was a constant source of guidance, hope, and encouragement during this significant journey. I extend sincere thanks to my friends and colleagues for their unwavering assistance and encouragement, which uplifted me in every possible manner.

TABLE OF CONTENTS

LIST OF TABLES

Page No.

LIST OF FIGURES

Page No.

LIST OF SYMBOLS, ABBREVIATIONS AND ACRONYMS

A	Pre-exponential factor
BFA	Biomass Fly ash
E_a	Activation Energy
FTIR	Fourier Transform Infrared Spectroscopy
GCV	Gass calorific value
PET	Polyethylene terephthalate
P_f	Pyrolysis factor
R^2	Regression factor
R_m	Mean reactivity
RL	Residue Left
T_p	Peak decomposition temperature
TGA	Thermogravimetric analysis
WL	Weight loss
XRD	X-ray Diffraction
A	Conversion factor
ΔS	Change in entropy
ΔH	Change in enthalpy
ΔG	Change in Gibbs free energy

ABSTRACT

Plastic waste stands as the most alarming challenge for environmental and human health, which needs to find some techniques to use for energy recovery. This investigation evaluates the plastic waste material polyethylene terephthalate (PET) through GCV, RAMAN, FTIR, and XRD, and the catalyst biomass fly ash (BFA) is characterized via XRD, FTIR, and TGA. The pyrolysis at a heating rate of 5,10,15 and 20 ºC/min is carried out in a thermogravimetric analyzer (TGA), the only catalytic PET blend i.e. 10 wt.% BFA-PET which showed a major shift in the peak temperature for the pure PET catalytic blends along with the increment in the weight loss, which will consider as an optimum catalytic blend. The thermo-kinetic study is performed by using twelve (12) mechanisms of model fitting (coats-Redfern method), and model free (Friedman, KAS, FWO) to find activation energy (E_a) based on regression factor (R^2). The activation energy (E_a) for pyrolysis of Pure PET is 200-220 kJ/mol and after catalyst loading it lies in the range of 140-200 kJ/mol and the same trend follows for change in enthalpy (ΔH), the change in Gibbs free energy (ΔG) and the change in entropy (ΔS) decreases as the catalyst ratio increases. The catalytic blend 10 wt.% BFA-PET lower the values for E_a, ΔH, ΔG, and ΔS of the pure PET indicates the reaction reaching equilibrium at a slow pace. Reactivity analysis for 10 wt.% BFA-PET considering mean reactivity (R_m) and pyrolysis factor (P_f) are 38.7563 and 0.8517 respectively. The catalytic pyrolysis of PET has been proposed as a viable alternative for energy sources and its kinetics study is important for important for design an efficient large-scale reactor system.

Keywords: *Biomass fly ash (BFA), Catalytic Pyrolysis, Polyethylene Terephthalate (PET), Reactivity Analysis, and Thermo-Kinetics*

Chapter 1: Introduction

1.1 Background

The quick depletion of finite oil resources and rapid increase in energy demand has enforced researchers to find out new ways to place conventional energy sources to produce high quality oils [1]. To solve this issue, energy from solid waste is one of the best techniques thus biomass and plastic are the two main sources of solid waste. In the future, biomass waste will be used for practical purposes, but the products obtained will have low thermal stability, calorific value, and a high oxygen value. Therefore plastic has a higher hydrogen-to-oxygen ratio, which can increase product quality [2], also plastic has exceptional characteristics such as affordability, ease to manufacture, and lightweight nature [3]. Plastic manufacturing has expanded twenty times over the last fifty years, and it is expected that yearly plastic output will reach 500 million tonnes in the future years [4]. However, about 90% of this plastic waste generated is not recycled and ends up in landfills or oceans [5].

Major types of plastic are polyethylene terephthalate(PET), high-density polyethylene (HDPE), polyvinyl chloride (PV), low-density polyethylene (LDPE), polypropylene (PP), and polystyrene (PS). [6]. Polyethylene terephthalate (PET) plastic has exceptional properties like transparency, and gas impermeability and has the highest demand than any other type of plastic, also it is commonly used to make drink bottles, packaging, electronics, etc [7, 8]. As pure PET is non-biodegradable, and can resist in the environment for longer periods [9], because it has some adverse effects on the environment, human health, and wildlife [10]. So, it is necessary to devise a practical way to dispose of or use it sustainably and cost-effectively. One method for energy recovery is Incineration which is a widely used method that significantly reduces waste production and produces energy but it releases air contaminants such as ammonia, carbon dioxide, and No_x [11]. The various method of chemical recycling of PET plastic includes hydrolysis, alcoholysis, glycolysis, and pyrolysis, but pyrolysis is extensively used nowadays due to more valuable products [12, 13].

Biomass Fly ash (BFA) is solid waste residue from the combustion of biomass and coal in power plants. BFA is typically a waste of biomass combustion in industries, which highly affects the environment. As it has high thermal stability and contains metal oxides which can act as a supporting catalyst as it is readily available in the breakdown of plastics and also a waste product [14]. Fly ash has been used as a catalyst in the catalytic pyrolysis of various plastic materials such as waste electrical and electronic equipment (WEEE) [15] which achieves significant improvements in the pyrolysis process thus enhancing the quality and yield of light oil fraction, whereas in HDPE and LDPE pyrolysis improves the oil yield at lower mass fraction but improves the properties of derived oil as compared to the standard fuels [16, 17]. PET plastic pyrolysis using a low-cost concrete waste catalyst has been conducted which showed no change in the decomposition temperature but enhances the deoxygenation reaction to produce more valuable aromatics products [18].

1.2 Problem Statement

Majority of plastics used in the society are not biodegradable and they remain in the environment for several centuries [19]. The literature identifies conventional recycling, which entails sorting and grinding, as efficient in reusing between 15% and 20% of the plastic waste in circulation [20]. Hence, thermal and catalytic pyrolysis, gasification, and plasma arc gasification are increasing their popularity as the methods of recycling plastic waste [21].

Pyrolysis is a sophisticated thermochemical process that may be done with or without a catalyst, at temperatures between 400-700 °C, in a non-oxidant environment for degrading waste plastic because of the minimal raw material demands, high effectiveness, and less expensive chemicals [22]. This process involves heating organic materials without oxygen or under controlled oxygen-deficient conditions [23]. Plastic waste may be pyrolyzed to generate three fractions: solid residue, gas, wax, liquid, or oil which is made up of both aromatic and aliphatic hydrocarbons [24]. Aiming to better understand the pyrolysis process, several researchers have studied the pyrolysis of PET using Thermogravimetric Analysis (TGA). TGA is commonly used for analyzing devolatilization and has been extensively discussed in the literature, containing plastics [23]. Despite its most significant advantage, environmental friendliness, the oil faces severe technical obstacles for commercialization due to its high concentration of oxygenated chemicals i.e. acids, ketones, ethers, aldehydes, and alcohols, which can have a negative impact on fuel characteristics, such as poor calorific value, combustion efficiency, corrosion, and instability [25]. To overcome these challenges, a catalyst can be added to the pyrolysis process. The main role of the catalyst is to accelerate the formation of the desired product, under lower reaction temperatures, and reduced residence times [26], and increase process efficiency, lowering the activation energy needed for conversion of polymers into hydrocarbons, leading to a decrease in energy consumption [27]. It removes the oxygenated compounds that lower the quality of oil produced from plastic. Various types of catalysts are utilized to enhance process efficiency and optimize pyrolysis of plastic waste overall [28]. Pyrolysis process converts plastic waste into liquid oil, solid residue (char) and gases at high temperatures (300–900 °C) via thermal decomposition. However, there are certain limitations with conventional thermal pyrolysis, where the whole process is temperature dependent. The liquid oil from thermal pyrolysis may contain impurities and residues. Therefore, catalytic pyrolysis is being developed to overcome the problems of thermal pyrolysis. Furthermore, activation energy required for pyrolysis of plastic is very high due to complex chemical reaction, which limits these processes.

1.3 Research Hypothesis

Catalyst is very important in the pyrolysis of PET and biomass fly ash (BFA) makes the process efficient and effective. The arrangement of the process used in this study as catalytic pyrolysis is expected to reduce the activation energy hence enhance the opportunity for faster degradation of the PET than in the non-catalytic pyrolysis. Moreover, the obtained catalyst should also enhance the thermodynamics characteristic values, the enthalpy change (ΔH) and Gibbs free energy change (ΔG) thus, the reaction is a more efficient one. Based on the above exposition, it is postulated that the incorporation of biomass fly ash will result to increased production of desired products, the gases and oil, with minimized generation of unfavorable compounds during pyrolysis, thereby improving the efficiency of the process. A detailed reactivity analysis is also conducted to envisage effects of the catalyst on the reaction pathways. An additional advantage associated with using biomass fly ash as a catalyst is that it is a waste product, thus, its use will promote green waste management. The objective of this work is to affirm that biomass fly ash can enhance the kinetic, thermodynamic, and reactivity characteristics of PET pyrolysis to contribute to the enhancement of the processes and technologies involved in the conversion of waste flows.

1.4 Objectives of the study

The goal of this study is to develop and investigate the characterization of PET-BFA blends to assess the chemical and physical properties, as well as how these qualities may change when coal and biomass are blended. The experimental work reported in this study is consistent and agrees with previous studies. The study's key objectives are as follows:

- ✓ Preparation of the plastic (PET) material and catalyst for catalytic pyrolysis.
- ✓ To characterize the various catalytic blends of BFA and PET plastic.
- ✓ To perform pyrolysis and catalytic pyrolysis in thermogravimetric (TGA) analyzer.
- ✓ To find out the kinetics and thermodynamic parameters through the Coats-Redfern method will help in approaching the most suitable reaction mechanism.
- ✓ To find out more about kinetics parameters though model free methods (FWO, KAS, and Friedman).
- ✓ To perform the reactivity analysis by using the TGA-DTG data.

1.5 Scope of the study

This study focuses on the PET plastic waste recovery through pyrolysis process and its catalytic pyrolysis over biomass fly ash. The scope of the study is described in Figure 1.1, starting from the material and catalyst preparation and its blends formation. Pure PET plastic was analyzed and discussed by GCV, FTIR, RAMAN, XRD and TGA. The catalyst was characterized via XRD, FTIR, and TGA. Pyrolysis and catalytic pyrolysis of Pure PET via BFA are done through a Thermogravimetric Analyzer (TGA) at heating rate of 5,10,15 and 20 °C/min. The thermodynamic and kinetic study was performed applying a model fitting technique (coats-Redfern method) by applying 12 integral models to select a suitable reaction mechanistic model to better understand it through conversion of the material. Model free kinetics methods (Friedman, KAS and FWO) are also applied to calculate and justify the kinetics and thermodynamic parameters. Through this study, the best ratio of catalyst loading is found to give the best products at the lowest activation energy and temperature. Also, the reactivity analysis was carried out using the TGA-DTG data to evaluate the pyrolysis performance of pure PET and catalytic PET blends through mean reactivity and pyrolysis factor.

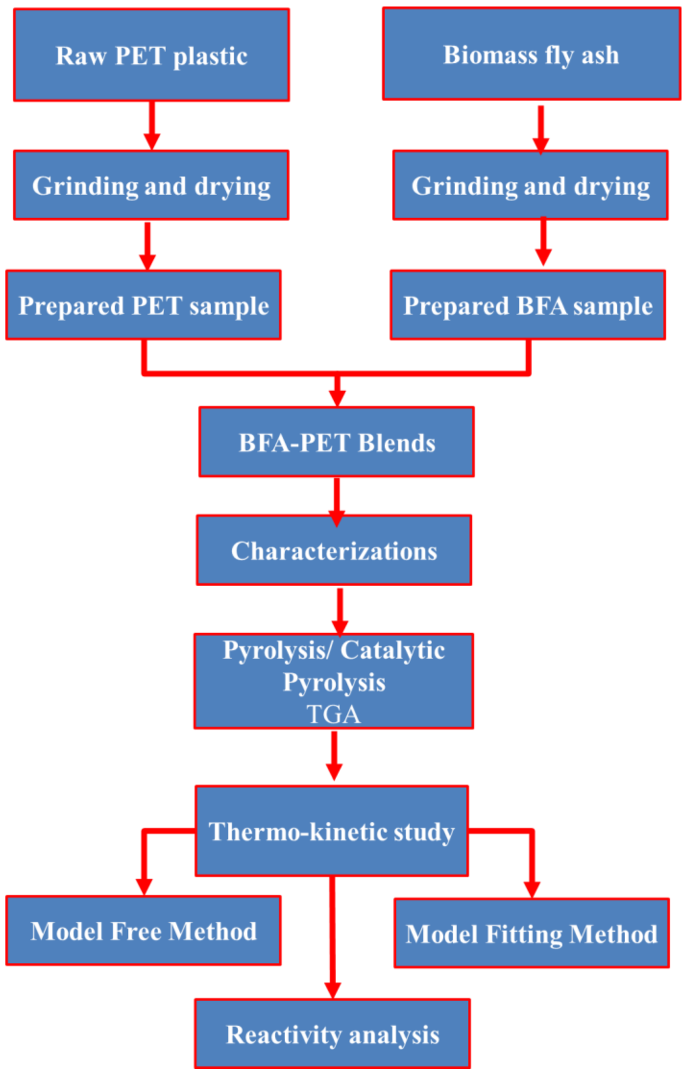

Figure 1. 1: Scope of the study

1.6 Flow chart

The flow chart of the thesis is shown in Figure 1.2, The study's goal was to evaluate how plastic and fly ash may be used more economically and sustainably rather than being thrown away in landfills or polluting the environment. For this goal, a literature review was conducted on existing plastic and biomass fly ash data and utilization. PET-BFA blends were prepared and characterized using CHN-S, GCV, FTIR, and TGA. The kinetics and thermodynamics of the pyrolysis process were also described using TGA data. In the end reactivity analysis is also performed. In the results and discussion section, the data from the results were carefully reviewed.

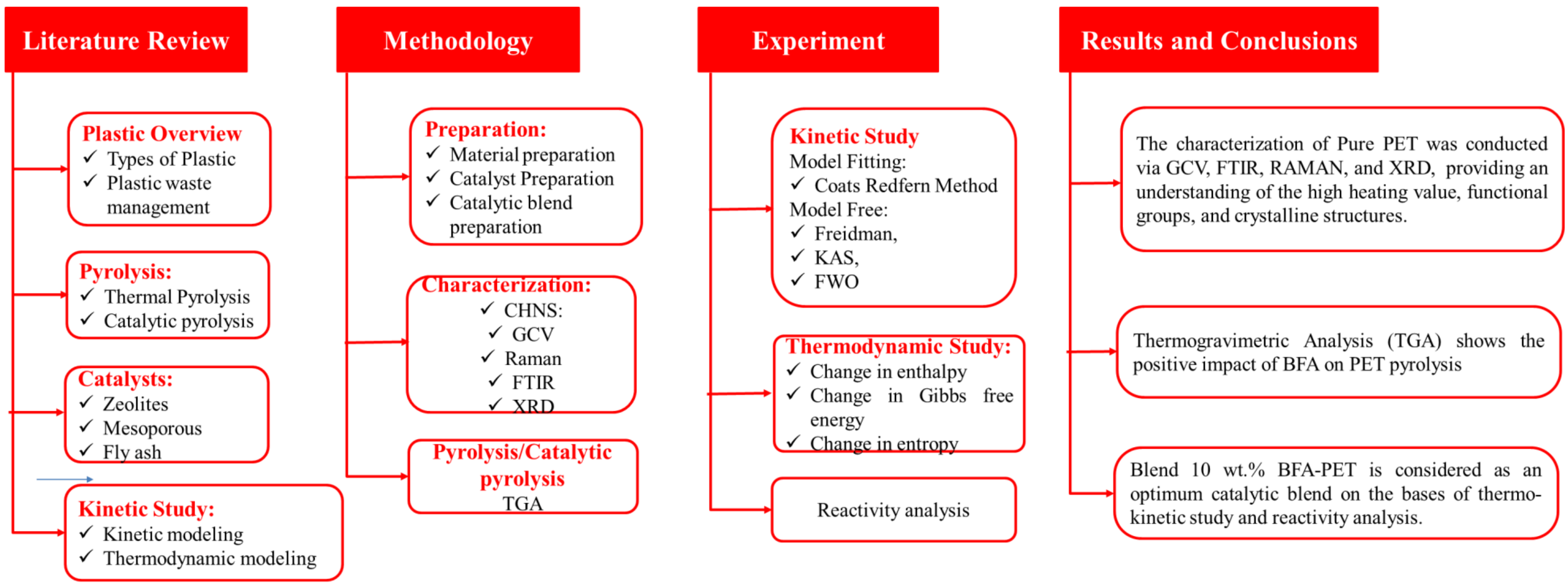

Figure 1. 2 : Flow chart of thesis

Chapter 2: Literature review

2.1 Plastic waste overview

The word ‘plastic’ derives from ‘pliable’, which translates as ‘easily shaped.’ Thus, the nature of plastics is their ability to undergo changes from one form to another to fulfill a definite set of requirements [29]. Due to their excellent physical and chemical characteristic, plastics have become one of the leading products in the global market with infinite uses in calibrated commercial and industrial products [30]. The production and use of plastics around the world has risen sharply in the past few years due to high demand this is because the material is versatile [31]. They are preferred because plastic products are cheap to produce, they require less energy to produce and in the process of production, they emit less CO_2 than other materials. This trend is reinforced by considerable population growth, and thus, analysts expect an improvement in the consumption of plastics per capita in the upcoming decades. As such, with the continually growing global population, the use of plastics is likely to rise further encouraging the promotion of management and recycling of plastics to address these effects. The Organization for Economic Co-operation and Development (OECD) further estimates that [32], the world consumption of plastics will increase by more than three times by the year 2060 to an astounding figure of 1231 million tonnes shown in Figure 2.1. Hence the life cycle of the plastic products is shorter; there is a huge plastic wastes formation that goes straight to the trash bins at the municipal sites. At the level of production by type of industry, packaging items including containers and bags predominate as they account for nearly 36 percent of plastics, while construction industry products come second at a ratio of 16 percent and fibers taking the third position with 14 percent. Disposable plastics are usually classified as single use plastics and comprise of items that are designed for one use before disposal or recycling. These consist of carry bags, food trays, bottles, straws, tubs, cups, and cutlery. According to the estimates conducted in 2015 [33], the largest share, amounting to 47 percent, was taken by plastic packaging waste, shown in Figure 2.2.

The major products made from these plastics include LDPE, HDPE, PP, PVC, PETE, PLA among others, are non-biodegradable, and would remain in the landfills for longer period causing serious environmental challenges. This has raised post-consumer disposal challenges especially due to legations from environmental protection agencies [34].

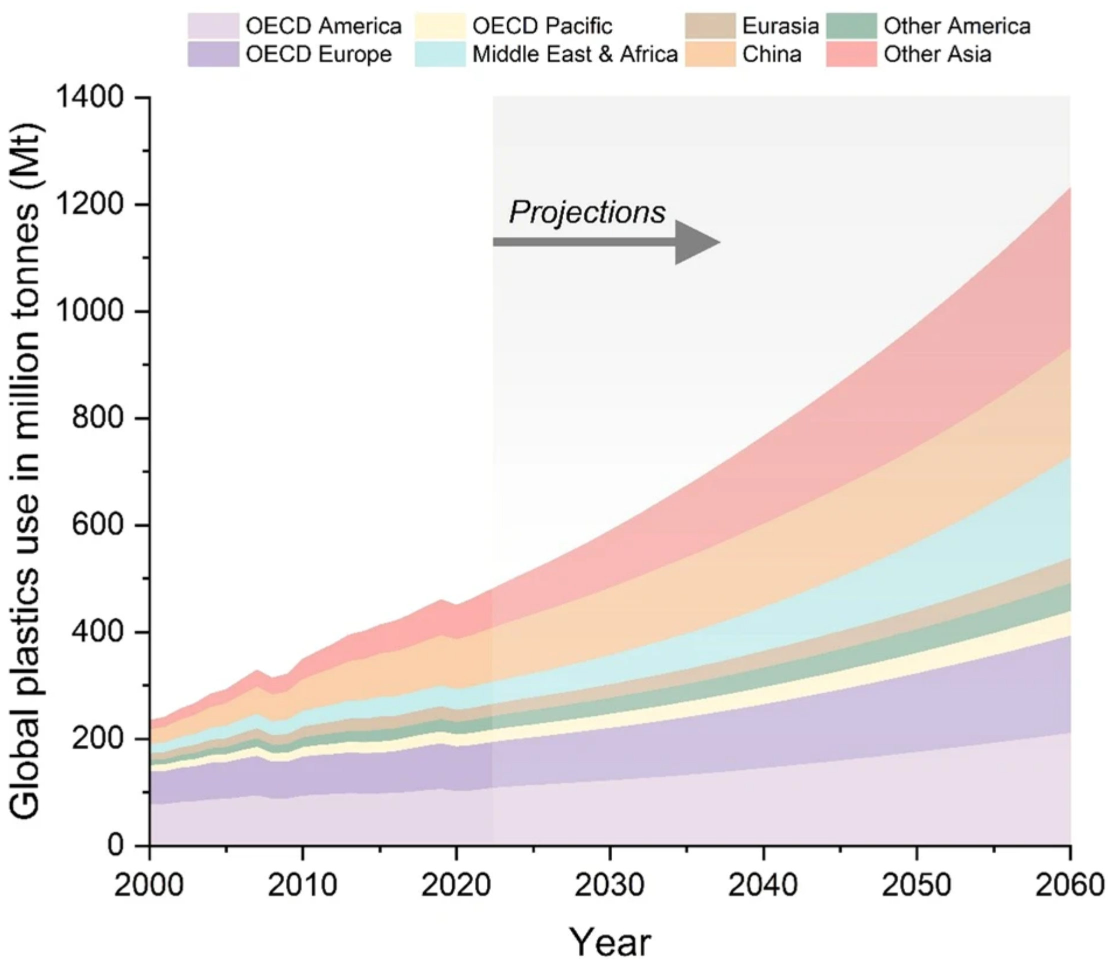

Figure 2. 1: Global Plastic Production trend [32]

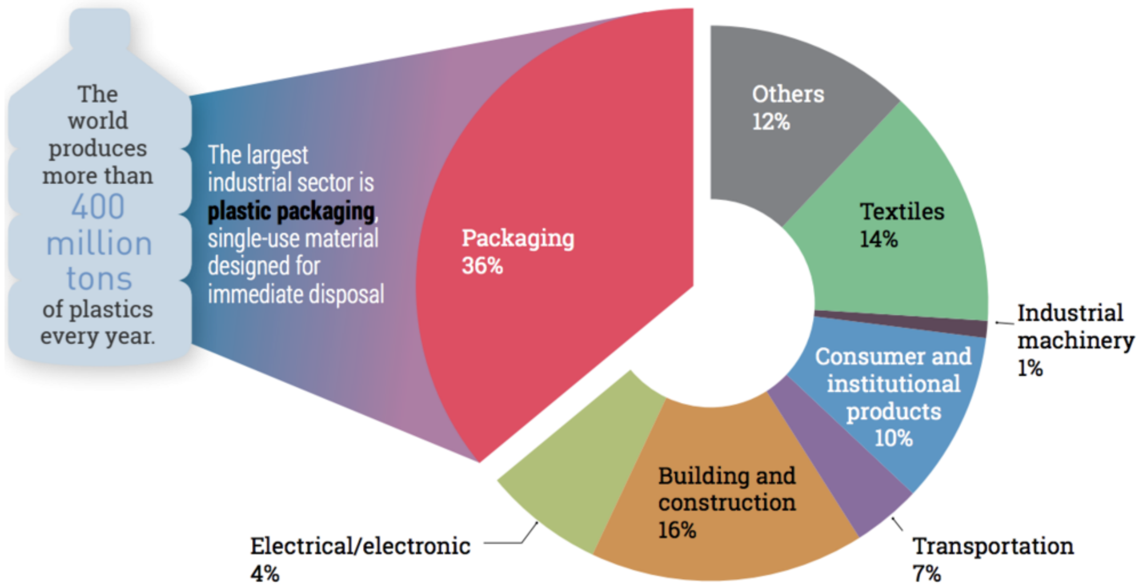

Figure 2. 2: Global plastic production by industrial sector [33]

2.2 Types of Plastics

2.2.1 Polyethylene terephthalate (PET)

Polyethylene Terephthalate (PET) is a type of polyester resin synthesized from ethylene glycol and terephthalic acid (or its dimethyl ester, dimethyl terephthalate). It's a long-chain polymer consisting of repeating units of ethylene terephthalate [35]. PET is transparent, allowing consumers to see the contents of the packaging. PET is hard and more resistant which make it more appropriate for packaging use [36]. Light in weight, PET is easy to transport hence translating into less energy use and cost. Moreover, PET is a good barrier to gases such as; oxygen, carbon dioxide as well as moisture to prevent deterioration of packaged commodities [37]. PET is easily recyclable and among the most recycled types of plastics in the world today where the bottles can be transformed into fibers for apparels, carpeting and packaging bottles [38].

PET is widely utilized for one time usage in packaging of beverages such as water, soft drinks, juices and sports drinks because it is transparent, strong and light weight. Specifically, some of the common products that are placed in PET include salad dressings, condiments, peanut butter, and sauces. The process is also applied to reach non-food and other items such as washing soap, detergents, gels, shampoos, conditioners, creams, lotions, medicines, etc. Recycled PET material is adopted for its usage of fibers in clothing products consisting of polyester fabric for shirts, pants, jackets, and other apparel. PET is deployed in construction applications that include thermal insulation, roofing and underlaying materials [39].

PET material can be easily recycled and recycled products can be manufactured out of it. Recycling percentages are not the same globally as they are determined by aspects like collection facilities and consumer habits. These last types, PET, are recyclable although the process of manufacturing them involves the use of fossil fuels and energy. Littering is a way of discarding waste in the environment, which is not the correct way of disposing wastes hence pollutes the environment. Development research continues on making PET derived from renewable raw materials, not fossil based materials and thus creating a more environmentally friendly product [40].

The recycling of PET is not fully effective as it may be combined with other materials like the residue from the food it contained or other plastics that can affect the PET quality in recycling. The morphological structure of recycled PET may have lower mechanical properties than virgin PET slightly, reducing certain applicationsHigh-density polyethylene (HDPE)

High-Density Polyethylene (HDPE) is a type of plastic manufactured from ethylene; a simple hydrocarbon substance induced from natural gas and petroleum [41]. Polymerization is used to make it and is a chemical reaction that involves combing many ethylene molecules to form chains. This is because HDPE possess good molecular weight which contributes to its high strength and environmental stability. Unlike other types of plastics, this one has very low amounts of branching, giving high density and crystalline structure to the HDPE. This makes the HDPE to be even more rigid and to be able to able to withstand shock, chemicals, and temperatures. Like LDPE, HDPE also has good chemical resistance hence widely used in packaging industries. The substance can be contained in bottles for milk, detergents, household cleaning agents, motor oil, and shampoo. They include moisture, light and temperature and they influence the suitability of the material for use in outdoor installations. Besides, packaging, HDPE is applied in construction, such as: rooftops, corrosion pipelines, plumbing, gutters, and profiles [42]. It has been utilized in the production of water and gas distribution, sewage and drains, and in the case of agriculture, irrigation. HDPE geomembranes are applied to the environmental constructions as landfill linings, ponding and wastewater treating systems because of its impermeability and chemicals resistance [43]. Another feature characteristic of HDPE is the possibility of recycling. Currently it is the most recycled of all the plastics, and tends to be reused to make new bottles, containers, lumber, and many other products. The reuse of the HDPE decreases the use of virgin plastic and therefore has an added advantage of decreasing environmental pollution [44].

2.2.2 Polyvinyl chloride (PVC)

Polyvinyl Chloride (PVC) is a widely used type of plastic characterized by its versatility and durability. It is composed of repeating vinyl chloride monomers. PVC can exist in both rigid and flexible forms, depending on the addition of plasticizers [45]. Construction is one of the biggest areas where rigid PVC is used for pipes, window frames, and siding because of its strength and chemical resistance. Whereas flexible PVC is suitable for uses in electrical cable, medical tubing and inflatable structures and production. Thus, although PVC has good economic characteristics, for example, a low cost per kilogram and high resistance to weathering, its manufacture and recycling are hazardous to the environment [46]. For its production, PVCs use chemicals that are dangerous and if burned or disposed in a wrong way, it poses a health risk by releasing fine particles of dioxins into the atmosphere. Recycling PVC is difficult due to its property and thus additives that are usually incorporated into this type of plastic are not frequently recycled compared to other types of plastic [47]. However, the following drawbacks are seen: In spite of all these, steps are being taken to enhance PVC recycling and to advance the formation of other ecofriendly materials [48].

2.2.3 Low-density Polyethylene (LDPE)

Low-Density Polyethylene (LDPE) is a kind of flexible plastic widely used in packing such as plastic bags, shrink wrap and flexible packaging [49]. There is also use in squeeze bottles, lids and some food packaging as it possesses good moisture barrier. LDPE is easy to process, and it is comparatively cheap; thus, it can be utilized for numerous consumers as well as industrial products. Nonetheless, it remains a low recycling rate mainly attributed to the issues of sorting and processing and contamination of the material. Continued attempts to increase the take-back and recycling of LDPE, as well as boosted utilization of recycled LDPE in new products are present to prevent negative environmental impacts [50, 51].

2.2.4 Polystyrene (PS)

Polystyrene commonly referred to as PS is a popular type of plastic commonly used due to its light nature and insulating abilities [52]. Daily it is utilized in disposals, cups, carry away containers, and other packing materials. PS can be rigid or foamed or expanded polystyrene, EPS or extruded polystyrene, XPS The uses for PS range from food packaging, insulation, etc. But the recycling rates of PS are comparatively lower because of minimum collection and sorting and its low recycling destination in some parts of the world [53].

2.2.5 Polypropylene (PP)

Polypropylene or PP is a polymer which is in the group of thermoplastic polymers that are flexible and have high heat resistant properties [54]. Known to be widely used in containers and films for food and beverages, for instance, yogurt cups, tubs for margarine and microwavable food trays. Non-carrying uses of PP also exist as in car components, toys, health care equipment and fabrics which attribute the material strength and flexibility. Despite being recyclable, PP can have varying recycled rates which are affected by contamination as well as sorting issues [55].

2.2.6 Other Plastics (Miscellaneous)

This will include any other type of plastic not included in the above categories for instance the polycarbonate often found in CDs and DVDs and some food packing materials; other specialty plastics.

Figure 2. 3: Types of Plastic

Table 2. 1: Plastic types, symbols, recyclability and its common uses

Sr. No	Symbols	Description	Recyclability	Common Uses
1.	1 PET	Polyethylene terephthalate	Yes	Soft drinks, water bottles, containers, salad dressing, biscuit trays and salad domes.
2.	2 HDPE	High-density polyethylene	Yes	Shopping bags, freezer bags, buckets, shampoo, milk bottles, ice cream containers, and detergent bottles, rigid agricultural pipe, crates
3.	03 PVC	Polyvinyl chloride	Yes, but not common	Cosmetic container, plumbing pipes, electrical conduct, blister packs, wall garden hose, Shoe soles, cable sheathing, blood bags and tubing.
4.	4 LDPE	Low-density polyethylene	Yes	Refuse bags, Irrigation tubing's, garbage bags, squeeze bottles.
5.	5 PP	Polypropylene	Yes	Microwave dishes, lunch boxes, packaging tape, garden furniture, kettles, bottles and ice cream tubs, potato chip bags, straws
6.	06 PS	Polystyrene	Yes, but not common	CD cases, plastic cutlery, imitation glassware, low-cost brittle toys, , protective packaging, building and food insulation
7.	7 OTHER	Others	Some	Automotive and appliance components, computers, electronics, cooler bottles, packaging

2.3 Plastic Waste Management

The management of plastic waste (PW) is broadly categorized into six methods [56]: i.e., landfilling, recycling by sort, pyrolysis, liquefaction, utilization for road construction and tar, and concrete production [54, 57]. These methods are captured in Figure. 2.4 and will be explained in the following section in briefly.

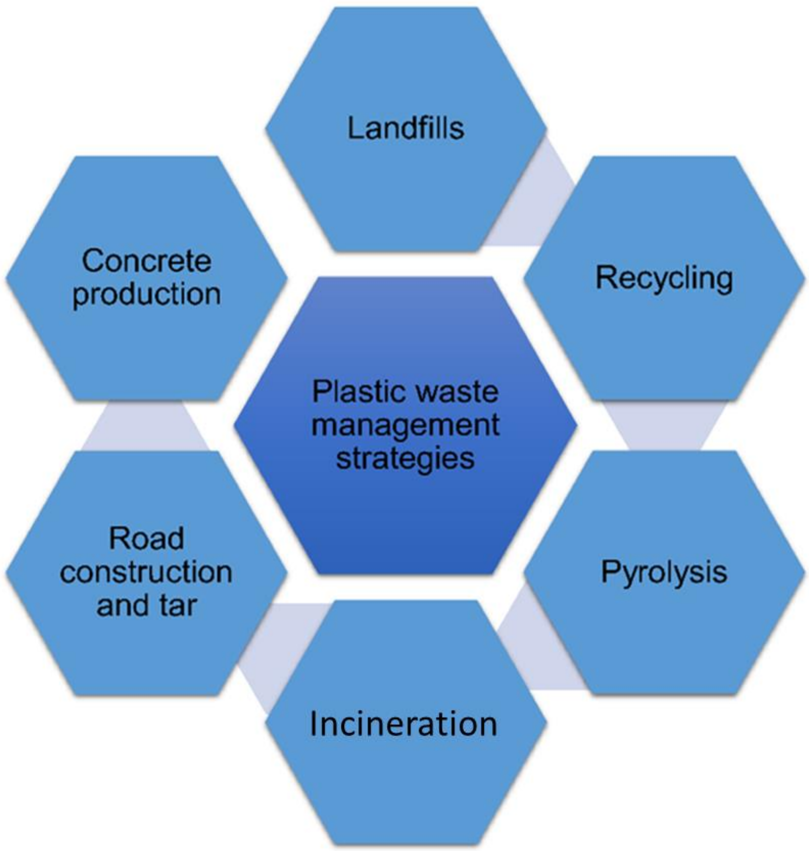

Figure 2. 4: Plastic waste management strategies [57]

2.3.1 Landfilling

Landfilling is the simplest way to dispose of PWs but creates great environmental and health hazards like soil pollution, water pollution, and compounding the scarcity of land. Landfill is depicted in Fig 2.5 (a, b) with an indication of various problems linked to the process. Thus, better PW management approaches, which will be described in the next sections, should be implemented to save the environment [57].

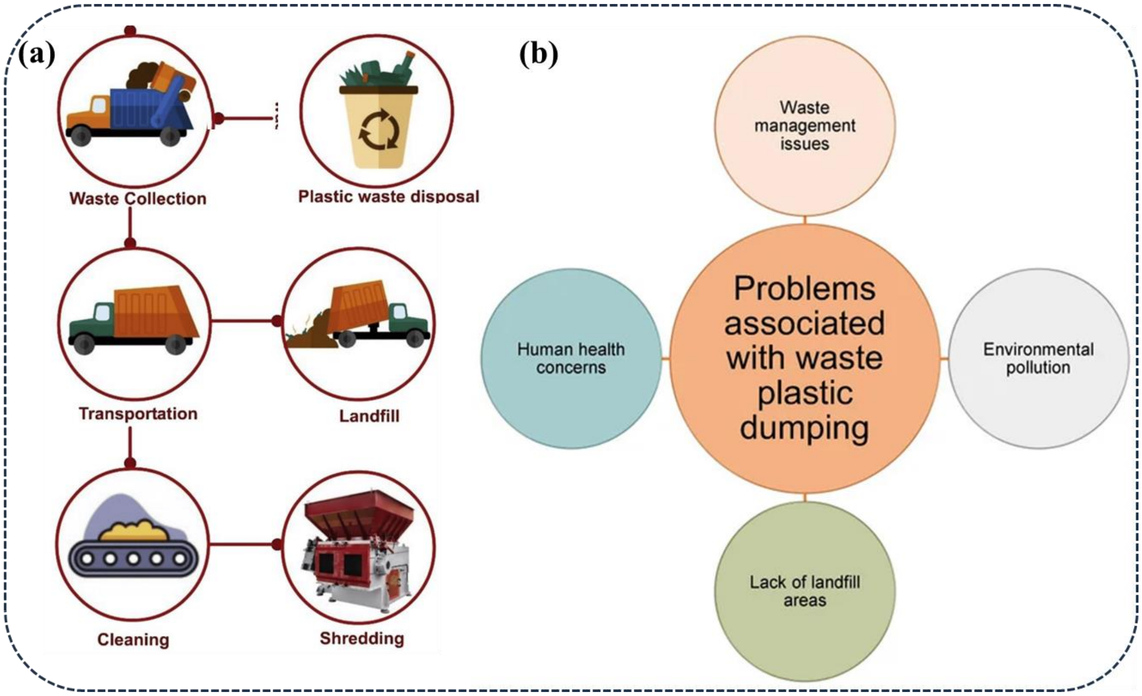

Figure 2. 5: (a) Flow chart for plastic waste landfilling (b) problems associated/disadvantages of plastic waste dumping [57]

2.3.2 Recycling

Plastic waste recycling, on the other hand, is a mechanically reprocessing of PW mainly by shredding, segregating contaminants, milling, chemical washing and then extruding the waste into new products [58]. However, it is important to note that there are tendencies with recycling where it is less costly but there are disadvantages like the use of energy and the shortness of the products. Other innovations with PW include woody biomass such as WPC which when incorporated with PW have potential but more work is needed to establish their sustainability in the long-term.

2.3.3 Incineration

Incineration is the method of disposal whereby waste is burned. Typically, most of the facilities employ the produced heat to create a minimal amount of electricity, therefore earning the title Waste-to-Energy (WTE) facilities. Incineration can burn mixed municipal solid waste of which 45% is plastic waste, but pre-treatment or sorting of the waste is done to remove water or have less of items such as electrical appliances Figure 2.6 Shows the global plastic waste management market map [59].

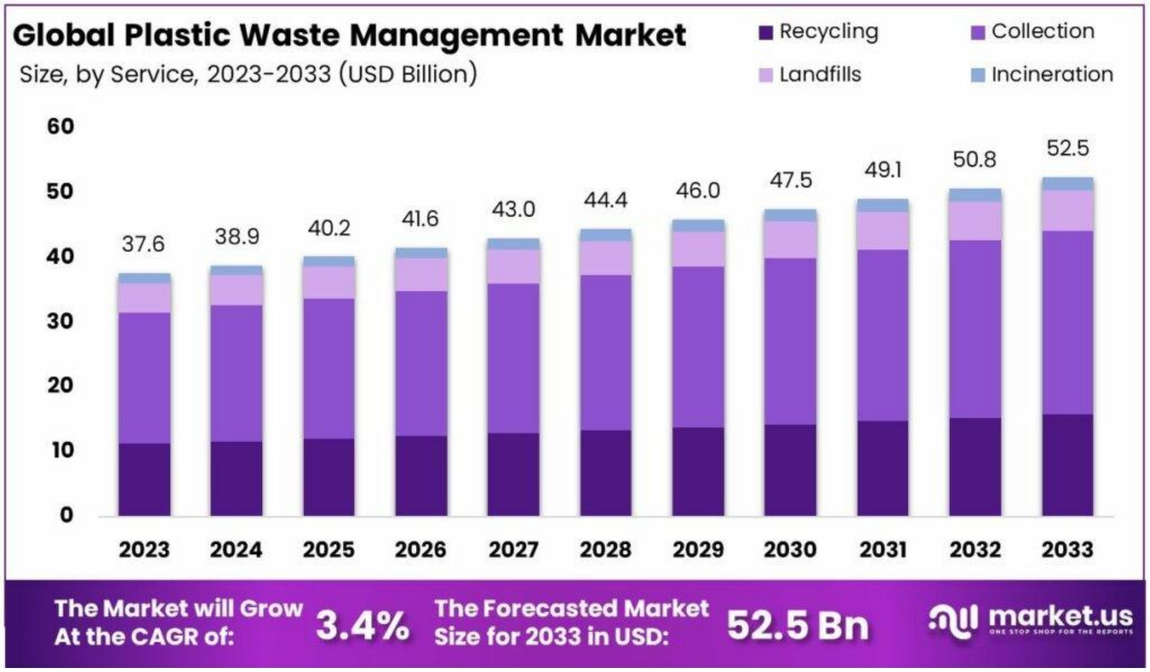

Figure 2. 6: Global Plastic waste management [60]

2.4 Pyrolysis

A process of pyrolysis is heating of the plastic waste in the inert environment through the help of carrier gases like nitrogen, helium, argon, steam, pyrolytic gas or hydrogen at a temperature of 450 to 800 °C is another method of waste recycling too. [61]. This technique is relevant in the conversion of mixed plastic waste to fuel and other chemicals. Pyrolysis byproducts for the most part can be repolymerized into polymers owing to the cyclic nature of the carbon content and because the alkene products have adaptable carbon bonds as noted in the saturated form [62]. The nature of feedstock determines the yields of the product and correlates with its characterization in that the characterization will predict the yields of the final products. More beneficial chemical rare materials containing benzene, toluene and supplementary condensed aromatic hydrocarbons may be attained by purifying the pyrolytic oil.

Pyrolysis process carried out in the absence of catalyst is called thermal pyrolysis or pyrolysis, while with the addition of catalyst is called catalytic pyrolysis [63]. The products of pyrolysis are solid carburized char, volatile but condensable hydrocarbon oil and non-condensable gases of high calorific value. Authors reported that LDPE, PP, PVC, HDPE, PET, and PS have a proportionately low ash content of 2 wt.% maximum and highly explosive volatile matter [64]. Safdari et al. [65] investigated the impact of heating rate on pyrolysis products, and the study established that that at consistent heating rate of 0. 5 °C/s under the range of 500-765 °C [66]. Pyrolysis is the heating of organic material to break in an inert atmosphere. The method can be employed to create gaseous or liquid fuel and coke mostly valid in petrochemical industry [67].

2.4.1 Thermal Pyrolysis

Thermal cracking is an endothermic process where the temperature typically ranges from 350 – 500°C for waste plastics; however, higher temperatures from 700 – 900°C have been used to enhance the yields [68, 69]. This method always gives a huge list of hydrocarbons and in some cases the useful products need to be 'milked' out from the set list. Detailed investigation has been carried out on thermal degradation in different polymers like PE [70], and polyethylene terephthalate [38]. The common characteristics of thermal pyrolysis of plastic wastes are:

- ✓ Higher percentage of C1 and C2 range hydrocarbons of the gaseous product
- ✓ Olefins produced are linear.
- ✓ Some di-olefins are also prepared at elevated temperatures.
- ✓ High occurrence of narrow molecular weight in the generated liquid product (low selectivity towards gasoline).
- ✓ The yield of gaseous and coke product is considerably high.

Thermal cracking reactions are generally slow. The thermal decomposition of PET is shown in Figure 2.7. When PET is exposed to high temperatures (≥375 °C), in the first step, PET decomposes long chains to produce benzoic acid and vinyl ester group. Further, benzoic acid breaks down to produce phenol and carbon dioxide, and the vinyl group produces ethanol, carbon dioxide, and some aromatic compounds. Also the formation of more benzene ring compounds in the presence of a catalyst, which causes the hydrogen transfer within the structure of PET, (a) Ester bond cleavage formed carboxyl and vinyl end groups, (b) carboxyl and acetaldehyde groups formation by seven-membered-ring transition state; (c) Decarboxylation of TPA and benzoic acid; (d) Vinyl ester group rearrangement will convert vinyl benzoate to acetophenone [6]. The Empirical formula of Pure PET is $C_5H_5O_2$ [11].

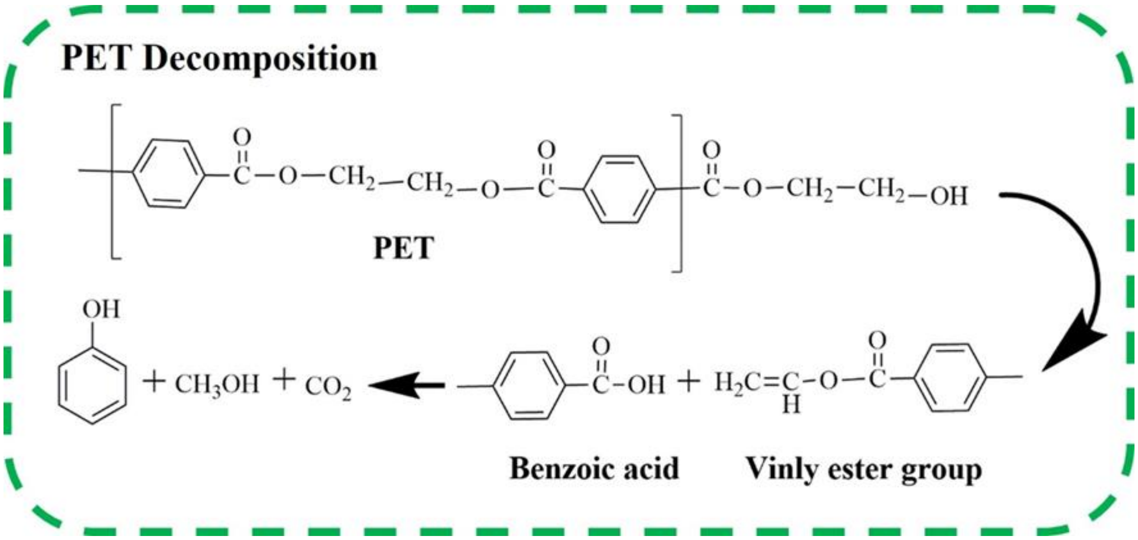

Figure 2. 7: Describes the Thermal decomposition of PET

2.4.2 *Catalytic Pyrolysis*

The quality of liquid oil generated by the decomposition of plastics has improved with the use of catalysts in pyrolysis, which is also referred as catalytic decomposition. Figure 2.8 illustrates the catalyst-pyrolysis schematic layout. Faster reaction resident times, decreased activation energies for cracking C–C bonds, being able to lower reaction temperatures, and the generation of lower molecular weight byproducts like petroleum are just several of the positive effects of catalysts [71, 72]. Catalytic cracking is performed with suitable catalysts at proper temperature, pressure and using environments such as N_2, H_2 or air consumes less energy most often at about 350-550 ºC. As a result, this method provides a limited chemical group of products, which means that more valuable outputs are generated. Catalysts also play a critical role in influencing the product distribution: catalytic processes produce gaseous products mostly with high value of C3 with a fewer number of liquid products, and these liquid products are majorly aromatic hydrocarbons and this is not so with non-catalytic processes. Several investigations have been carried out on the catalytic pyrolysis of plastic i.e. PET and PP plastic using different metal oxide catalysts such as ZSM-5 [73], metal oxides (ZnO, MgO, TiO_2) [6], TiO_2/SiO_2 [74], natural and synthetic zeolite [75], and sulphated zirconia [11]. Commercial catalysts are frequently costly and have a limited lifespan in a pyrolysis processes, thus the economics feasibility dependents on appropriate catalyst regeneration for recycle. As a result, discovering and manufacturing low-cost catalysts such as fly ash with comparable performance to commercial catalysts might prove very intriguing for the pyrolysis of plastic waste [15, 16, 76].

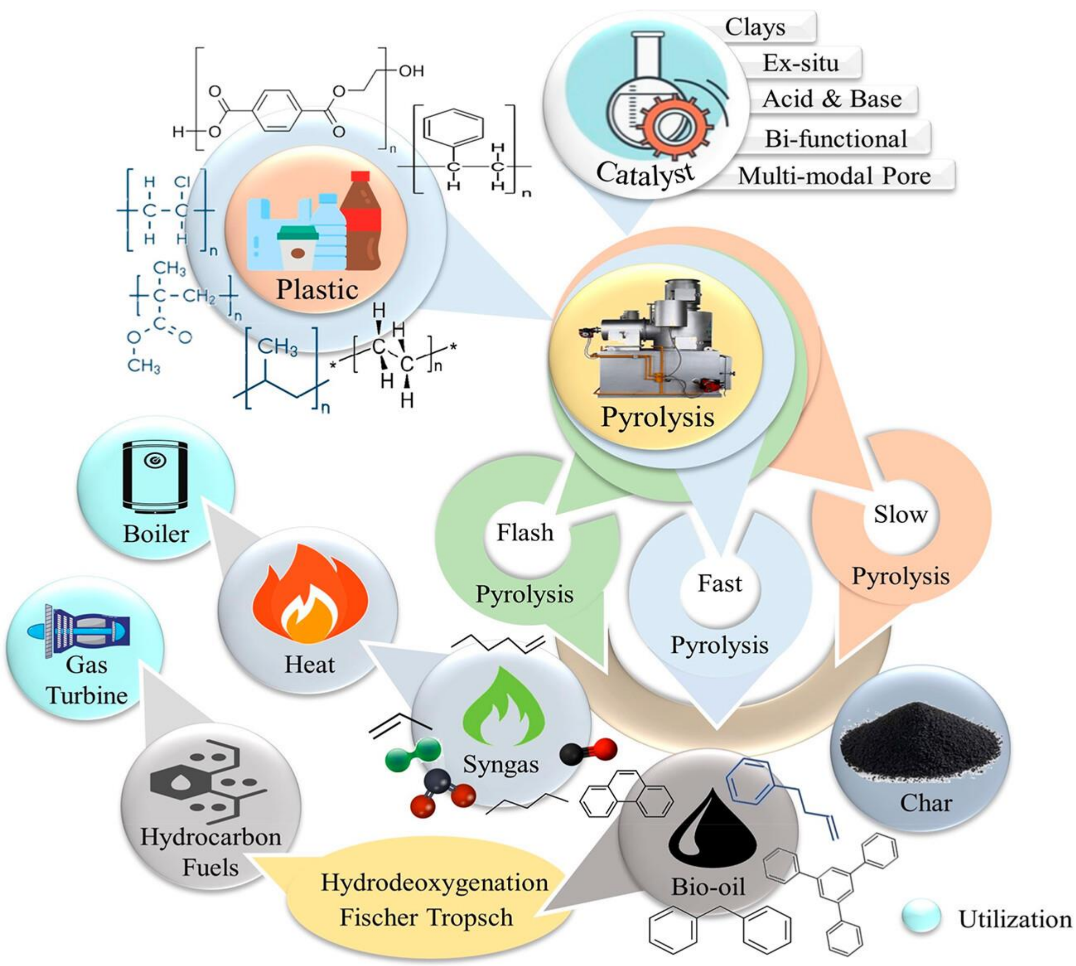

Figure 2. 8 : Schematic Diagram of catalytic pyrolysis [77]

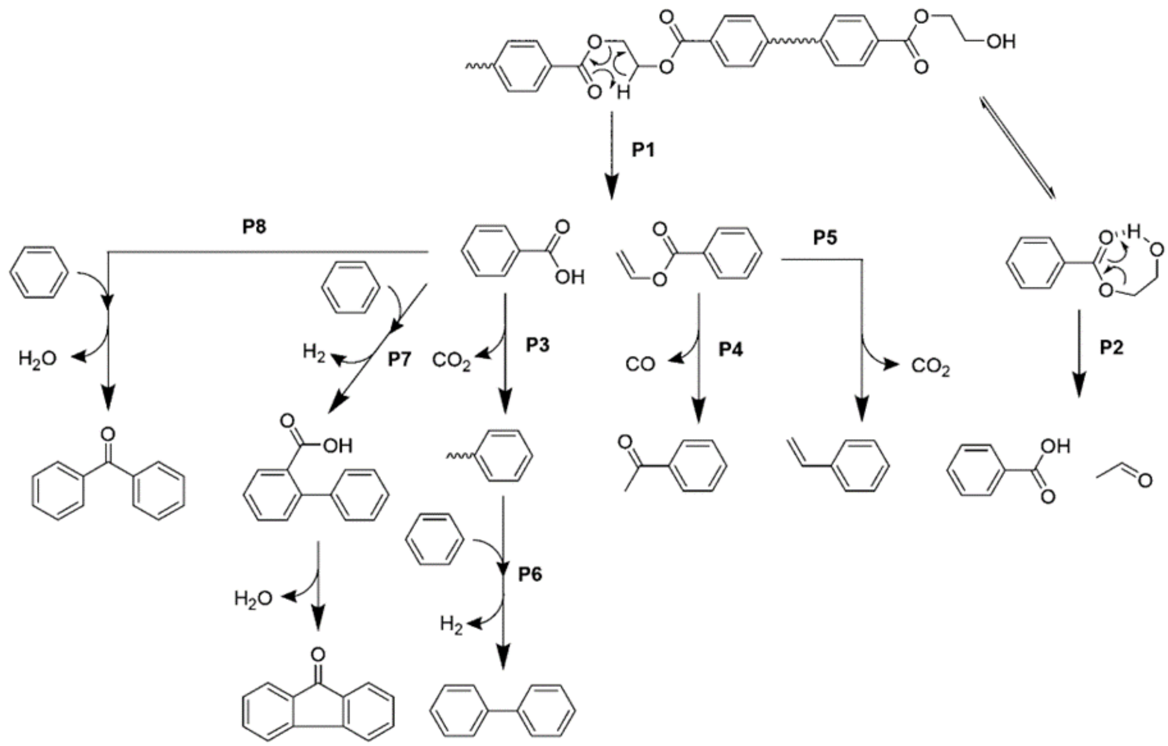

Figure 2. 9: Mechanism of catalytic pyrolysis of PET [78]

2.5 Catalysts used for pyrolysis

Plastic waste becomes contaminated with nitrogen, sulphur, and chlorine as because of surface contamination, additives, and heteroatom-containing plastics like PVC. The resultant liquid oil's quality is compromised by these contaminants. In addition, endothermic cracking and limited thermal conductivity enable thermal pyrolysis an extremely energy-intensive process. Various catalysts are utilised in the pyrolysis process through "in situ" methods to mitigate those challenges, specifically feedstock contamination. Figure 2.10 outlines these catalysts' properties and how they influence the pyrolysis process. During the pyrolysis of plastic waste to obtain higher chemical assets in the industries, different homogenous and heterogenous catalysts are used. Classical examples of solid Lewis acid heterogeneous catalysts have been used; these include Aluminum chloride and metal tetra chloroaluminates [79]. Nevertheless, such systems present problems like the capturing of the used catalyst from the final product. To deal with these problems the use of heterogeneous catalyst systems has been implemented in the catalytic cracking of plastics. Some of the regular heterogeneous catalysts are conventional zeolites , mesoporous catalysts [80], nanostructured and hierarchical kinds of catalysts , ionic liquids [81] and industrial Ziegler-Natta catalyst [81]. However, there are problems like corrosion and environmental issues with these catalysts though they are useful. Molecular sieves refer to a group of solid materials that have porous structures on the microscopic level and must be either acidic or basic so they could be effectively involved in catalytic processes.

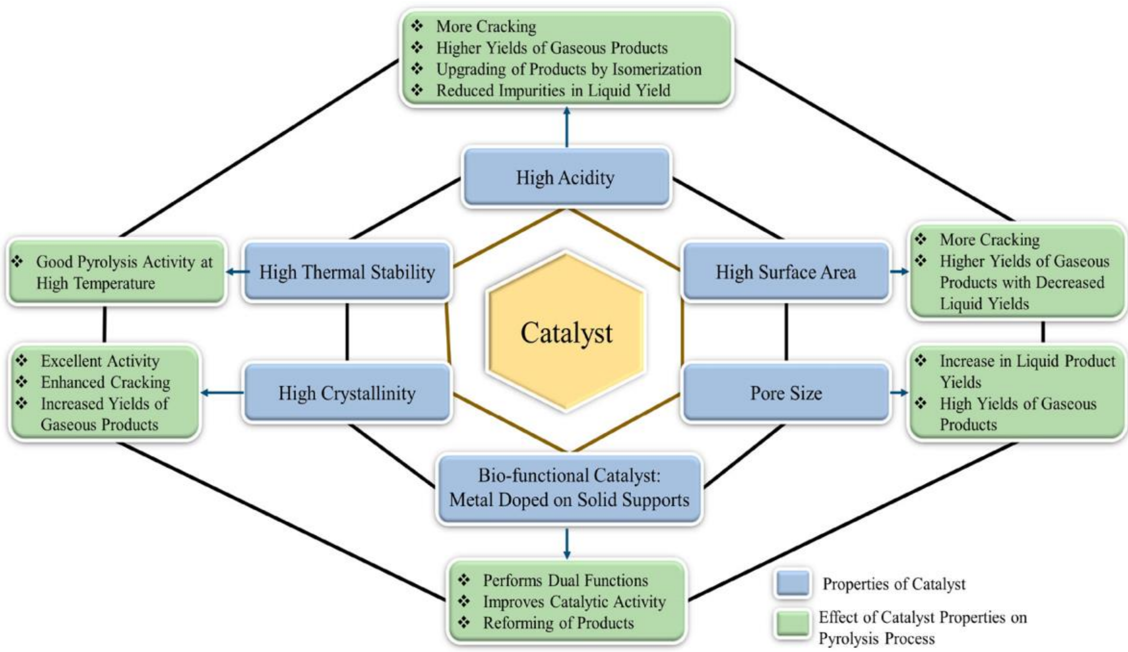

Figure 2. 10 : Catalysts properties and its impacts on pyrolysis [77]

2.5.1 Zeolites

Zeolite catalysts have distinct characteristics of pore structures that are well suited to the needs of the specific reactions, allowing excellent diffusion for the guest molecules to reach Brønsted and Lewis acid sites. It is very commonly used in plastic cracking processes. Zeolites used in plastic-to-fuel processes typically fall into two categories: intercrystallite microporous types containing narrow channels include HZSM-5, HY, HMOR HUSY and a group of mesoporous catalysts with relatively larger channels including MCM-41and SBA-15 [82, 83].

2.5.2 Mesoporous catalysts

Due to the bulky polymeric wastes hinder access to micropores of zeolitic catalysts because of steric lumens or diffusion barriers, mesoporous materials are emerging. This means that these materials possess relatively favorable acid site accessibility and useful in managing the large sizes of plastics wastes [84]. For instance, mesoporous silica exhibits a BET surface between 693- 800 m^2/g with a pore diameter of 2-50 nm [85]; thus, renders mesoporous materials suitable to be used as heterogeneous catalyst in many processes. They have comparatively low acidity, and their selectivity can be adjusted such that during their preparation process elements like aluminum, gallium, iron or zirconium can be incorporated into the catalyst. Solid acid catalysts to convert polyolefin plastic wastes to fuels has attracted more attention because of the desirable products like gasoline and diesel. Many papers and research articles have been published to analyze various catalysts like zeolites, silica-alumina, and mesostructured materials in the catalytic cracking of polyolefins. Other studies of the recent past have discussed micro/mesoporous materials [86], with hierarchical Beta zeolite with bimodal micro and microporosity being used copiously. Interestingly, Ni/H-Beta catalyzed the gasoline production better than the other two catalysts out of the tested standards.

2.5.3 Fly ash catalysts

Biomass Fly ash (BFA) is solid waste byproduct resulting from coal and biomass combustion in power plants. BFA is typically a waste of biomass combustion in industries, which highly affects the environment. It is known that major components of fly ash are SiO_2 and Al_2O_3. Following the high temperature combustion the oxides that are produced are of high thermal stability and this makes fly ash to be a good catalyst support. Like the non-single oxide components, other minor metal oxides including Fe_2O_3, TiO_2, CaO, MgO, K_2O, and Na_2O are also good candidates for the catalytic components. Typically, in quite a number of catalyst systems, the active components are transition metal oxides and other metal oxide components work as promoters, such as alkali or alkaline earth metal oxides. Hence, fly ash has to potential to be implemented in the role of a catalyst as well as the support of the catalyst in a range of reactions. It has high thermal stability and contains metal oxides which can act as a supporting catalyst as it is readily available in the breakdown of plastics [14]. In catalytic pyrolysis of various plastic materials, fly ash has been utilized as catalyst [15], which achieves significant improvements in the pyrolysis process thus enhancing the quality and yield of light oil fraction, whereas in HDPE and LDPE pyrolysis improves the oil yield at lower mass fraction but improves the properties of derived oil as compared to the standard fuels [16, 17]. PET plastic pyrolysis using a low-cost concrete waste catalyst has been conducted which showed no change in the decomposition temperature but enhances the deoxygenation reaction to produce more valuable aromatics products [87].

Table 2. 2: Pyrolysis of plastic over different catalysts

Types of Plastic	Catalysts	Conditions	Conversion	Ratio (catalyst/plastic)	References
Plastic mixtures (PET/PP/PS/PVC)	ZSM-5	500 C, 30 min	58 % gases	1: 10	[88]
Plastic mixtures (PET/PP/PS/PVC)	Regenerated ZSM-5	440 C, 30 min	60 % liquids	1: 10	[89]
HDPE	Co-Y-zeolite	600 C, 30 min	40% gases	2:1	[90]
PS	Natural zeolites	450 C,30 min	60.8 % ethylbenzene	0.1 kg: 1 Kg	[75]
PS/PO	Y-zeolite	600 C, 30 min	-	1: 1	[91]
PE/PP	USY-zeolite	500 C	80 % liquid	1: 10	[92]
Corn stalk/ HDPE	ZSM-5	700 C, 1 atm	90 % gases	1:2	[93]
Rise Husk/PE	Ni/ gema-A2O3	600 C	80 % hydrogen	50-75 % PE	[93]
LDPE	Mo-MgO, Fe	400 C	-	0.5 g: 15 g	[94]
PP	La2O3	500 C, 2.5 h	-	0.5 g: 15 g	[95]
PET	-	500	26 % liquid	-	[96]
Mixed	-	500	90% Liquid	-	[97]
PET	-	500	15% Liquid	-	[98]

2.6 Kinetic study

A variety of models and methodologies were used to investigate pyrolysis kinetics. Model-fitting method provide helpful information about reaction mechanism involve in pyrolysis and determination of Ea [99]. For estimating the apparent Ea for fixed mass conversions, model-free method are also a reliable method [100]. Based on the calculated kinetic triplet such as Ea, and A, and mechanism function, a major way to explore the thermal degrading process of plastic is currently extensively employed [101]. Non-isothermal approaches for determining kinetics had the benefit of executing the temperature program more rapidly and readily than isothermal methods [102].

Table 2.3 presents the most frequent models used in the evaluation of kinetics parameters and discusses the assumption that has been made to perform these models. The model free and model fitting methods were employed in the non-isothermal kinetics. The two model free methods are the Kissinger-Akahira-Sunose (KAS) [102] and Flynn Wall Ozawa (FWO) [103] method, that assuming the reaction rate was only dependent on the reaction temperature for a fixed conversion. Various heating rate were used instead of a single heating rate without information of the reaction mechanism to calculate more reliable kinetic parameters. The mode fitting technique, on the other hand, was developed using a specific reaction mechanism such as diffusion, order-based, or power-law models to depict the conversion reliance on the reaction rate [104]. The most crucial step in using a mode-fitting approach, such as in Coats Redfern [105] method, was to find an adequate reaction mechanism that describe degradation of sample [106]. Therefore, both methods have pros and cons. The combined, can obtain not only the Ea, and A but also find the most probable reaction mechanism [107]. Vyazovkin et al. [108]believe that the kinetic parameters attained by model free methods are more accurate and consistent. The model free procedures provide less specific information than model fitting methods [109].

Table 2. 3: Comprehensively used model fitting and model free methods, general forms, rules, and plotting variables [110]

Kinetic models	**General equation form**	**Rules**	**Plotting variables**
Coats-Redfern Method	$\ln\left(\frac{g(\alpha)}{T^2}\right) = ln\left[\frac{AR}{\beta E_a}\right] - \frac{E_a}{RT}$	In this method, taylor series used, and assumed the value of reaction order	$\frac{g(\alpha)}{T^2}\ vs\ \frac{1}{T}$
Kissinger Akahira Sunose (KAS) method	$\ln\left(\frac{\beta}{T^2}\right) = \frac{-E_a}{R}\left(\frac{1}{T}\right) - \ln\left[\left(\frac{E_a}{AR}\right)\int_0^\alpha \frac{d\alpha}{f(\alpha)}\right]$	T: temperature At max reaction rate Assumes conversion is fixed.	$\ln\left(\frac{\beta}{T^2}\right)\ vs\ \left(\frac{1}{T}\right)$ and $Slope\ =\ E_a$
Flynn Wall Ozawa (FWO) method	$\ln\beta = \ln\frac{AE_a}{Rg(\alpha)} - 5.331 - 1.052\frac{E_a}{RT}$	Assumes apparent activation energy remains constant during the degradation and Doyle approximation is applicable for mathematical formulation.	$\log\beta\ \ vs\ \left(\frac{1}{T}\right)$ and slope = $-0.4567\ \frac{E_a}{R}$
Friedman method	$\ln\left(\frac{d\alpha}{dt}\right) = \ln\left[\beta\left(\frac{d\alpha}{dt}\right)\right] = \ln\left[A\ \mathrm{f}(\alpha)\ \right] - \frac{E_a}{RT}$	Assumes f(α) remains constant. degradation is independent of temperature and depends only on the rate of mass loss.	$\ln\left(\frac{d\alpha}{dt}\right)\ vs\ \left(\frac{1}{T}\right)$ and $Slope\ =\ -\frac{E_a}{R}$

Table 2. 4: Literature review on kinetic study of plastic pyrolysis

Plastic type	Catalyst	Method	Operating Conditions	Kinetics Parameters	References
PET	-	Fridman	P = atmospheric, β = 5,10,15 K/min	E_a = 225.1 kJ/mol A = 4.08 x 10^{24}	[111]
LDPE	-	Fridman	β = 2,5,20,50 K/min	E_a = 221 kJ/mol	[112]
PP		Fridman	β = 2,5,20,50 K/min	E_a = 207 kJ/mol	[113]
PET	-	KAS	β = 10,15,20 K/min	E_a = 162.15 kJ/mol	[114]
PS	Fe	KAS	β=0.25-0.5-1-2 K/min	E_a = 138 kJ/mol	[115]
PET	-	FOW	β=5,10,15,20.25 K min^{-1}	E_a = 177-255 kJ/mol	[116]
PET		KAS	β = 10,3,50 K/min N_2 : 40 ml/min	E_a = 207.10-230.10 kJ/mol Lnk_0 = 27.06−30.62	[117]
PET		Starnik method	β = 10,3,50 K/min N_2 : 40 ml/min	E_{mean} = 131.3 kJ/mol	[117]
Mixed plastic	ZSM-5	DAEM	5,10,15,20, 25,30 °C/min	E_a = 350 kJ/mol	[118]
PET	BFA	CR, Fridman, KAS, FOW	5,10,15,20 C/min	160-180 kJ/mol	This study

Chapter 3: Materials and Methods

3.1 Material Preparation

The waste collected consisted of pure PET plastic; they were bought locally and were then washed with water and soap separately. Subsequently, the cleaned PET was dried in an oven for 24 h at a temperature of 105 °C to remove every form of moisture content. Following the drying process, the PET material was crushed manually and then sieved using RX-29–10 WS Tyler sieving machine, sourced from USA, and this was to ensure that it has a constant particle size of 0. 2 mm This holistic procedure enables collection, cleaning, drying, grinding, and sieving of the PET waste, making them a clean, easy to work with, and of a uniform particle size. It is crucial to prevent any negativity that may affect the reliability of the PET in future uses, for instance in recycling or research, and because the quality of the material should be homogeneous to avoid disruptions [119, 120]. Figure 3.2 explains the schematic diagram of material pure polyethylene terephthalate (PET) preparation.

3.1.1 Catalyst synthesis

The synthesis of the biomass fly ash (BFA) catalyst shown in Figure 3.1, as outlined in the research literature [121]. begins with drying, grinding, and sieving the BFA sample to reduce its particle size. This is followed by washing the sample with deionized water to remove any non-volatile components. Finally, the BFA undergoes calcination at 700 °C for 5 hours, a process that eliminates any remaining moisture and volatile components, resulting in a purified catalyst material.

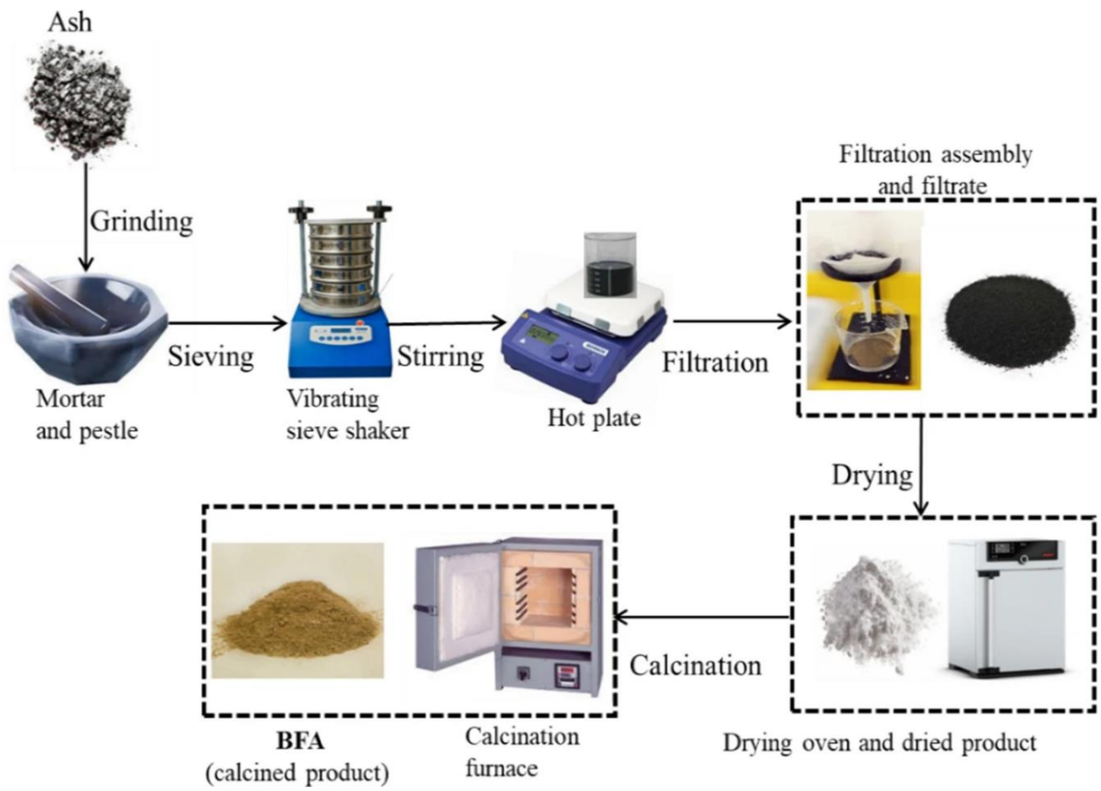

Figure 3. 1: Schematic Diagram of catalyst synthesis

3.1.2 Catalytic Blends Preparation

In catalytic pyrolysis, the in-situ catalytic pyrolysis technique was used for the preparation of the material where the catalyst or the active phase was incorporated with the pyrolyzing material. Namely, biomass fly ash (BFA) was chosen as a catalyst and was blended with pure polyethylene terephthalate (PET). The BFA and PET mixture was thoroughly ground using a hand mortar and pestle so that the fine particle size was achieved to give a better interaction with the catalyst during the pyrolysis process.

The BFA catalyst was incorporated into the pure PET at three different weight ratios: This was after one of the components of the rubber vulcanizing process known as sulfur increased to 5 wt. %, 10 wt. %, and 15 wt. %. These different ratios enabled the studies of effects of catalyst loading on the pyrolysis process and productions of the pyrolytic products. The blends for the catalytic pyrolysis were thereafter named depending on the specific proportion of the catalyst to the PET. The blends were as follows: Complete

PET without using any catalyst (0. 00:1. 00), 5 wt. % BFA-PET (0. 05:0. 95), 10 wt. % BFA-PET (0. 10:0. 90), and 15 wt. % BFA-PET.

Thus, an accuracy of the measures was accomplished by using a digital GSM balance to weigh the BFA and PET. Subsequently, the mixtures were properly mixed by using a vortex mixer for at least 5 to 10 minutes. This stage was particularly important to ensure that the blends were rather homogeneous was important so as to attain uniform distribution of the catalyst in the PET material. This uniform distribution is needed in order to have a uniform catalytic activity throughout the pyrolysis process.

The preparation of the mixtures, combining, and the grinding processes which leads to homogeneity of the mixture is illustrated in the PFD as shown in Fig. 1. This elaborate procedure helps to implement the catalyst with the PET optimally which in turn helps in carrying out the catalytic pyrolysis research and observe the impact of the catalyst at varying quantities.

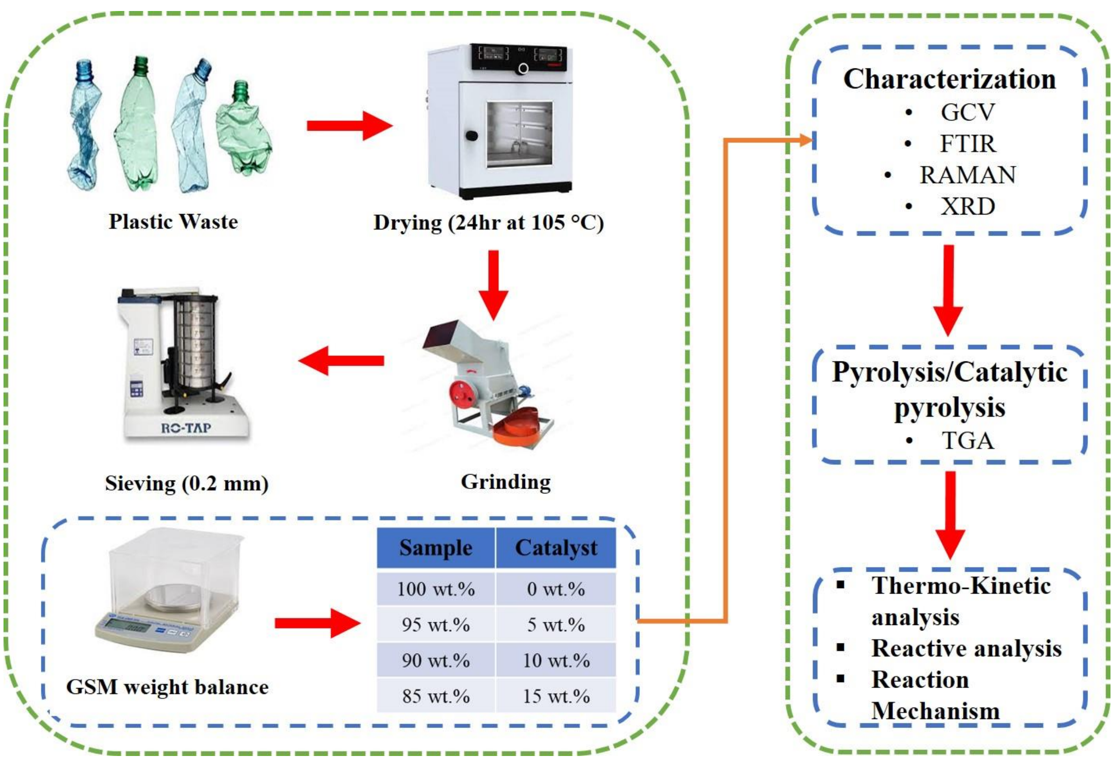

Figure 3. 2: Schematic diagram of material and catalytic blends preparation

3.2 Non-Catalytic Pyrolysis and Catalytic Pyrolysis of PET in TGA

Experiments involving pyrolysis and catalytic pyrolysis of both pure PET and its catalytic blends were carried out using TGA 5500 (TA Equipment, USA), weighing between 8-12 mg for each sample. The process was performed from room temperature to 900 ºC using the inert (N_2) environment supplying 25 ml/min flow rate. The heating rate was 10 ºC/min for pure PET or 0%BFA-PET, 5%BFA-PET, 10%BFA-PET, and 15%BFA-PET. Weight loss (WL%) and Residue Left (RL%) concerning temperature are used to determine TGA and DTG curves respectively. Further, TGA data were used to examine the kinetic study and reactivity analysis of this work. Schematic Diagram of Pyrolysis/Catalytic Pyrolysis in TGA as shown in Figure 3.3.

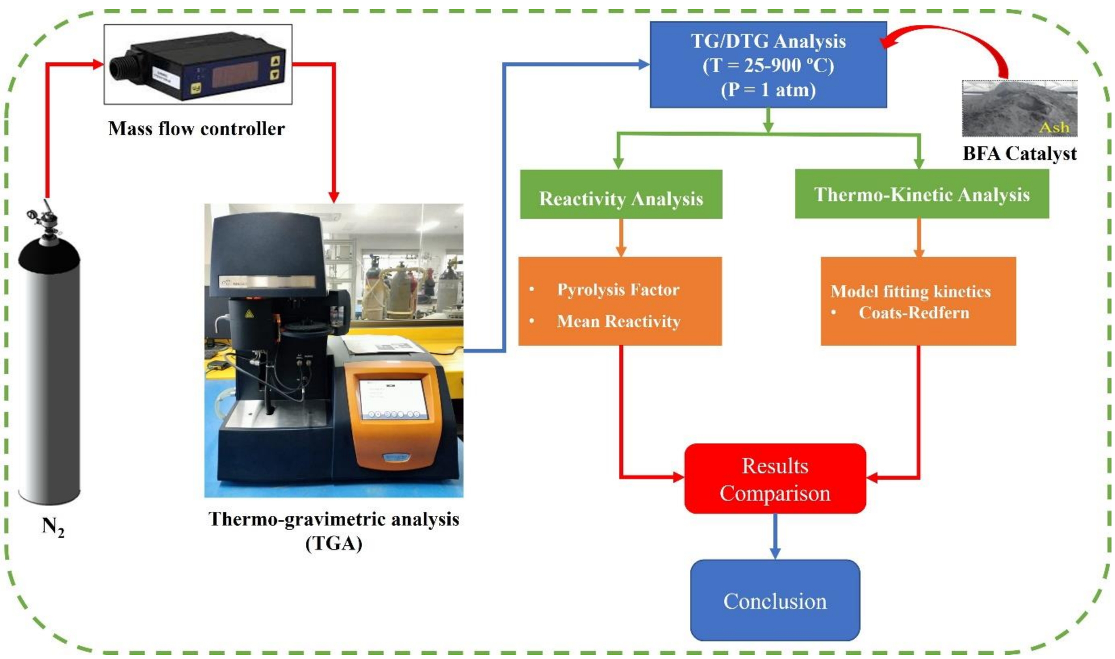

Figure 3. 3: Schematic Diagram of Pyrolysis/Catalytic Pyrolysis in TGA

3.3 Material Characterizations

The gross calorific value (GCV) of material was determined in the PAR-6200 bomb calorimeter following standard of ASTM D5865-13. Fourier transform infrared (FTIR) spectroscopy module: attenuated total reflection (ATR) with the wavelengths ranging 600-4000 cm^{-1} (model: Cary 630 by Agilent Technologies, USA) was used to analyze the functional groups in pure PET and BFA. To identify the vibrational characterization of the sample, RAMAN spectrometry is used to analyze Pure PET and BFA samples and is performed via Raman (BAC 102–532) of BWTEK. The TGA analysis of the Biomass fly ash (BFA) was performed in TGA 5500 (TA Equipment, USA) to study its thermal stability. The XRD analysis to determine the crystalline structure of Pure PET and BFA samples was performed in an X-ray diffractometer (D8 Advance). The diffracted pattern was in the range of (2(θ) = 10-80°).

3.4 Kinetic Study

The kinetic study of any process represents the relationship between reaction rate and different parameters [122]. The reaction occurring in single step, the thermal breakdown of PET and its catalytic blends under specific temperature ranges produce volatiles (tar & gases) and char (solid & residue) termed as Eq. 1.

$$A \rightarrow B + C \quad (1)$$

The fundamental equation Eq. 2 is used for the investigate of the kinetics of solid-state thermal decomposition.

$$\frac{d\alpha}{dt} = k_n f(\alpha) \quad (2)$$

where the reaction of rate (dα/dt) can be represented as a function involving temperature-dependent term k_n and the explain the dependency of the extent of conversion(α) on reaction model f(α). According to Arrhenius's Equation, Eq. 3 represents the rate constant k_n [123],

$$k_n = A \exp\left(\frac{-E_a}{RT}\right) \quad (3)$$

The conversion rate of a solid material is expressed in Eq. 4 [124], which is derived by putting Eq. 3 in Eq. 2;

$$\frac{d\alpha}{dt} = A \exp\left(\frac{-E_a}{RT}\right) f(\alpha) \quad (4)$$

Where α is the conversion rate, while Ea stands for activation energy, A indicates pre-exponential factor. R is the universal gas constant (8.314 J/ (mol. K)), T represents temperature, and f(α) is the reaction model. Eq. 5 gives the degree of conversion during pyrolysis [125]. The constant heating rate is defined as β in Eq. 6 [126] as,

$$\alpha = \frac{m_o - m_t}{m_o - m_e} \tag{5}$$

$$\beta = \frac{dT}{dt} = \frac{dT}{d\alpha} \times \frac{d\alpha}{dt} \tag{6}$$

$$f(\alpha) = (1 - \alpha) \tag{7}$$

m_o represents the initial weight of the sample, m_t denotes weight at any given time t, and m_e indicates the final weight.

3.4.1 *Coats-Redfern Method*

The Coats-Redfern method is a model-fitting technique employed for studying the kinetics of materials decomposition [120]. thermogravimetric analysis (TGA) data used to determine the important kinetics parameters, including activation energy (E_a) and pre-exponential factor (A). The Arrhenius equation Eq. 3 is employed in the Coats-Redfern method to relate the rate of thermal degradation of a sample to its activation energy and temperature [119, 127]. The decomposition of materials through pyrolysis is commonly believed to be a first-order reaction with a value of n equal to 1 and is associated with this type of reaction as shown in Eq. 7. From Eq. 4, Eq. 6, and Eq. 7 we get Eq. 8,

$$\frac{d\alpha}{dT} = \frac{A}{\beta} \exp\left(\frac{-E_a}{RT}\right)(1 - \alpha) \tag{8}$$

After integrating Eq. 8, the integral function of conversion is g(α) of the reaction model, which takes the form in Eq. 9.

$$g(\alpha) = \int_0^\alpha \frac{d\alpha}{f(\alpha)} = \frac{A}{\beta}\int_0^T \exp\left(\frac{-E_a}{RT}\right) dT \tag{9}$$

Taking the integral and rearrangement of Eq. 9 can be expressed in following form Eq. 10

$$\ln\left(\frac{g(\alpha)}{T^2}\right) = ln\left[\frac{AR}{\beta E_a}(1-\frac{2RT}{E_a})\right] - \frac{E_a}{RT} \tag{10}$$

Where $(1-\frac{2RT}{E_a})$ is very small and can therefore be neglected, then Eq. 10 becomes,

$$\ln\left(\frac{g(\alpha)}{T^2}\right) = ln\left[\frac{AR}{\beta E_a}\right] - \frac{E_a}{RT} \tag{11}$$

Plotting $\frac{g(\alpha)}{T^2}$ vs $\frac{1}{T}$ gives the slope $-\frac{E_a}{R}$ which is applied to calculate the Activation energy (E_a).

Table 3. 1: Reaction models and their algebraic expressions

Symbols	Reaction mechanism	$f(\alpha) = \frac{1}{k}\frac{d\alpha}{dt}$	$g(\alpha) = -kt$
		Model: Reaction Order	
F1/3	One-third order	$(1-\alpha)^{\frac{1}{3}}$	$-\frac{3}{2}\left[(1-\alpha)^{\frac{1}{3}}-1\right]$
F1	First-order	$(1-\alpha)$	$-ln(1-\alpha)$
F3/2	One and a half-order	$(1-\alpha)^{\frac{3}{2}}$	$2\left[(1-\alpha)^{\frac{-1}{2}}-1\right]$
F2	Second-order	$(1-\alpha)^2$	$(1-\alpha)^{-1}-1$
F3	Third order	$(1-\alpha)^3$	$\frac{1}{2}[(1-\alpha)^{-2}-1]$
		Model: Diffusion mechanism	
D1	Parabolic law	$\frac{1}{2}\alpha$	α^2
D2	Valansi law	$-[ln(1-\alpha)]^{-1}$	$\alpha+[(1-\alpha)ln(1-\alpha)]$
D3	Jander equation	$-2(1-\alpha)^{\frac{2}{3}}\left[1-(1-\alpha)^{\frac{1}{3}}\right]^{-1}$	$\left[1-(1-\alpha)^{\frac{1}{3}}\right]^2$
		Model: Geometric Contraction	

R1	Contracting disk	1	A
R2	Contracting cylinder	$2(1-\alpha)^{\frac{1}{2}}$	$1-(1-\alpha)^{\frac{1}{2}}$
	Model: Power Law		
P2	Power Law; P2	$2(\alpha)^{\frac{1}{2}}$	$(\alpha)^{\frac{1}{2}}$
P3	Power Law; P3	$3(\alpha)^{\frac{2}{3}}$	$(\alpha)^{\frac{1}{3}}$

3.4.2 Combined kinetics

Empirical mechanism model was employed to obtain the combined kinetics method by fitting the theoretical reactions with adjustment of suitable parameters. The ordered reaction mechanisms for pyrolysis is generally different from the mechanism actually taking place for the biomass conversion. Therefore, multi-mechanisms are addressed with the help of this approach. A linearized rate equation is proposed for the combined kinetics for the single step reactions as $f(\alpha) = c(1-\alpha)^n\alpha^m$ in which different parameters like c, n and m somehow be obtained by maximizing the R^2 for linear equation that is depicted in Eq. 12 as,

$$\ln\left[\frac{d\alpha/dt}{(1-\alpha)^n\alpha^m}\right] = \ln[cA] - \frac{E_a}{RT} \tag{12}$$

3.4.3 Master plot method

For the kinetic mechanistic function analysis, ICTAC (International Confederation for Thermal Analysis and Calorimetry) Kinetics Committee recommendations has recommended the method of master plots. By employing the [Eq. 8], [Eq.13] can be obtained as,

$$f(\alpha) = \frac{\beta}{A}\exp\left(\frac{E}{RT}\right) d\alpha/d \tag{13}$$

At conversion of α =0.5 which is probably a reference point, [Eq. 14] can be obtained as

$$\frac{f(\alpha)}{f(0.5)} = \frac{\left(\frac{d\alpha}{dT}\right) \exp\left(\frac{E}{RT}\right)}{\left(\frac{d\alpha}{dT}\right)_{0.5} \exp\left(\frac{E_{0.5}}{RT_{0.5}}\right)} \tag{14}$$

Where the $(\boldsymbol{d\alpha/dT})_{0.5}$ is basically the rate of conversion which somehow related to $\boldsymbol{\alpha}$ = 0.5 and f (0.5), $E_{0.5}$ and $T_{0.5}$ certainly dictates the mechanism of kinetic function, E_a along with temperature that somehow related to $\boldsymbol{\alpha}$=0.5 respectively. Moreover, the experimental values of f($\boldsymbol{\alpha}$)/f(0.5) vs $\boldsymbol{\alpha}$ could have been estimated based on the [Eq. 14].

3.4.4 *Friedman Method*

The Friedman model equation is presented in Eq. 15 which is the logarithmic form of Eq. 5 [128],

$$\ln\left(\frac{d\alpha}{dt}\right) = ln\left[A[f(\alpha)]\right] - \frac{E_a}{RT} \tag{15}$$

Plotting the Graph $\ln\left(\frac{d\alpha}{dt}\right)$ vs $\frac{1}{T}$ gives the slope $-\frac{E_a}{R}$ a form where activation energy E_a can be calculated. Friedman method is an iso-conversional method that is more noise sensitive. This noise is one of the main reasons for errors in activation energy (E_a) estimation [124]. For the comparison, further conversional integral methods are applied to estimate E_a.

3.4.5 *Ozawa-Flynn-Wall (OFW) method*

Ozawa-Flynn-Wall (OFW) method is a conversional integral method Eq. 16 describes the relationship between the heating rate and the conversion rate [129].

$$ln\beta = ln\left[\frac{AE_a}{R \times g(\alpha)}\right] - 5.331 - 1.052\left[\frac{E_a}{RT}\right] \tag{16}$$

This method employs the approximation of Doyle for the calculation of the energy of activation. The Ozawa-Flynn-Wall (FWO) shows that there is a relationship between the logarithm of the heating rate and the inverse of the ambient temperature and plotting the graph $ln\beta\ vs\ \frac{1}{T}$, the slope will be $-1.052\left[\frac{E_a}{R}\right]$ which gives activation energy E_a [130].

3.4.6 *Kissinger-Akahira-Sonuse (KAS) method*

The correlation between activation energy and the heating rate is expressed by Eq. 17. When the conversion rates at different heating rates are the same, there is a linear relationship between $ln\left(\frac{\beta}{T^2}\right)$ and 1/T and $-\frac{E_a}{R}$ will be the slope [131].

$$ln\left(\frac{\beta}{T^2}\right) = ln\left[\frac{AR}{E_a g(\alpha)}\right] - \frac{E_a}{RT} \tag{17}$$

3.5 Thermodynamics Study

Enthalpy is a measure of the heat exchanged during a chemical reaction while keeping the pressure constant. The change in enthalpy for a system is denoted as (ΔH) (kJ/mol). Entropy is a measure of the heat energy that is exchanged throughout a chemical reaction, and it is often used as a degree of disorder, which is usually denoted by (ΔS) with the unit of (kJ/mol K). Gibbs free energy, which signifies the maximum work possible in a closed system, is only feasible through a completely reversible process. Indicated as (ΔG) (kJ/mol), provides a metric for a system's energy content and is useful for studying energy production. By studying kinetic parameters, various thermodynamic properties involving enthalpy (ΔH), entropy (ΔS), and Gibbs free energy (ΔG) can be derived as described in Eq. (18-20) [132].

$$\Delta H = E_a - RT_p \tag{18}$$

$$\Delta S = \frac{(\Delta H - \Delta G)}{T_p} \tag{19}$$

$$\Delta G = E_a + RT\, ln\left(\frac{k_b T_p}{hA}\right) \tag{20}$$

Where T_p is highest decomposition temperature, k_b represents the Boltzmann constant (1.38×10^{-23} J/K), R denotes universal gas constant (8.314 J/mol· K), h stands the Planck's constant (6.63×10^{-34} J.s).

Chapter 4: Results and Discussion

4.1 Catalyst Characterization

Figure 4.1 illustrates the FTIR of the BFA sample which shows major absorption peaks have appeared in its structure. The first peak is at 682 cm^{-1} wavelength (680-690 cm^{-1}) which shows the S-O bending which indicates the presence of sulphates in BFA [121]. The next major peak at 885 cm^{-1} is due to the plane bending of C-O in calcite $CaCO_3$ [133]. The next two peaks at 976 cm^{-1} and 1094 cm^{-1} present the bending and stretching vibrations of Si-O respectively with similar peaks in literature [121, 134]. Lastly, a minor adsorption peak at 2200 cm^{-1} shows O-H bending which indicates the carboxylic acid in BFA [135].

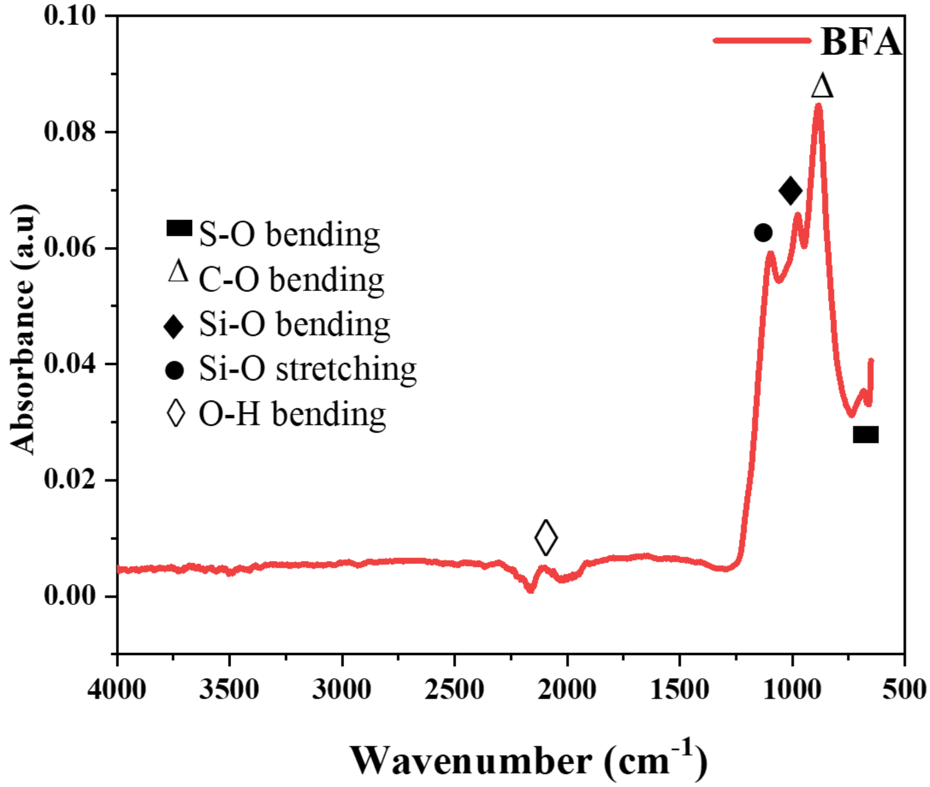

Figure 4. 1 : FTIR Pattern of Biomass Fly Ash (BFA) catalyst

The thermal stability of the catalyst is analyzed by using TGA, the curve shows that between 200-700 °C, weight loss remains negligible but after 700 °C an abrupt loss occurs till 900 °C only 5-6 %wt. loss is analyzed which clarifies the thermal stability of BFA catalyst as shown in Figure 4.2.

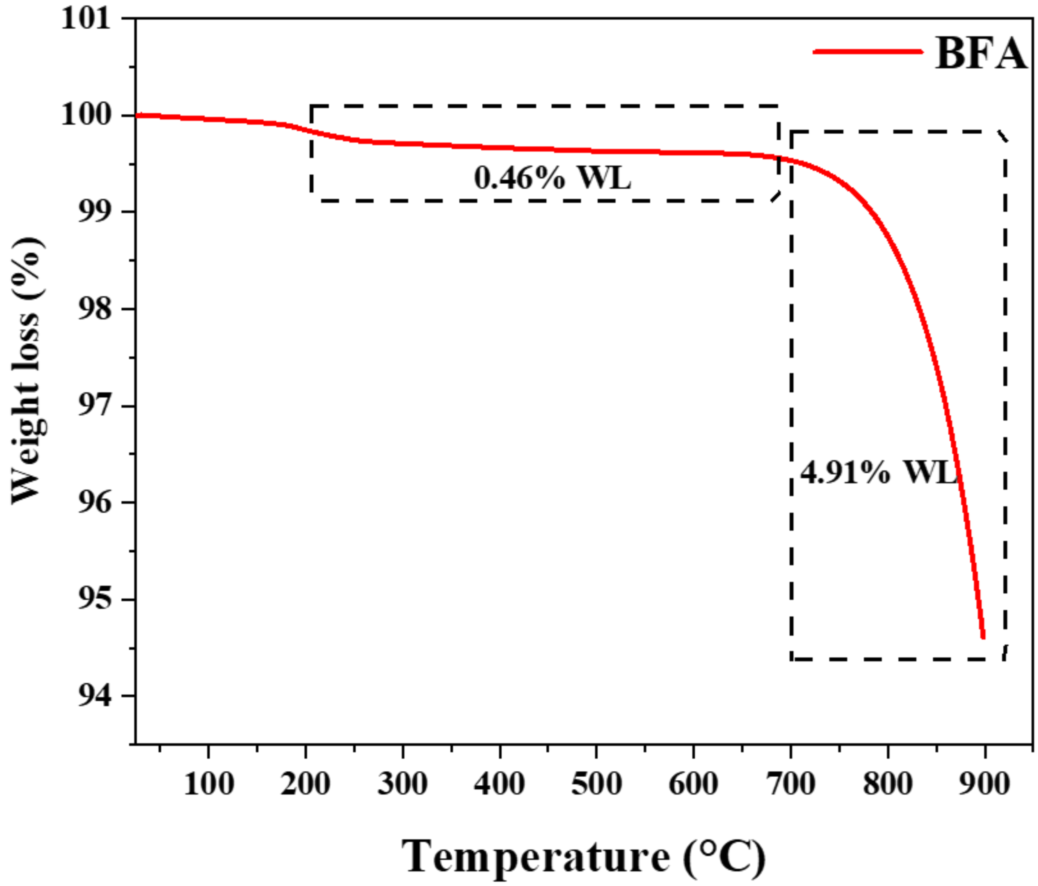

Figure 4. 2 : TGA Pattern of Biomass Fly Ash (BFA) catalyst

XRD pattern of BFA is illustrated in Figure 4.3 explain the crystallinity of the structure. BFA contains different diffraction peaks of various compounds such as oxides, carbonates, and aluminates. Major peaks represent SiO_2, Ca, K_2O, Fe, and Al_2O_3 with miller indexes of (001), (110), (220), (102), and (440) respectively. SiO_2 was detected at $2\theta = 26.2^o$ with PDF#47-1144 while Calcium (Ca) at $2\theta = 28.3^o$ with (PDF# 10-0348), K_2O at $2\theta = 39.5^o$ (PDF# 06-0615), Fe at $2\theta = 49.4^o$ (PDF# 15-0131) and Al_2O_3 at $2\theta = 66.7^o$ (PDF# 29-0063). A minor peak at 31.2^o, miller index (015), and (PDF# 06-0615) represented the trace amount of $K_2Ca(CO_3)$. All these peaks represent the crystallinity behaviour of BFA [121].

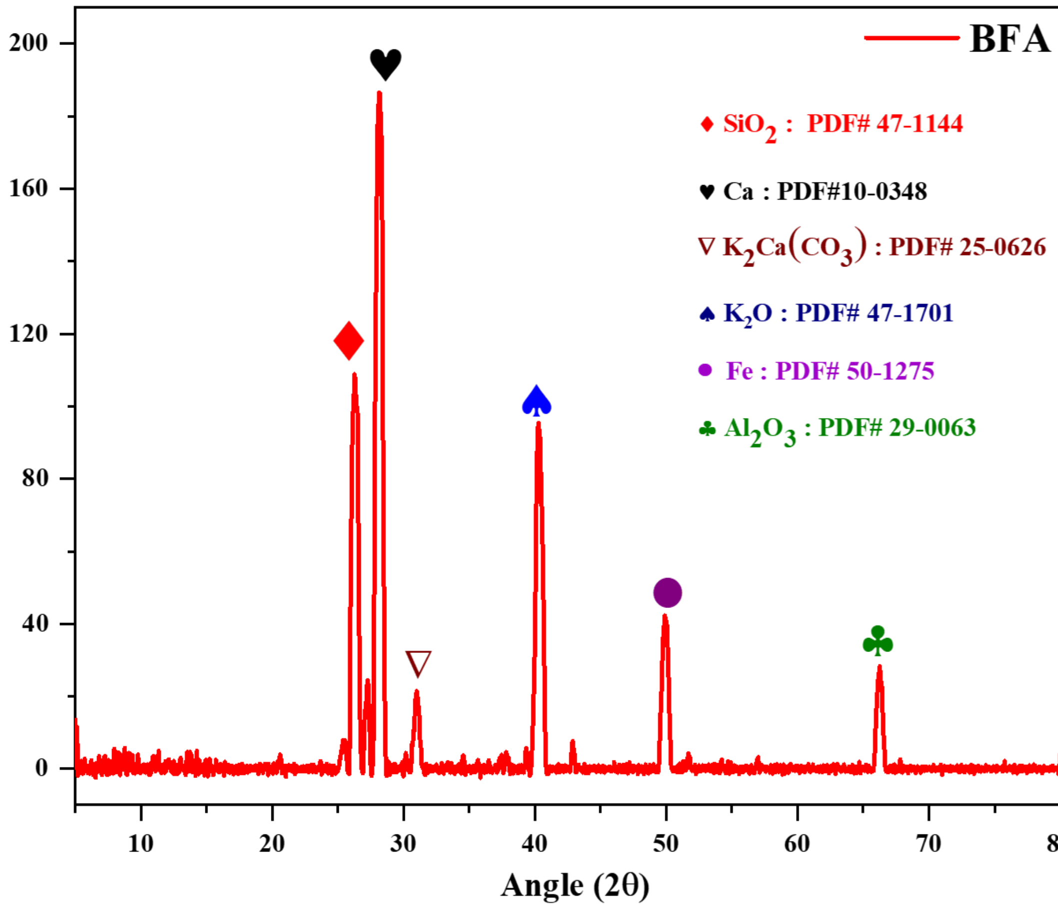

Figure 4. 3 : XRD Pattern of Biomass Fly Ash (BFA) catalyst

4.2 Material Characterization

PET is a rigid, semi-crystalline polymer created by repeating structural units. Temperature, catalyst type and quantity, and volatile residence time all affect how quickly PET decomposes and distributes its products [136].

GCV is used to find the heat of combustion, which gives the energy content of the fuel. The weight of the sample taken was 500 mg. GCV of Pure PET was found to be 24.13 MJ/kg, similar results were reported in the literature [137]. The high calorific value of PET matched that of bituminous coal (17-29 MJ/kg) or lignite coal (15-27 MJ/ kg) [11, 119].

Figure 4.4 illustrates the FTIR of a pure PET sample which shows four major absorption peaks have appeared in its structure. The first peak is at 715 cm^{-1} wavelengths in the range of (710-730 cm^{-1}) indicates the C-H bond stretching vibration in the aromatic structure of the benzene ring. The next two peaks at 1090 cm^{-1} and 1240 cm^{-1} show the stretching vibration of asymmetric –O-C-C and –C-C-O bonds respectively with similar peaks in literature [138]. A strong adsorption peak at 1710 cm^{-1} indicates the stretching vibration of C=O in the carboxylic group [139]. The last peak at 2962 cm^{-1} is due to the symmetrical vibration of CH in the ethylene group [140].

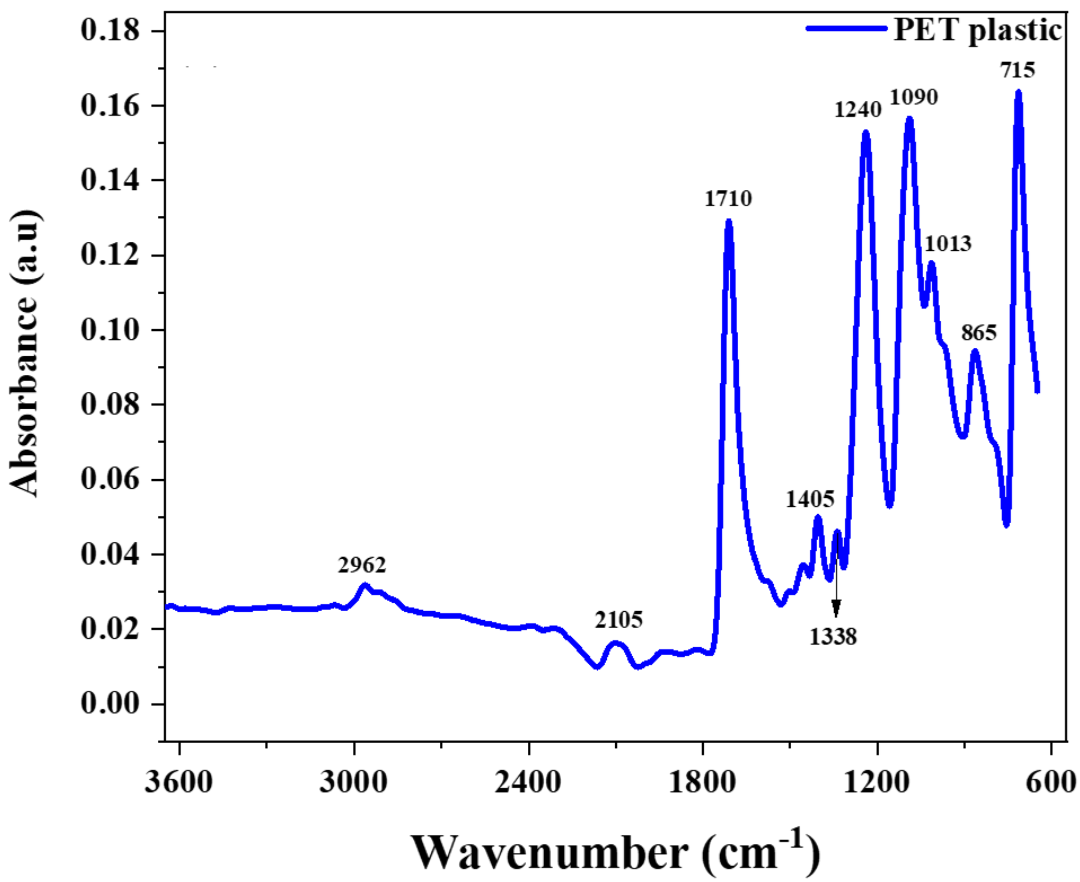

Figure 4. 4 : FTIR of Pure Polyethylene Terephthalate (PET)

Figure 4.5 shows the Raman spectroscopy of pure PET plastic, where the major two characteristic bands at 1615 cm^{-1} and 1737 cm^{-1} identified (G-band, crystalline state) the C=C aromatic stretching and C=O stretching vibration, respectively. Further, the bands between 1400-1450 cm^{-1} (D-band, amorphous state) are due to CH_2 and CH bending vibration, the bends at 1112 cm^{-1}, 1298 cm^{-1} (in the range of 1000-1300 cm^{-1}) belong to C(O)-O stretching and O-C-O stretching. The bend at 994 cm^{-1} corresponds to C-O bending (O-CH_2), and the bend at 780 cm^{-1} associated is bending vibration peak of C-H with isolated adjacent hydrogen and hydrogen bonds on the benzene ring. The bends at 618 cm^{-1} and 700 cm^{-1} are attributed to ring modes of a benzene ring and C-H out-of-plane bending with similar peaks in literature [141-144].

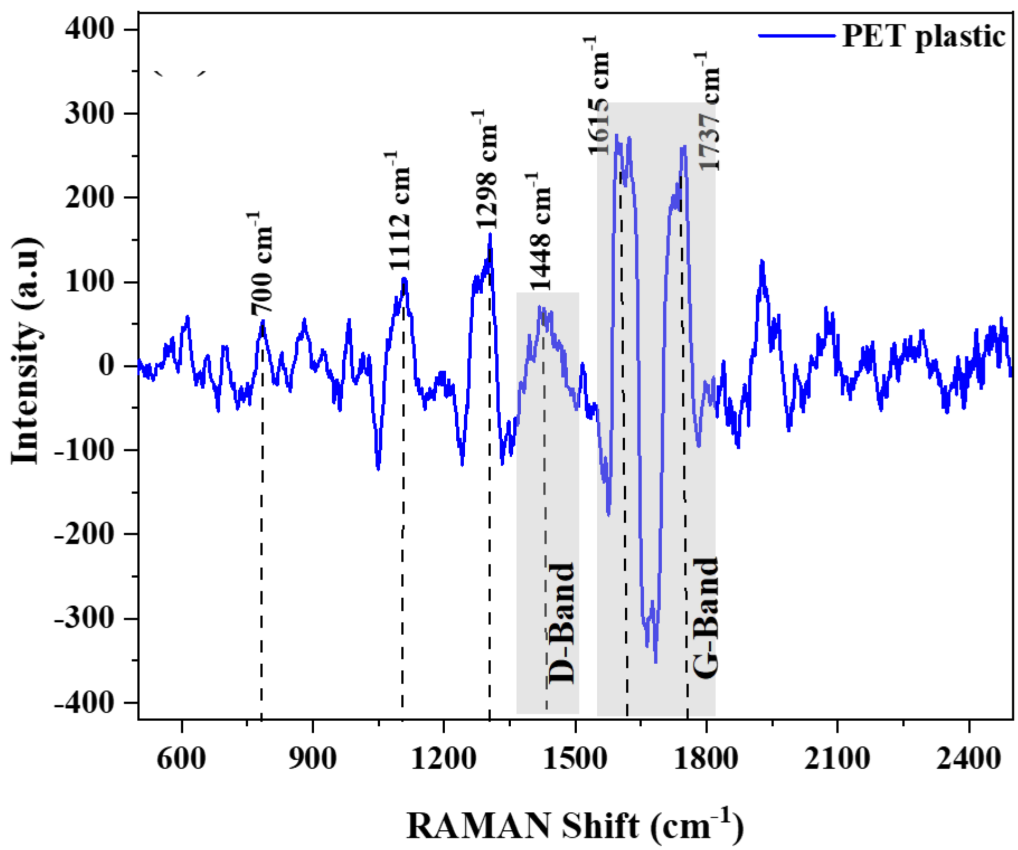

Figure 4. 5 : Raman of Pure Polyethylene Terephthalate (PET)

Figure 4.6 represents the crystalline and amorphous structure phases of the Pure polyethylene terephthalate (PET) which was studied via X-ray Diffraction (XRD) peak patterns. Pure PET can be found in both semi-crystalline as amorphous states. Depending on its crystalline and amorphous form, PET can seem opaque, white, or transparent. Processing variables like processing temperature, cooling rate, stretching process, etc. have a significant impact on its crystallinity and, subsequently, its physical and mechanical qualities [145]. The XRD peak for PET signify their crystallographic structure which demonstrates the main phase with miller indices and their structure which is polyethylene terephthalate (PET) (PDF# 50-2275) at 2θ = 26.1° with the hkl *(100)* having a triclinic structure [146, 147].

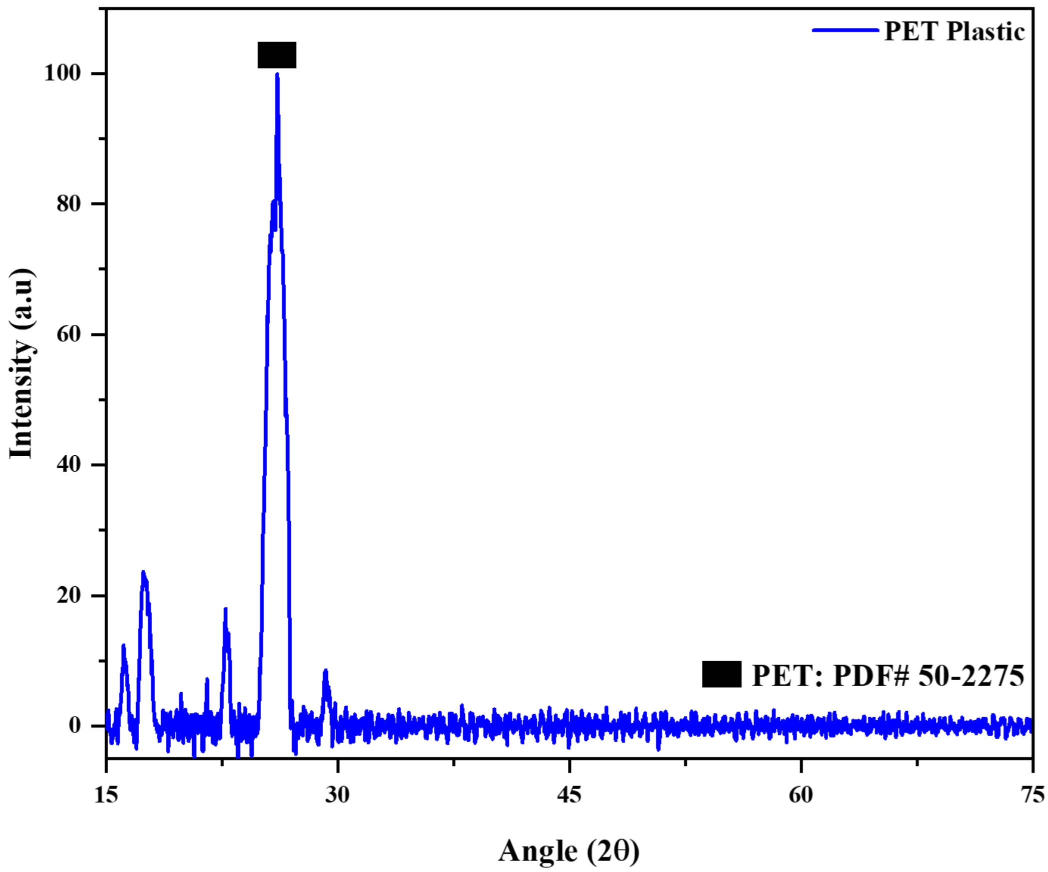

Figure 4. 6 : XRD pattern of Pure Polyethylene Terephthalate (PET)

4.3 Non-catalytic and Catalytic pyrolysis of PET in TGA

The TGA and DTG curves of Pure PET plastic waste in an inert atmosphere of nitrogen at heating rates 10 ºC/mi are shown in Figure 4.7 (a-b) respectively. TGA curve shows that weight loss occurs in three phases which are (a) moisture loss, (b) active pyrolysis, and (c) passive pyrolysis. The first stage lies between 25 and 375 ºC shows a very small amount of weight loss which is due to moisture removal. The second stage occurs between 375 to 500 ºC in which most of the decomposition of the volatile matter occurs. In this stage, larger molecules thermally degrade into minor molecules to produce benzoic acid and vinyl ester groups. The third stage lies between the range of 500 to 900 ºC which represents passive pyrolysis [148]. This stage is associated with the thermal degradation of char products that were formed during the previous decomposition step [149]. Weight loss (WL) of 87.32% and a residual mass of 12.68%, with a peak DTG rate of -18.91 wt.%/min at a peak decomposition temperature (T_p) of 440.26 °C as shown in Figure 4.7 (b). The weight loss (WL%) and residue left (RL%) are given in Table. 1 that are similar to the literature [150].

Table 4. 1 : TGA and DTG analysis with active pyrolysis range and peak degradation temperature.

Sample Name	Active pyrolysis range (ºC)	Peak Temp. (T_p) (ºC)	Weight Loss (WL) (%)	DTG (wt.%/min)
PET plastic	375-500	440.26	87.32	-18.91
5 wt.% BFA-PET	375-500	436.00	83.82	-16.75
10 wt.% BFA-PET	375-500	435.80	86.31	-16.89
15 wt.% BFA-PET	375-500	434.40	76.68	-15.39

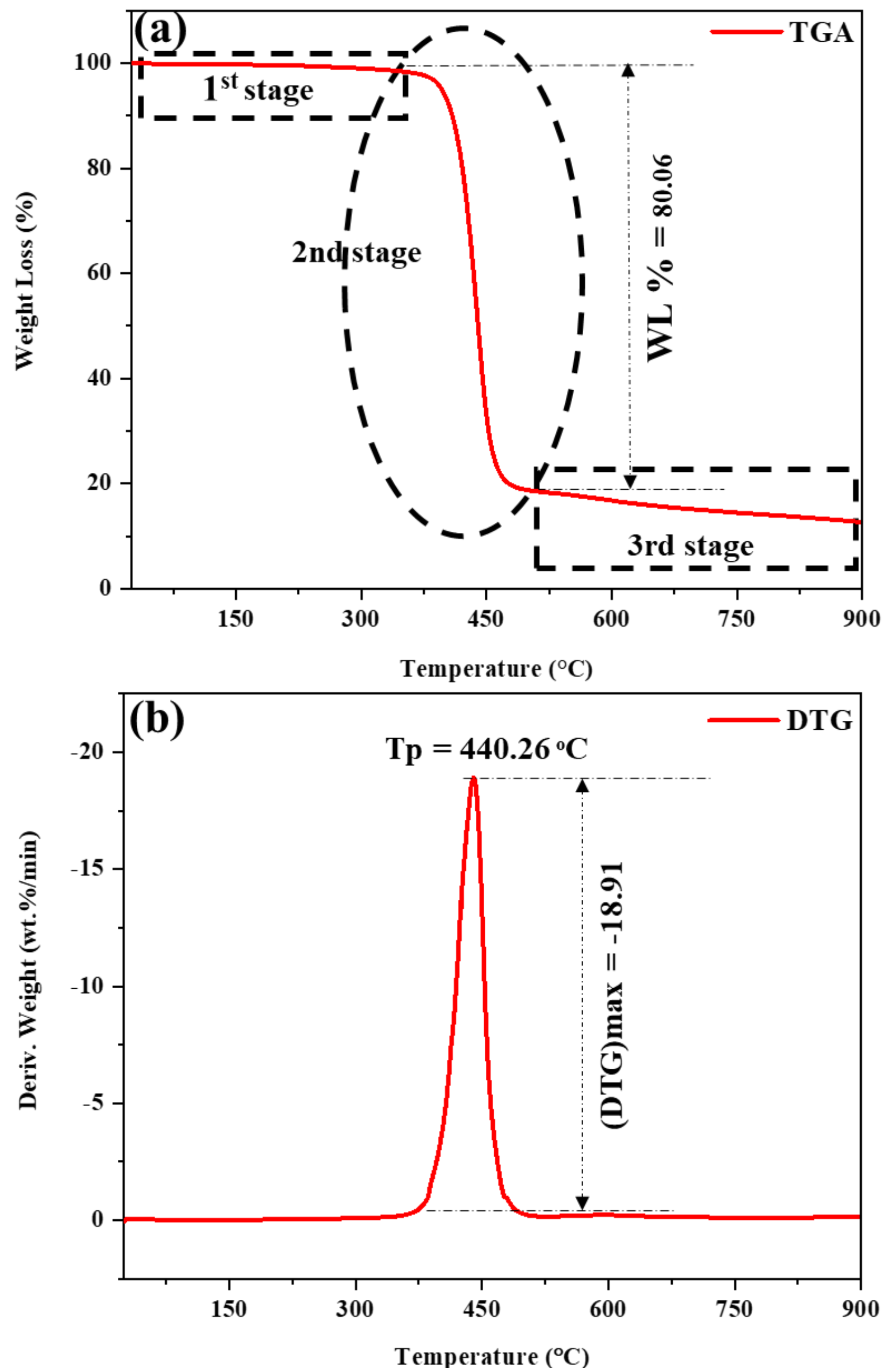

Figure 4. 7: TGA curve of Pure PET (b) DTG curve of Pure PET at 10 C/min

These studies were also analyzed at heating rate of 10 °C/min for catalytic pyrolysis. The experimental data is shown in the Figure 4.8 (a-b)

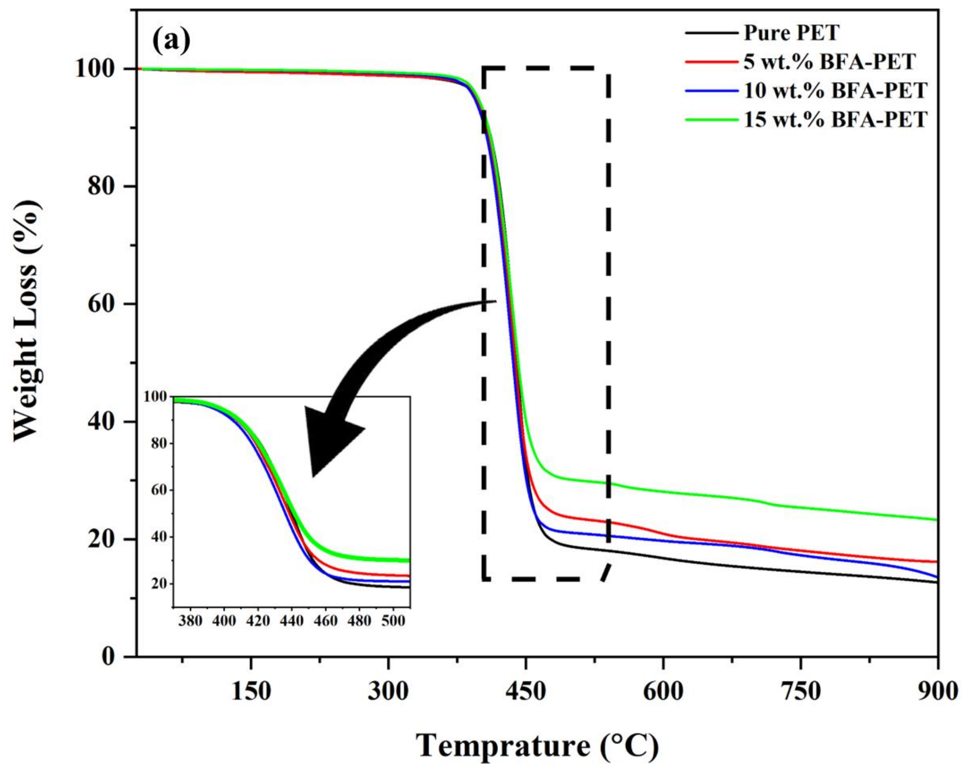

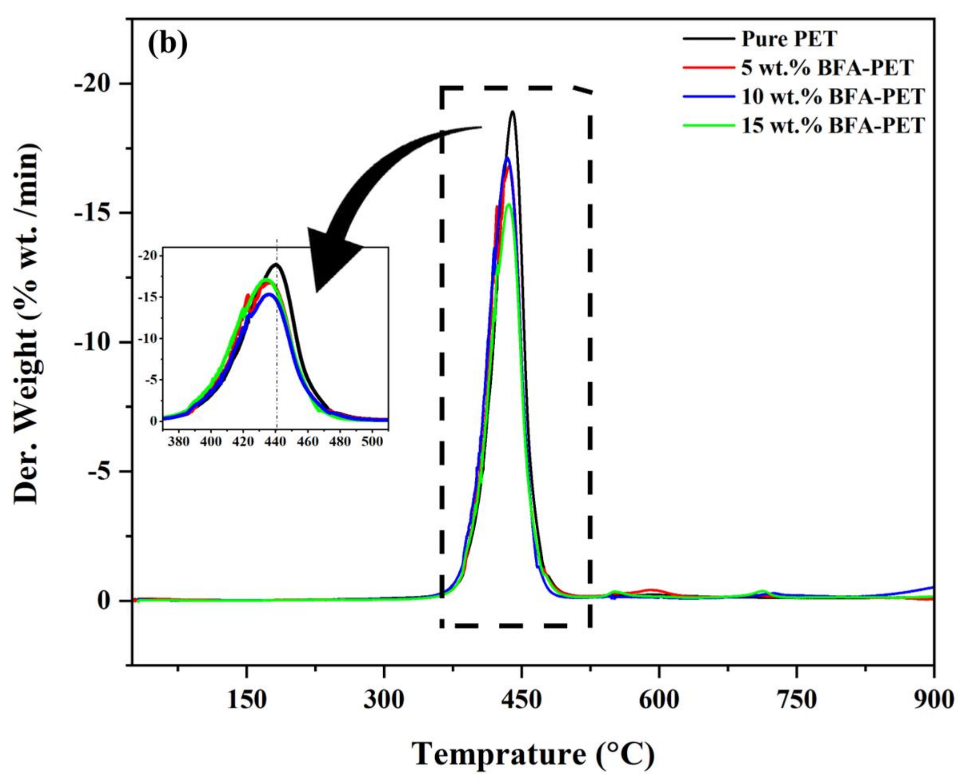

Figure 4. 8 : (a) TGA (b) DTG curves for Pure PET and its catalytic blends at 10 C/min

4.3.1 *Model Fitting Method*

Model-fitting thermo-kinetics was performed by using twelve (12) reaction models of coats Redfern method to calculate the kinetics triplets (E_a, A, and R^2) and thermodynamic parameters (ΔH, ΔG, and ΔS) for pure PET, 5 wt.% BFA-PET, 10 wt.% BFA-PET, and 15 %wt. BFA-PET are shown in Figure 4.9 (a-b), Figure 4.10 (a-c), and Table 4.3 respectively. Kinetics was done for the active pyrolysis region where the maximum weight loss occurred. Regression factor R^2 was used to select the suitable model for the mechanism for the highest R^2 value lying in range (0.90-0.99).

For pure PET, the suitable (highest) R^2 was 0.9861 at F3/2, and the activation energy (E_a) was 218.72 kJ/mol as shown in Figure 9 (a-b). These results are almost similar to the reported literature [2, 38]. For 5 wt.% BFA-PET the highest R^2 was 0.9575 for model F3/2, respectively and the corresponding activation energy (E_a) was 197.30 kJ/mol. activation energy (E_a) for 10 wt.% BFA-PET with highest R^2 value and with model F3/2 was 185.10 kJ/mol. Similarly, for 15 wt.% BFA-PET, the suitable model was F1, and the respective activation energy (E_a) was 140.55 kJ/mol. The best or most suitable model varies for the different concentrations of catalyst as the reaction mechanism is very complex and it's not always a first-order reaction [151]. The activation energy (E_a), the pre-exponential factor (A) concerned with the (E_a), and the regression factor (R^2) are described in Table. 4.2 and Figure 4. 9 (a-b).

Table 4. 2: Kinetics Triplets for Pure PET and its catalytic blends

Sample Name	Best Model	Regression Factor (R^2)	Pre-Exponent Factor (A)	Activation Energy (E_a)
Pure PET	F3/2	0.9861	3.85973E+15	218.72
5 wt.% BFA-PET	F3/2	0.9575	1.48456E+14	197.30
10 wt.% BFA-PET	F3/2	0.9872	9.96641E+12	185.10
15 wt.% BFA-PET	F1	0.9786	3953675437	140.55

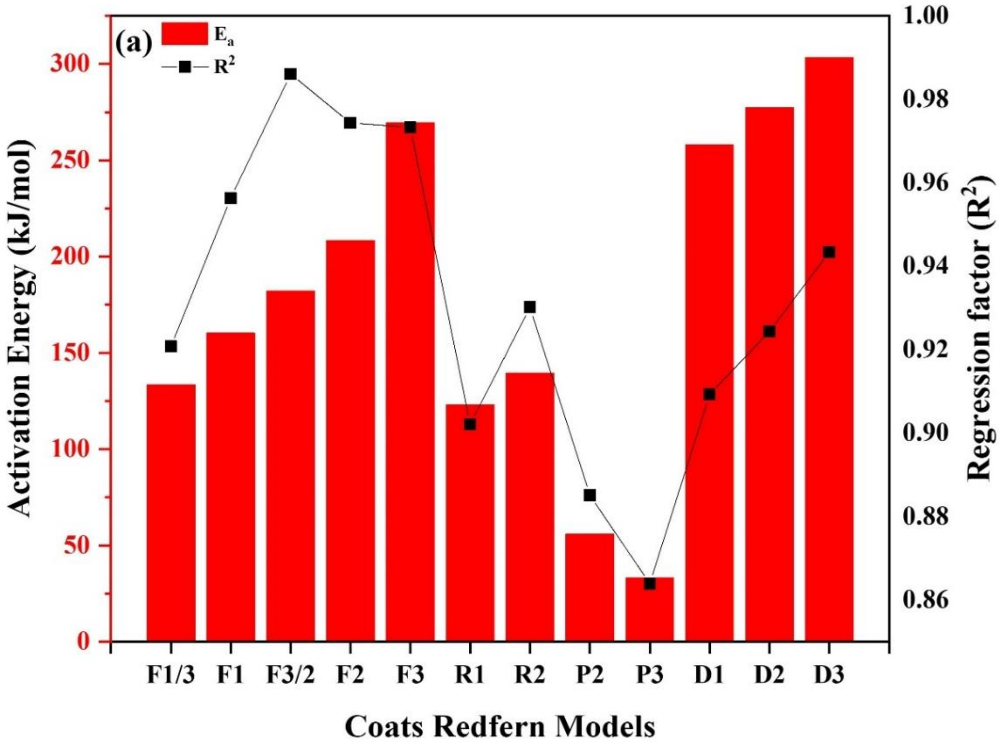

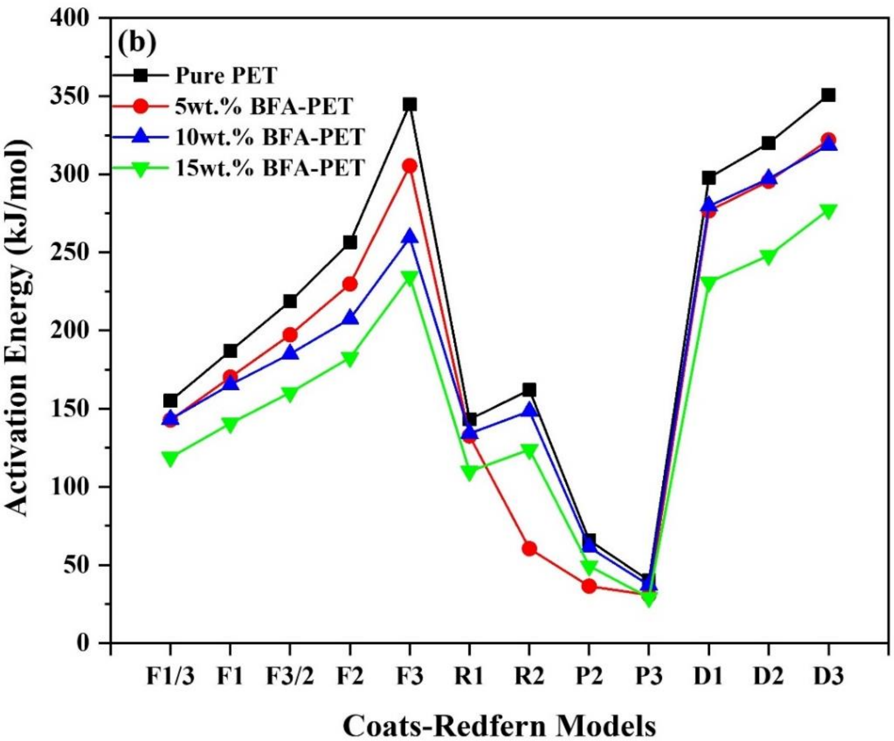

Figure 4. 9 : (a) activation energy (Ea) of Pure PET and the (b) activation energy (Ea) of the catalytic blends through 12 kinetic functions

Table 4. 3: Model Fitting Kinetic Parameters of Pure PET and its catalytic blends at 10 ºC/min

Model	Sample code	Peak Temp. Tp (°C)	Kinetics Parameters		
			E_a (kJ/mol)	R^2	A (min)$^{-1}$
F1/3	Pure PET	440.27	155.11189	0.9395	22298807990
	5 wt.% BFA-PET	436.4	142.78286	0.9442	4744679284
	10 wt.% BFA-PET	435.8	143.3403	0.9451	3231895913
	15 wt.% BFA-PET	434.4	118.85538	0.966	56319975.17
F1	Pure PET	440.27	187.0144	0.9575	9.65153E+12
	5 wt.% BFA-PET	436.4	170.09476	0.957	8.62775E+11
	10 wt.% BFA-PET	435.8	165.31316	0.9615	2.23772E+11
	15 wt.% BFA-PET	434.4	140.54941	0.9786	3953675437
F3/2	Pure PET	440.27	218.72623	0.9861	3.85973E+15
	5 wt.% BFA-PET	436.4	197.3042	0.9575	1.48456E+14
	10 wt.% BFA-PET	435.8	185.09879	0.9872	9.96641E+12
	15 wt.% BFA-PET	434.4	160.23154	0.9646	1.82018E+11
F2	Pure PET	440.27	256.5278	0.9651	4.71033E+18
	5 wt.% BFA-PET	436.4	229.75032	0.9492	6.67652E+16
	10 wt.% BFA-PET	435.8	207.61256	0.9722	7.36055E+14
	15 wt.% BFA-PET	434.4	182.71136	0.9558	1.27035E+14

F3	Pure PET	440.27	344.74875	0.9447	6.90566E+25
	5 wt.% BFA-PET	436.4	305.33244	0.9197	9.35577E+22
	10 wt.% BFA-PET	435.8	259.47032	0.9671	1.41012E+19
	15 wt.% BFA-PET	434.4	234.56138	0.9306	2.7258E+18
R1	Pure PET	440.27	143.12674	0.9283	2241885091
	5 wt.% BFA-PET	436.4	132.5335	0.9354	664270553.9
	10 wt.% BFA-PET	435.8	134.16706	0.9351	544423549.3
	15 wt.% BFA-PET	434.4	109.85234	0.9615	9526514.554
R2	Pure PET	440.27	162.0257	0.9448	41751754560
	5 wt.% BFA-PET	436.4	60.496644	0.923	3042.553894
	10 wt.% BFA-PET	435.8	148.37604	0.9469	4273513736
	15 wt.% BFA-PET	434.4	123.80203	0.9675	1525092693
P2	Pure PET	440.27	65.81087	0.9131	3390.176854
	5 wt.% BFA-PET	436.4	36.484359	0.907	591.757422
	10 wt.% BFA-PET	435.8	61.401687	0.9227	1630.088623
	15 wt.% BFA-PET	434.4	49.321586	0.9524	194.088489
P3	Pure PET	440.27	40.03891	0.893	30.67365451
	5 wt.% BFA-PET	436.4	30.798155	0.9108	28.04842145
	10 wt.% BFA-PET	435.8	37.146563	0.9066	18.44371387

	15 wt.% BFA-PET	434.4	29.144667	0.94	4.09073351
D1	Pure PET	440.27	297.76431	0.9345	4.31222E+20
	5 wt.% BFA-PET	436.4	276.61303	0.9406	1.37695E+19
	10 wt.% BFA-PET	435.8	279.70362	0.9403	2.65134E+19
	15 wt.% BFA-PET	434.4	230.91967	0.9651	9.72545E+15
D2	Pure PET	440.27	319.91078	0.9433	1.39881E+22
	5 wt.% BFA-PET	436.4	295.55878	0.9474	2.43642E+20
	10 wt.% BFA-PET	435.8	297.12147	0.9479	3.65352E+20
	15 wt.% BFA-PET	434.4	247.96766	0.9685	1.30552E+17
D3	Pure PET	440.27	350.75076	0.9534	1.48304E+22
	5 wt.% BFA-PET	436.4	321.93322	0.9551	1.48304E+22
	10 wt.% BFA-PET	435.8	318.77938	0.9573	4.94346E+21
	15 wt.% BFA-PET	434.4	277.319	0.9745	6.46775E+19

Thermodynamics analysis includes the study of enthalpy change, Gibbs free energy change and change in entropy (ΔH, ΔG, ΔS) respectively. All these kinetics models were used to calculate these factors (ΔH, ΔG, and ΔS) represented in Figure 4.10 (a-c) and Table 4.5.

Change in enthalpy (ΔH) is the amount of energy lost or gained during a chemical reaction. Positive ΔH indicates a gain of energy means an endothermic reaction [152] as represented in Figure 4.10 (a). All values of ΔH for these models were positive, which shows all are endothermic reactions. Change in enthalpy (ΔH) followed the same trend as activation energy E_a which decreases with the increase of catalyst loading up to some extent. The value of ΔH, for pure PET at 10 °C/min heating rate with suitable model F3/2, was 212.89 kJ/mol. While for 5 wt.% BFA-PET, ΔH was 191.35 kJ/mol corresponding to selected suitable model F3/2. Value of ΔH for 10 wt.% BFA-PET was 179.29 kJ/mol for the best model F3/2 and for 15 wt.% BFA-PET was 134.74 kJ/mol for the best model F1. The variance between E_a and ΔH is within a narrow range of 5-6 kJ/mol, which shows that these reactions are easily possible due to a small potential barrier [153].

The change in Gibbs free energy (ΔG) indicates the overall energy rise in the system as the reactants approach and the activated complex is formed [154] as depicted in Figure 4.10 (b). Reactions characterized by a negative ΔG indicate exergonic processes, where energy is spontaneously released, helping the reaction without external input (are spontaneous). On the other hand, reactions with a positive ΔG denote endergonic processes, demanding an external energy source to proceed (are non-spontaneous). The value of ΔG, for pure PET, 5 wt.% BFA-PET, and 10 wt.% BFA-PET for the best model F3/2 was 186.23 kJ/mol, 235.10 kJ/mol, and 187.30 kJ/mol respectively, and for 15 wt.% BFA-PET, the ΔG value for the optimal model F1 was 188.24 kJ/mol.

While the change in entropy (ΔS) is positive for some cases and some negative. The lower value of entropy shows the reaction is close to the equilibrium state. A negative ΔS indicates that the produced devolatilization products show lower disorder. On the contrary, a positive ΔS indicates an increase in entropy, reflecting a higher degree of randomness in the products. For pure PET, the change in entropy (ΔS) was (0.0381 kJ/mol. K), for 5 wt.% BFA-PET the ΔS was -0.0610 kJ/mol.K, and for 10 wt.% BFA-PET the change in entropy was -0.011 kJ/mol.K, all have the same reaction model F3/2 and for 15 wt.% BFA-PET the value of ΔS was -0.076 kJ/mol.K for the reaction model F1 shown in Figure 4.10 (c).

From Table. 4.2 and Table. 4.4 we can see a decreasing trend in the values of Change in enthalpy (ΔH) as the loading of the catalyst (BFA) increases by the difference of 5 wt.% an analogous trend was observed in the values of activation energy (E_a). The change in Gibbs free energy (ΔG) and the change in entropy (ΔS) showed an increasing and decreasing trend as the ratio of the catalytic increases at regular intervals. The best blend is 10 wt.% BFA which has lower values for ΔH, ΔG, and ΔS among the catalytic blends thus lowering it for Pure PET. A lower ΔH value signifies that less energy is required to break the material's bonds during the decomposition process. Similarly, a lower ΔG value indicates a lowered energy demand for initiating the activated complex, while a higher value of ΔG denotes decreased reaction favorability, resulting in reduced spontaneity. Also, a lower negative value for ΔS in the optimal blend indicates a slower approach to equilibrium in the reaction. As per the study utilizing the thermos-kinetic model, catalytic PET blends are found effective in upgrading sustainable fuel production and converting them into valued products.

Table 4. 4: Most suitable Thermo-kinetic results of Pure PET and its catalytic blends

Sample Name	**Suitable Reaction Model**	**ΔH (kJ/mol)**	**ΔG (kJ/mol)**	**ΔS (kJ/mol. K)**
Pure PET	F3/2	212.90	186.23	0.0381
5 wt.% BFA-PET	F3/2	191.35	235.10	-0.061
10 wt.% BFA-PET	F3/2	179.29	187.30	-0.011
15 wt.% BFA-PET	F1	134.74	188.24	-0.076

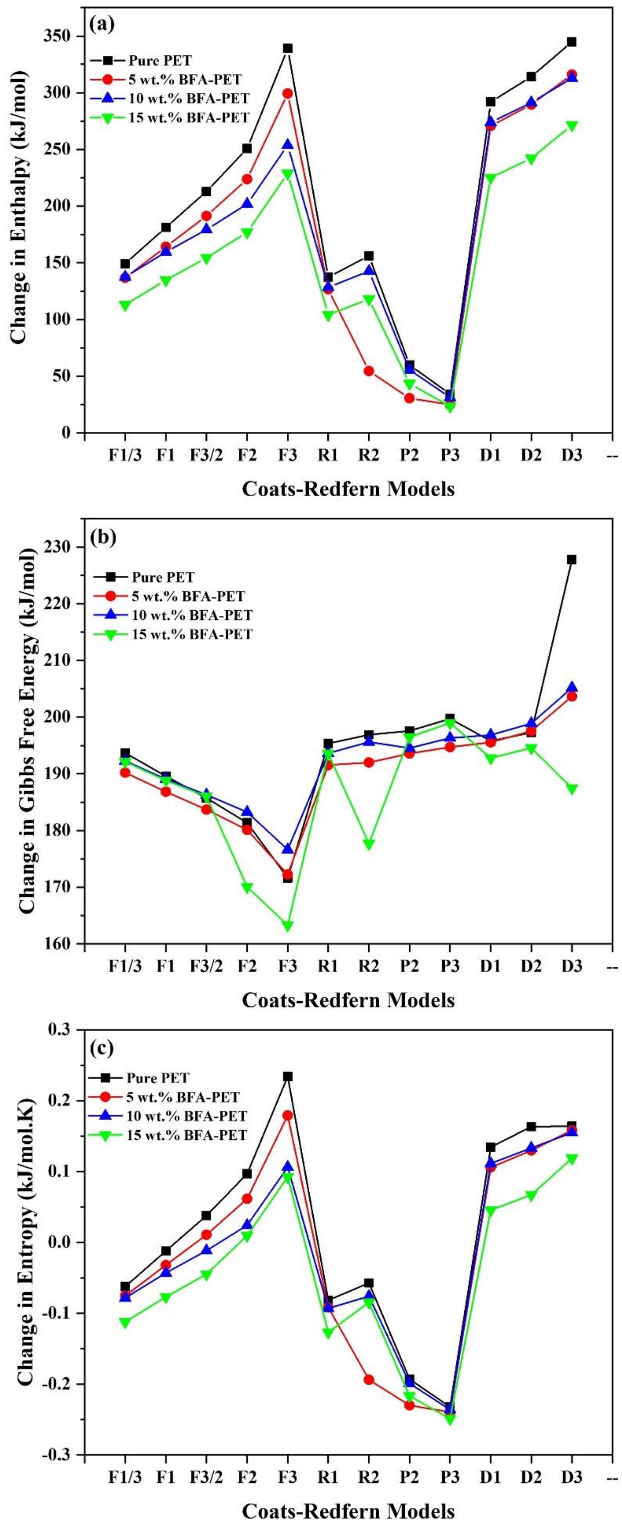

Figure 4. 10: Thermodynamic Parameters of Pure PET and its catalytic blends through 12 kinetic functions (a) ΔH (b) ΔG (c) ΔS

Table 4. 5: Model Fitting Thermodynamic parameters of Pure PET & catalytic blends at 10 ºC/min

Model	Sample Name	Thermodynamics Parameters		
		∆H	**∆G**	**∆S**
F1/3	Pure PET	149.2852698	192.8957223	-0.062227751
	5 wt.% BFA-PET	136.8282101	190.7412836	-0.07527446
	10 wt.% BFA-PET	137.5417004	192.2051765	-0.078258377
	15 wt.% BFA-PET	113.0478038	191.2332626	-0.111928563
F1	Pure PET	181.1877784	189.4286882	-0.011758953
	5 wt.% BFA-PET	164.1401066	187.0703421	-0.032015631
	10 wt.% BFA-PET	159.5058288	189.5604046	-0.04302731
	15 wt.% BFA-PET	134.7418349	188.2372357	-0.076582825
F3/2	Pure PET	212.8996089	186.2318827	0.038052176
	5 wt.% BFA-PET	191.3495497	235.1014831	-0.061087282
	10 wt.% BFA-PET	179.2914627	187.2993962	-0.011464472
	15 wt.% BFA-PET	154.4239622	185.6794692	-0.044744688
F2	Pure PET	250.7011797	182.6241714	0.097139078
	5 wt.% BFA-PET	223.7956684	179.6971284	0.061571221
	10 wt.% BFA-PET	201.8052331	184.8295496	0.024303054
	15 wt.% BFA-PET	176.9037778	170.1306091	0.009696317
F3	Pure PET	338.9221285	174.7019764	0.234325721

	5 wt.% BFA-PET	299.3777823	171.0035853	0.179238498
	10 wt.% BFA-PET	253.6629925	179.4243233	0.106282991
	15 wt.% BFA-PET	228.7537995	164.056949	0.092618571
R1	Pure PET	137.3001261	194.2955784	-0.081326806
	5 wt.% BFA-PET	126.5788472	192.1993022	-0.091620529
	10 wt.% BFA-PET	128.3597303	193.3666209	-0.093066415
	15 wt.% BFA-PET	104.0447642	192.5501177	-0.126702294
R2	Pure PET	156.1990821	196.155032	-0.057013142
	5 wt.% BFA-PET	54.54199132	193.3674479	-0.193830746
	10 wt.% BFA-PET	142.5687113	195.6098088	-0.075935716
	15 wt.% BFA-PET	117.9944554	177.0220999	-0.084502662
P2	Pure PET	59.98425222	195.0677146	-0.192750581
	5 wt.% BFA-PET	30.52970632	179.1050484	-0.207443721
	10 wt.% BFA-PET	55.5943581	194.463786	-0.19881092
	15 wt.% BFA-PET	43.51400748	194.7486143	-0.216504097
P3	Pure PET	34.21229432	196.711351	-0.23186989
	5 wt.% BFA-PET	24.84350202	191.5755605	-0.232794474
	10 wt.% BFA-PET	31.339234	196.2351711	-0.236071492
	15 wt.% BFA-PET	23.33708858	196.9865664	-0.248592727

D1	Pure PET	291.9376907	197.5426365	0.134692295
	5 wt.% BFA-PET	270.6583754	194.8273322	0.105876746
	10 wt.% BFA-PET	273.8962917	195.9909434	0.111532353
	15 wt.% BFA-PET	225.1120943	193.1454314	0.045762763
D2	Pure PET	314.0841578	199.4163211	0.163619527
	5 wt.% BFA-PET	289.6041288	196.6638892	0.129764932
	10 wt.% BFA-PET	291.3141424	198.1749477	0.133341725
	15 wt.% BFA-PET	242.1600798	195.1109707	0.067354457
D3	Pure PET	344.9241468	229.9156311	0.164105642
	5 wt.% BFA-PET	315.9785661	198.5722556	0.163924926
	10 wt.% BFA-PET	312.9720548	204.7050106	0.154999347
	15 wt.% BFA-PET	271.511422	188.4239965	0.118946109

4.3.2. Combined kinetic analysis and the master plots

Based on the linear regression R^2, (10wt% BFA-PET) was selected for the combined kinetic analysis at the varied heating rate of 10, 15 and 20 °C/min to validate the results obtained from the Coats-Redfern method. Figure 4.11 (a) shows the combined kinetics plot of (10 wt % BFA-PET) pyrolysis from the conversion range of 0.2 to 0.8. As the active pyrolysis region of (10wt % BFA-PET) occurs in the temperature range of (375 °C - 500 °C) where the maximum degradation occurs that typically lies in the conversion range of 0.2 to 0.8. The optimization procedure for these three heating rates yields the straight line. From the slopes and the intercepts, the activation energy obtained as E_a = 183.5 (±10) $kJmol^{-1}$ which is in approximation with the E_a (185.10 $kJmol^{-1}$) obtained by Coats-Redfern method for the model F3/2. Similarly, ln (cA) = 27.1 (±1.7) s^{-1}, n=1.56

(±0.12) while m = 0.6 (±0.52) were being evaluated. High linear regression (R^2= 0.9544) for (10wt % BFA-PET) pyrolysis that shows that values correspond with experimental results. However, the reaction order (n=1.56) for pyrolysis was obtained that shows the conversion rate of (10wt % BFA-PET) during the phase of maximum dissociation somehow has a noticeable impact on the reaction. In the previous studies combined kinetic analysis of almonds shells at three heating rates (10, 15, 20 °C/min) were also evaluated where the findings retrieves the different parameters like E_a = 190.6 (±9.3) $kJmol^{-1}$, ln(cA)= 32.1 (±1.8)$s^{-1}$and the n=2.33 (±0.11) while m= -1.79 (±0.11) is obtained [155]. Similarly combined kinetic analysis for the combustion and pyrolysis of the sludge obtained from the tannery are also reported in previous literature at four different heating rates (5,10, 20 and 40 °C/min) where the results dictates E_a = 165.9 (±7.8) $kJmol^{-1}$, pre exponential factor which is ln(cA)= 32.4 (±1.9)s^{-1}, n=11.25 (±0.52), m= 1.19 (±0.52) for the combustion while for the pyrolysis the findings revealed that E_a = 65.2 (±2.1) $kJmol^{-1}$, ln(cA)= 0.3 (±0.4)s^{-1}, m= -4 (±0.1), n=0.57 (±0.14) respectively [156].

Figure 4. 11 (b) shows the master plots of the (10wt% BFA-PET) pyrolysis parameters that certainly be obtained from the combined kinetic analysis when used in model function form that somehow corresponds to the F1/3, A3/2, F3/2 and A2 model functions. For solid materials degradation various mechanisms that somehow act together, and it continuously changes the order of reaction. During the process of pyrolysis with in particle random nucleation attributes to higher reaction order [157]. As the combined kinetics can be applied to the single- step reaction, its application to the various complicated processes is certainly limited [158].

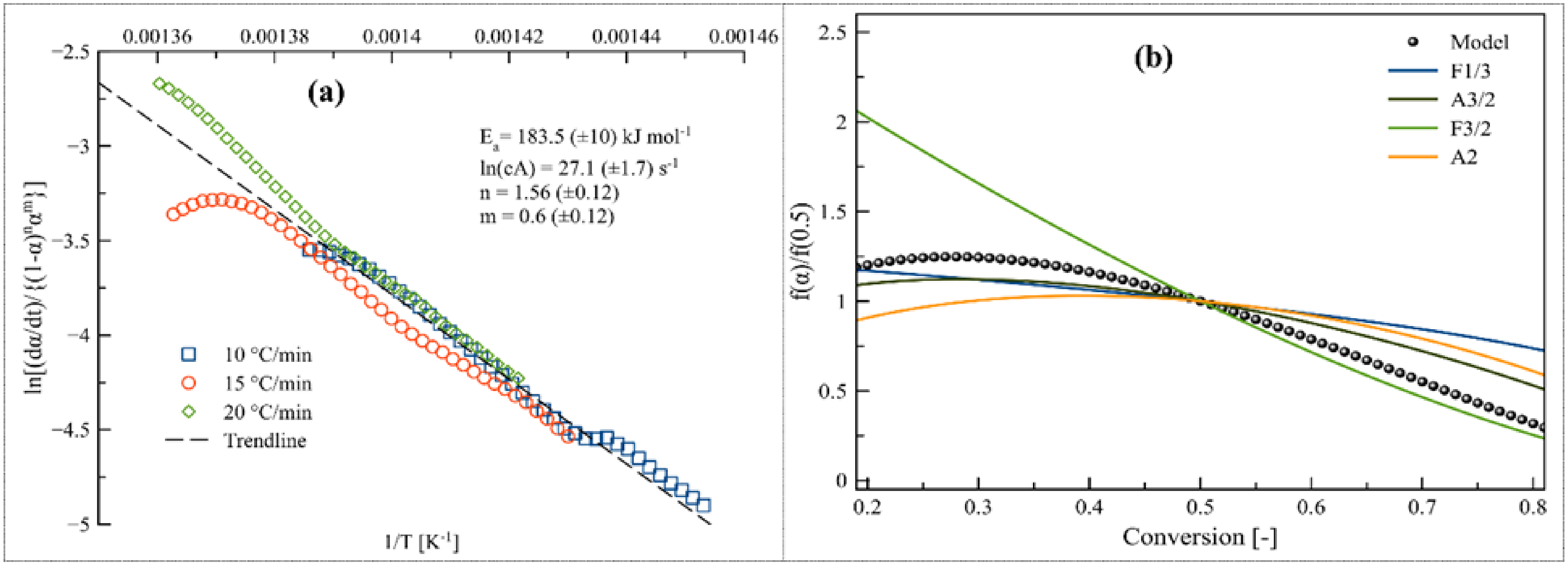

Figure 4. 11: (a) combined kinetic analysis (b) master plot for (10wt% BFA-PET

4.3.2. Model Free Method

For model free kinetics, pyrolysis of PET plastic and catalytic pyrolysis of 10 wt.% BFA-PET was performed at heating rate of 10,15 and 20 C/min. Figure 4.12 shows the DTG and conversion trend for PET sample.

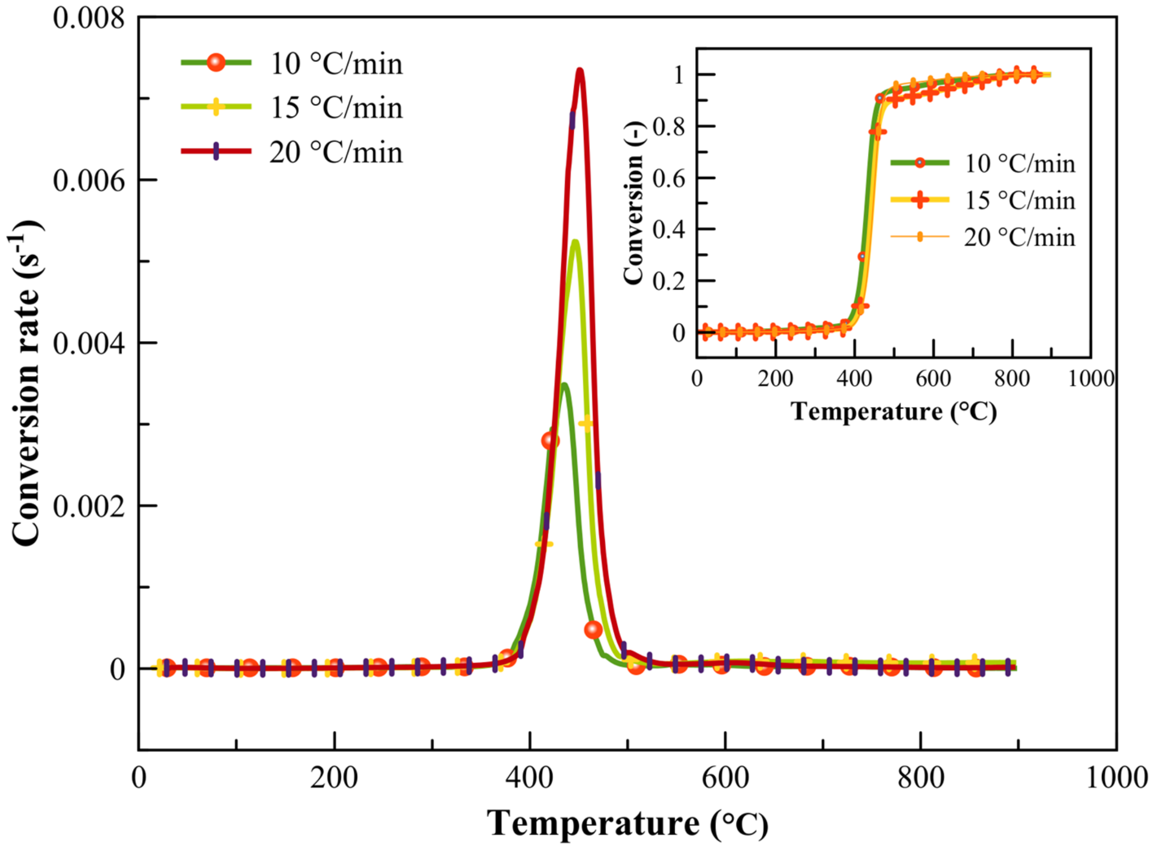

Figure 4. 12: DTG curves for PET plastic at heating rate of 10,15 and 20 °C/min

Activation energy is basically the critical kinetic parameters that surely gives an idea that how easily the plastic would disintegrate. Ea predicts that the minimum quantity of energy required for the breakage of the chemical bond and surely it is also responsible for the sensitivity and the reactivity of a reaction rate. Ea was being calculated by the linear fitting in the non-isothermal TG data using the model free iso-conversional method which include Friedman, KAS and the OFW at the four heating rates. From the corresponding slopes of each of the line the activation energies (E_a) can be calculated from the conversion degrees (α) from 0.1 to 0.8 with the corresponding linear regression (R^2). All values of the activation energies, pre-exponential factor increases with the increase of the conversion degree to about (α=0.35) and then activation energy starts decreasing with (α= 0.35 to (α=0.50). By all three iso conversional methods the linear fitting fits well with the correlation coefficient (R^2) which is 0.90 at α=0.65 for Friedman method. The iso-conversional model free plots fits well for the relation because it is the main solution.

The reason for this is that due to sharp weigh loss at the temperature range of 350°C to 550 C. the average activation energies for pure PET calculated by Friedman, KAS, OFW was found to be 265 kJ mol^{-1}, 255 kJ mol^{-1}, 253 kJ mol^{-} respectively shown in Figure 4.13. and for 10 wt.% BFA-PET, the graphs for Friedman, KAS and FWO are shown in Figure 4.14.

Enthalpy change, Gibbs free energy and Entropy as thermodynamic parameters were determined for the TSS pyrolysis at all the conversion values. The enthalpy values were positive for changing conversion degree that means that during the pyrolysis the reactions were endothermic. Gibbs free energy represents the total energy increase in the system for the activated complex development. The Gibbs free energy is in the range of 260 and 200 for all the models shown in Table 6. The entropy changes are positive for all conversion. The negative values of delta s indicate that produced substances are well organized in the molecular structure as compared to the initial substance that shows that before reaching at the thermodynamic equilibrium the substances undergo the chemically and the physically ageing process.

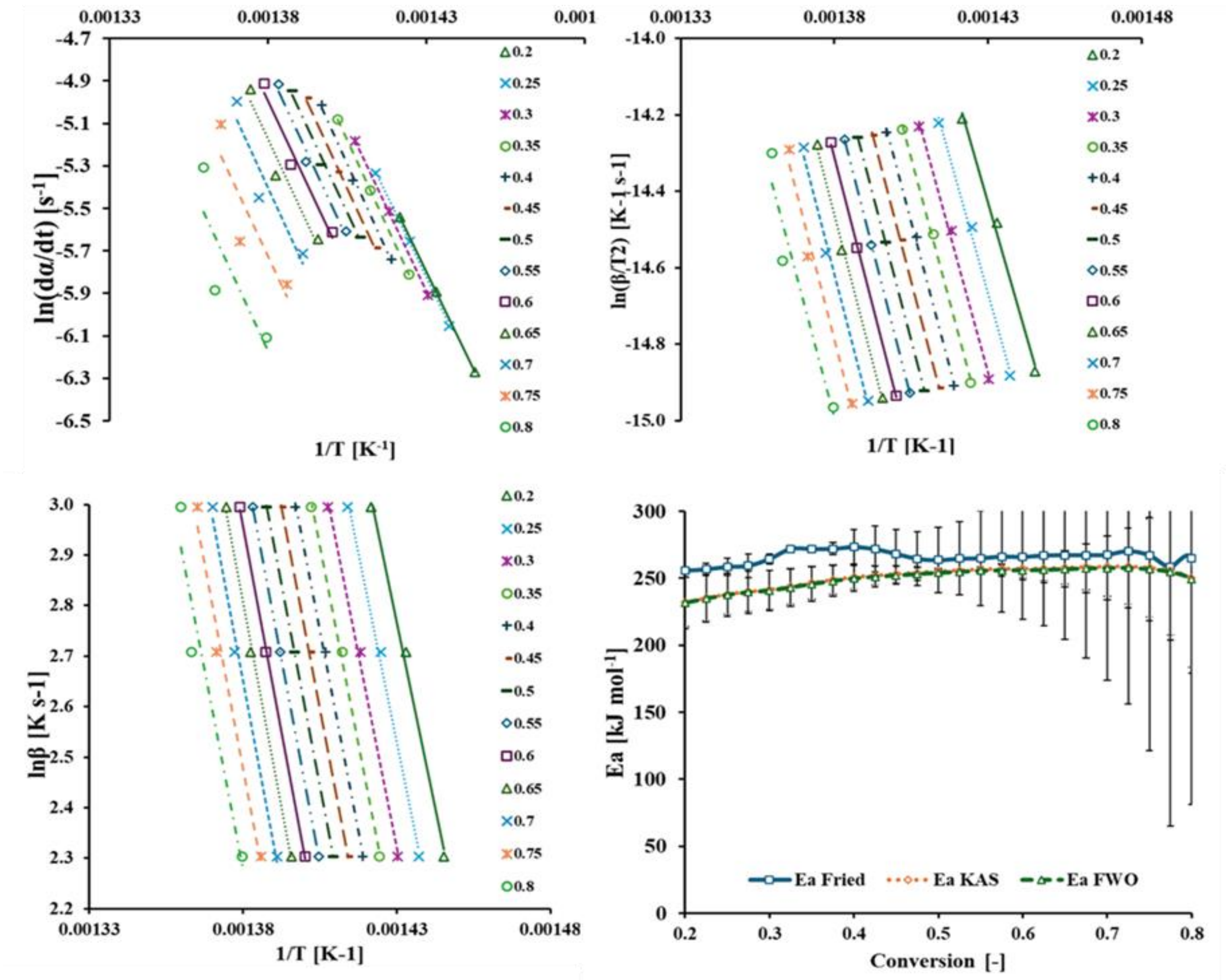

Fig 4. 13: Model free kinetics of Pure PET plastic

Table 4. 6: Model free Thermo-kinetics parameters of Pure PET

	Friedman meth		KAS method		OFW method					
α	E_a, kJ mol^{-1}	R^2	E_a, kJ mol^{-1}	R^2	E_a, kJ mol^{-1}	R^2	A, s^{-1}	ΔH, kJ mol^{-1}	ΔG, kJ mol^{-1}	ΔS, J mol^{-1} K
0.200	254.03	1.000	244.46	0.998	243.44	0.998	7.83E+15	238.87	206.12	45.68
0.225	254.48	1.000	245.66	0.998	244.61	0.998	9.62E+15	239.92	206.06	47.23
0.250	258.12	1.000	247.08	0.999	245.99	0.999	1.23E+16	241.21	205.99	49.12
0.275	258.36	1.000	248.24	0.999	247.12	0.999	1.50E+16	242.25	205.91	50.69
0.300	261.11	1.000	249.06	0.999	247.92	0.999	1.74E+16	242.96	205.85	51.77
0.325	267.57	1.000	250.36	0.999	249.17	0.999	2.16E+16	244.14	205.79	53.49
0.350	266.63	1.000	251.93	0.999	250.68	0.999	2.82E+16	245.58	205.73	55.60
0.375	265.97	1.000	253.27	0.999	251.98	0.999	3.53E+16	246.82	205.68	57.39
0.400	267.33	0.999	254.25	1.000	252.94	1.000	4.16E+16	247.72	205.67	58.66
0.425	266.93	0.999	255.04	1.000	253.71	1.000	4.73E+16	248.45	205.66	59.68
0.450	263.36	0.999	255.74	1.000	254.39	1.000	5.30E+16	249.09	205.66	60.57
0.475	260.67	0.999	256.23	1.000	254.88	1.000	5.74E+16	249.54	205.68	61.19
0.500	259.77	0.998	256.41	1.000	255.06	1.000	5.89E+16	249.70	205.71	61.36
0.525	261.01	0.997	256.80	1.000	255.46	1.000	6.27E+16	250.07	205.73	61.84
0.550	261.51	0.996	257.24	1.000	255.89	1.000	6.72E+16	250.48	205.76	62.38
0.575	261.87	0.994	257.35	1.000	256.01	1.000	6.81E+16	250.58	205.80	62.47

0.600	262.51	0.993	257.44	1.000	256.12	1.000	6.87E+16	250.67	205.85	62.52
0.625	263.57	0.991	257.70	1.000	256.38	1.000	7.13E+16	250.92	205.89	62.81
0.650	265.29	0.988	258.24	0.999	256.91	0.999	7.71E+16	251.43	205.95	63.44
0.675	266.91	0.982	258.76	0.999	257.42	0.999	8.29E+16	251.93	206.03	64.03
0.700	270.54	0.974	259.40	0.998	258.05	0.998	9.06E+16	252.55	206.13	64.75
0.725	275.54	0.963	260.35	0.997	258.98	0.997	1.04E+17	253.47	206.26	65.85
0.750	280.03	0.942	261.23	0.995	259.84	0.995	1.16E+17	254.33	206.44	66.79
0.775	284.75	0.903	262.41	0.991	260.99	0.992	1.35E+17	255.47	206.71	68.02
0.800	288.39	0.829	263.82	0.983	262.36	0.984	1.58E+17	256.83	207.12	69.34
Average	**265.85**		**255.14**		**253.85**		**6.03E+16**	**248.60**	**205.97**	**59.47**

Table 4. 7: Model free Thermo-kinetics parameters of 10%BFA-PET

α	Friedman method		KAS method		OFW method					
	E_a, kJ mol^{-1}	R^2	E_a, kJ mol^{-1}	R^2	E_a, kJ mol^{-1}	R^2	A, s^{-1}	ΔH, kJ mol^{-1}	ΔG, kJ mol^{-1}	ΔS, J mol^{-1} K
0.200	251.29	0.959	278.13	0.976	275.41	0.978	2.52E+18	270.56	203.59	93.28
0.225	253.51	0.958	274.59	0.975	272.07	0.977	1.36E+18	267.13	203.92	88.05
0.250	251.98	0.949	271.46	0.974	269.12	0.976	7.93E+17	264.10	204.20	83.45
0.275	242.84	0.928	268.02	0.971	265.87	0.974	4.39E+17	260.78	204.47	78.44
0.300	235.56	0.916	264.43	0.969	262.49	0.971	2.38E+17	257.34	204.74	73.27
0.325	235.70	0.913	260.95	0.965	259.21	0.968	1.32E+17	254.01	204.99	68.27
0.350	234.92	0.926	258.28	0.962	256.69	0.965	8.35E+16	251.45	205.20	64.43
0.375	227.13	0.931	255.26	0.961	253.85	0.964	5.00E+16	248.57	205.41	60.12
0.400	221.13	0.929	252.06	0.959	250.82	0.963	2.91E+16	245.52	205.63	55.57
0.425	218.55	0.922	249.05	0.958	247.98	0.962	1.75E+16	242.65	205.82	51.31
0.450	216.51	0.917	246.46	0.956	245.54	0.960	1.13E+16	240.19	205.98	47.65
0.475	214.19	0.908	243.62	0.954	242.86	0.958	7.01E+15	237.49	206.15	43.65
0.500	211.71	0.902	240.98	0.953	240.37	0.957	4.51E+15	234.98	206.30	39.95
0.525	208.60	0.895	238.28	0.951	237.82	0.955	2.87E+15	232.42	206.44	36.19
0.550	204.68	0.887	235.42	0.949	235.13	0.953	1.78E+15	229.71	206.59	32.20
0.575	198.75	0.873	232.61	0.946	232.48	0.951	1.12E+15	227.05	206.74	28.29

0.600	193.51	0.860	229.75	0.943	229.78	0.948	6.94E+14	224.34	206.89	24.32
0.625	186.84	0.838	226.29	0.940	226.52	0.946	3.91E+14	221.07	207.04	19.53
0.650	178.72	0.808	222.26	0.937	222.71	0.943	2.01E+14	217.25	207.22	13.98
0.675	167.41	0.759	217.90	0.933	218.59	0.939	9.74E+13	213.12	207.41	7.96
0.700	151.63	0.679	212.28	0.927	213.28	0.934	3.85E+13	207.80	207.63	0.24
0.725	126.63	0.528	204.27	0.919	205.70	0.927	1.03E+13	200.22	207.92	-10.73
0.750	90.11	0.293	192.56	0.906	194.62	0.916	1.52E+12	189.14	208.29	-26.68
0.775	41.22	0.065	173.74	0.881	176.81	0.895	7.02E+10	171.32	208.81	-52.23
0.800	-71.33	0.150	139.09	0.831	144.08	0.854	2.55E+08	138.58	209.62	-98.96
Average	**187.67**		**235.51**		**235.19**		**2.28E+17**	**229.87**	**206.28**	**32.86**

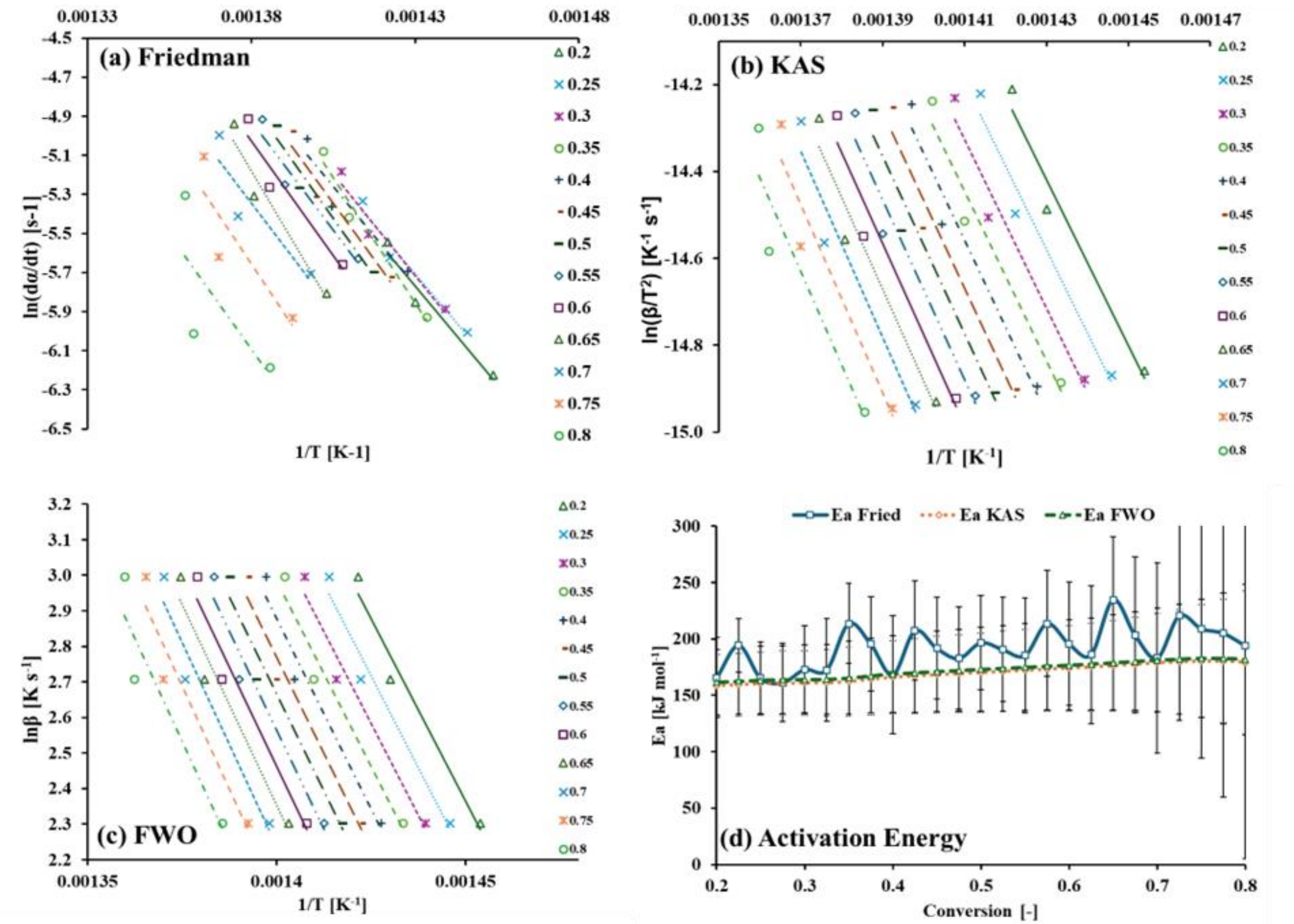

Fig 4. 14: Model free kinetics of 10 wt.% BFA-PET

4.4 Reactivity Analysis

The reactivity characteristics of both pure polyethylene terephthalate (PET) and its catalytic blends were thoroughly analyzed in this study, focusing on mean reactivity (R_m) and pyrolysis factor (P_f). Relative mean reactivity (R_m) was determined using a method established by previous research [159]. Pyrolysis factor (P_f) calculation provides an effective way to measure fuel's pyrolytic capability. P_f combines pyrolysis temperatures and devolatilization speed to compare pyrolytic performance [160]. Upon examination of the R_m, values tabulated in Figure 4.15 and Table 8, a clear ranking of sample reactivity appeared: pure PET displayed the highest reactivity, followed by 5 wt. % BFA-PET, 10 wt. % BFA-PET, and 15 wt. % BFA-PET, in descending order.

The observed trend can be explained by considering the influence of the catalyst biomass fly ash (BFA), on the reactivity of the PET samples. BFA acts as a catalyst, affecting the degradation kinetics of PET during pyrolysis. Notably, the characteristic stability examined becomes more pronounced with increasing concentrations of the catalyst. Therefore, as the concentration of BFA in the BFA-PET blends rises, the reactivity decreases gradually. This effect is clear in the reducing size of the maximum degradation peak, as well as its slight shift towards lower temperature ranges, as shown in Figure 4.13. It forms a pointed zigzag curve identical to convex mirror shape. This shows that the reactivity and the ignition of the samples are decreasing and becoming difficult as the ratio of the catalyst increases. Furthermore, the pyrolysis factor (P_f), which performs as an indicator of the overall pyrolysis behavior, shows a similar trend to that of mean reactivity. The pyrolysis factor holds several parameters including average degradation rate, peak degradation characteristics (such as temperature and rate), as well as the onset and offset temperatures of the active pyrolysis stage. The observed decrease in the pyrolysis factor (P_f) with increasing BFA concentration can be attributed to the differential devolatilization rates between plastic and the BFA catalyst. Plastic materials typically show higher devolatilization rates compared to their catalytic blends. Therefore, as the concentration of BFA increases, the overall devolatilization rates decrease, resulting in a decrease in the (P_f). The values of P_f showed that it was higher for Pure PET and 5 wt.% BFA-PET and were more reactive fuels than bituminous coal reported elsewhere [161] and will have better pyrolysis performance because of plastic's higher devolatilization rates when compared to coal. This analysis provides further validation of our selection of the optimum catalytic blend 10wt.% BFA-PET for the pyrolysis process consequently with the thermo-kinetic study because of the lower T_p and better maximum weight loss rate among the catalytic blends, although it couldn't establish a significant insight about the optimum blend rather it provided a better understanding of pure PET and its catalytic blends, as the product distribution is discuss.

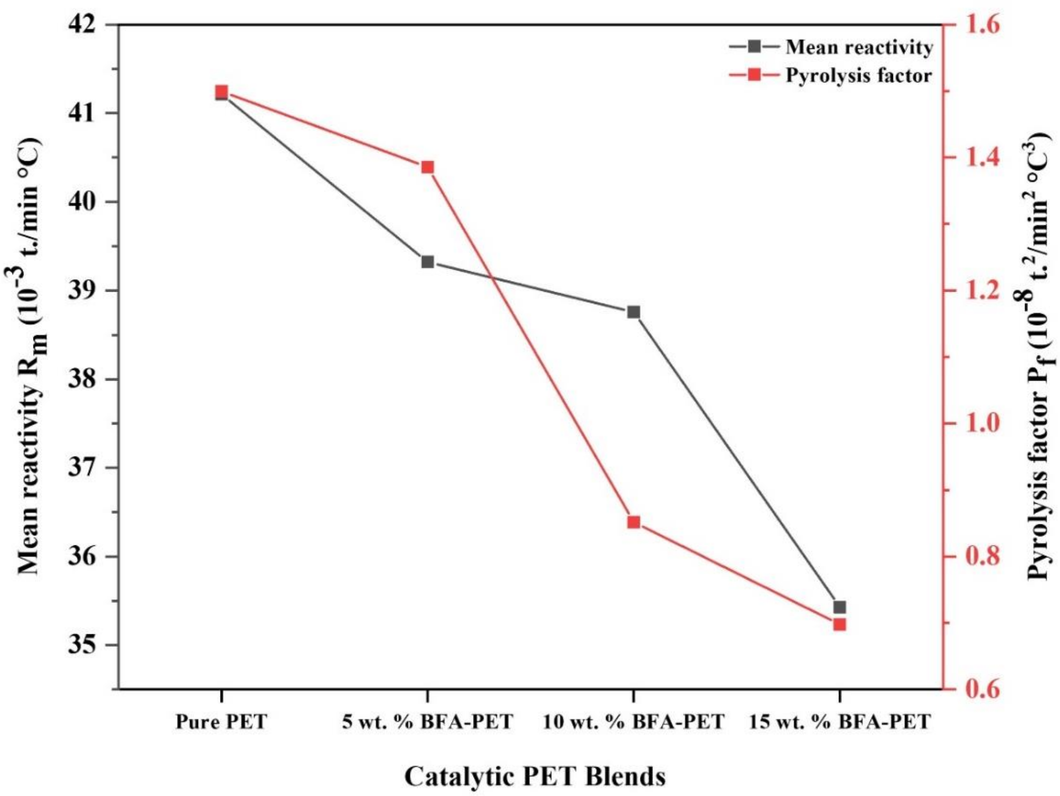

Figure 4. 15: Reactivity analysis of pure PET & its catalytic blends

Table 4. 8: Reactivity analysis of pure PET & its catalytic blends

Sample Name	T_s (°C)	T_p (°C)	T_f (°C)	$(DTG)_{max}$ (%wt./min)	$(DTG)_{avg}$ (%wt./min)	R_m (%wt./min °C)	P_f (%wt.^{2}/min^2 °C^3)
Pure PET	375	440.26	500	-18.91	-0.0505	41.21376	1.4995
5 wt.% BFA-PET	370	436.00	500	-16.75	-0.0494	39.3217	1.3857
10 wt.% BFA-PET	350	435.8	500	-16.89	-0.0309	38.7563	0.8517
15 wt.% BFA-PET	350	434.4	500	-15.39	-0.0277	35.4281	0.6979

Chapter 5: Conclusions And Future Recommendation

5.1 Conclusions

This study investigates the critical issue of plastic waste, particularly focusing on polyethylene terephthalate (PET), which poses significant challenges to both environmental sustainability and human health. The catalyst biomass fly ash (BFA) has been characterized through FTIR, XRD, and TGA. The presence of functional groups such as Sulphates, Si-O, and carboxylic acid are observed, also XRD explains the crystallinity of the structure, as BFA contains different diffraction peaks of various compounds and the major peaks represented are SiO_2, Ca, K_2O, Fe, and Al_2O_3 and about 5-6% weight loss is analyzed which clarifies the thermal stability of the BFA catalyst, all the catalyst characterizations are interrelated to each other. The characterization of Pure PET was conducted via GCV, FTIR, RAMAN, and XRD, thus providing an understanding of the high heating value, functional groups, and crystalline structures. The pyrolysis of polyethylene terephthalate (PET) was performed in the presence and absence of biomass fly ash (BFA) as a catalyst in Thermogravimetric Analysis (TGA) at a heating rate of 5,10,15, and 20 ºC/min which sheds light on a potential solution to address this alarming concern. Pure PET and the blends of PET with the catalyst BFA at a catalyst: mass ratios of 5 10, and 15 wt.% of B FA-PET were prepared. The TGA/DTG curves show that decompositions occur in three stages with the active stage lying in b 375-500 ºC where larger molecules thermally degrade into smaller molecules and the overall weight loss (WL%) of around 87 percent is calculated at this heating rate.

Catalytic pyrolysis was performed with 5 wt.% BFA-PET, 10 wt.% BFA-PET and 15 wt.% BFA-PET the active stage lies in the temperature range of 360-500 ºC with the overall weight loss (WL) existing in the range of around 76-87 percent calculated at this heating rate, thus showing that the catalyst BFA had a positive impact on the pyrolysis of PET, and the catalytic blend 10 wt.% BFA-PET remains impressive among the others. A model fitting technique is used to investigate the kinetics study by applying the twelve reaction mechanisms of the coats-Redfern method and model free technique by using three methods of Friedman, KAS, and FWO. The activation energy (E_a) for the pyrolysis of Pure PET was found to be in the range of 200-220 KJ/mol, while the introduction of BFA as a catalyst led to a reduction in activation energies, ranging from 140-200 KJ/mol. This trend was uniform across measurements of change in enthalpy (ΔH), change in Gibbs free energy (ΔG), and change in entropy (ΔS). The results specified that biomass fly ash (BFA) as a catalyst considerably affected the pyrolysis performance of PET by particularly influencing the primary and secondary reactions throughout the process.

The reactivity analysis confirms our selection of the optimum catalytic blend 10 wt.% BFA-PET for the pyrolysis process and provided a better understanding of pure PET and its catalytic blend performance as a fuel. The comparison of above mentioned two stats shows that catalytic pyrolysis with 10 wt.% is the best option because with produces more volatiles and reduced activation energy E_a along with a better regression factor which causes more chances of oil production through pyrolysis.

5.2 Recommendations

Based on thermos-kinetics analysis, future research should focus on pyrolysis and catalytic pyrolysis in reactor systems such as fixed bed reactors, and fluidized bed reactor, to identify the products (char, oil and gases). Investigating reaction mechanisms through experiments will further explain the role of catalyst. Assessing various catalysts, like metal oxides and zeolites will improve the pyrolysis process, and it can be performed in future. Thermo-kinetic modeling will help in reactor design and scale up, while evaluating reactor performance under various conditions will identify optimal parameters. Exploring co-pyrolysis with other waste can improve the product yield. Life cycle assessment and techno-economic assessment will ensure sustainability and economic feasibility.

In the future, these findings specify the probability of catalytic pyrolysis of Pure PET with a commercially viable catalyst like BFA for energy recovery. These also indicate the development of efficient waste plastics treatment technologies in the form of a pyrolysis reactor system. However, further sustainability and cost-benefit analyses are required to enhance their feasibility.

REFERENCES

1. Vijayakumar, A. and J. Sebastian. *Pyrolysis process to produce fuel from different types of plastic–a review*. in *IOP conference series: Materials Science and Engineering*. 2018. IOP Publishing.

2. Mishra, R., H.C. Ong, and C.-W. Lin, *Progress on co-processing of biomass and plastic waste for hydrogen production.* Energy Conversion and Management, 2023. **284**: p. 116983.

3. Peng, Y., et al., *A review on catalytic pyrolysis of plastic wastes to high-value products.* Energy Conversion and Management, 2022. **254**: p. 115243.

4. Sardon, H. and A.P. Dove, *Plastics recycling with a difference.* Science, 2018. **360**(6387): p. 380-381.

5. Sivagami, K., et al., *Conversion of plastic waste into fuel oil using zeolite catalysts in a bench-scale pyrolysis reactor.* RSC Advances, 2022. **12**(13): p. 7612-7620.

6. Kumagai, S., et al., *Catalytic Pyrolysis of Poly(ethylene terephthalate) in the Presence of Metal Oxides for Aromatic Hydrocarbon Recovery Using Tandem μ-Reactor-GC/MS.* Energy & Fuels, 2020. **34**(2): p. 2492-2500.

7. Solis, M. and S. Silveira, *Technologies for chemical recycling of household plastics – A technical review and TRL assessment.* Waste Management, 2020. **105**: p. 128-138.

8. Li, C., et al., *Catalytic pyrolysis of polyethylene terephthalate over zeolite catalyst: Characteristics of coke and the products.* International Journal of Energy Research, 2021. **45**(13): p. 19028-19042.

9. Panahi, L., M. Gholizadeh, and R. Hajimohammadi, *Investigating the degradability of polyethylene using starch, oxo-material, and polylactic acid under the different environmental conditions.* Asia-Pacific Journal of Chemical Engineering, 2020. **15**(1): p. e2402.

10. Khalid, U., et al., *Experimental and numerical techniques to evaluate coal/biomass fly ash blend characteristics and potentials.* Science of The Total Environment, 2024. **912**: p. 169218.

11. Diaz-Silvarrey, L.S., A. McMahon, and A.N. Phan, *Benzoic acid recovery via waste poly(ethylene terephthalate) (PET) catalytic pyrolysis using sulphated zirconia catalyst.* Journal of Analytical and Applied Pyrolysis, 2018. **134**: p. 621-631.

12. Wang, L., et al., *Glycolysis of PET Using 1,3-Dimethylimidazolium-2-Carboxylate as an Organocatalyst.* ACS Sustainable Chemistry & Engineering, 2020. **8**(35): p. 13362-13368.

13. Genta, M., et al., *Supercritical methanol for polyethylene terephthalate depolymerization: Observation using simulator.* Waste Management, 2007. **27**(9): p. 1167-1177.

14. Qiu, B., et al., *Application of industrial solid wastes in catalytic pyrolysis.* Asia-Pacific Journal of Chemical Engineering, 2018. **13**(1): p. e2150.

15. Benedetti, M., et al., *Pyrolysis of WEEE plastics using catalysts produced from fly ash of coal gasification.* Frontiers of Environmental Science & Engineering, 2017. **11**(5): p. 11.

16. Nalluri, P., P. Prem Kumar, and M.R. Ch Sastry, *Experimental study on catalytic pyrolysis of plastic waste using low cost catalyst.* Materials Today: Proceedings, 2021. **45**: p. 7216-7221.

17. Lai, J., et al., *Catalytic pyrolysis of linear low-density polyethylene using recycled coal ash: Kinetic study and environmental evaluation.* Korean Journal of Chemical Engineering, 2021. **38**(11): p. 2235-2246.

18. Lim, S. and Y.-M.J.A.C.f.E. Kim, *Catalytic pyrolysis of waste polyethylene terephthalate over waste concrete.* 2019. **30**(6): p. 707-711.

19. Kubowicz, S. and A.M. Booth, *Biodegradability of plastics: challenges and misconceptions*. 2017, ACS Publications.

20. Ragaert, K., L. Delva, and K.J.W.m. Van Geem, *Mechanical and chemical recycling of solid plastic waste.* 2017. **69**: p. 24-58.

21. Armenise, S., et al., *Plastic waste recycling via pyrolysis: A bibliometric survey and literature review.* 2021. **158**: p. 105265.

22. Liu, J., et al., *Catalytic Pyrolysis of Poly(ethylene terephthalate) with Molybdenum Oxides for the Production of Olefins and Terephthalic Acid.* Industrial & Engineering Chemistry Research, 2022. **61**(15): p. 5054-5065.

23. Shakya, B.D., *Pyrolysis of waste plastics to generate useful fuel containing hydrogen using a solar thermochemical process*. 2007, University of Sydney.

24. Bartolome, L., et al., *Recent developments in the chemical recycling of PET.* Material recycling-trends and perspectives, 2012. **406**: p. 576-596.

25. Hassan, H., J.K. Lim, and B.H. Hameed, *Recent progress on biomass co-pyrolysis conversion into high-quality bio-oil.* Bioresour Technol, 2016. **221**: p. 645-655.

26. Christopher, F.J., et al., *Assessment of product distribution of plastic waste from catalytic pyrolysis process.* Fuel, 2023. **332**: p. 126168.

27. Al-Salem, S., et al., *A review on thermal and catalytic pyrolysis of plastic solid waste (PSW).* 2017. **197**: p. 177-198.

28. Miandad, R., et al., *Catalytic Pyrolysis of Plastic Waste: Moving Toward Pyrolysis Based Biorefineries.* Frontiers in Energy Research, 2019. **7**.

29. Evode, N., et al., *Plastic waste and its management strategies for environmental sustainability.* 2021. **4**: p. 100142.

30. Frienkel, S.J.c., *Plastics: A Toxic Love Story. New York: Henry Holt, 2011.* 2020. **6**: p. 22.

31. Panda, A.K., et al., *Thermolysis of waste plastics to liquid fuel: A suitable method for plastic waste management and manufacture of value added products—A world prospective.* 2010. **14**(1): p. 233-248.

32. Tan, A.F., et al., *Reimagining plastics waste as energy solutions: challenges and opportunities.* 2024. **2**(1): p. 2.

33. Wang, C., et al., *Critical review of global plastics stock and flow data.* 2021. **25**(5): p. 1300-1317.

34. Patel, D., et al., *Rogue one: A plastic story.* 2022. **177**: p. 113509.

35. Karayannidis, G.P., D.S.J.M.M. Achilias, and Engineering, *Chemical recycling of poly (ethylene terephthalate).* 2007. **292**(2): p. 128-146.

36. Sousa, A.F., et al., *Recommendations for replacing PET on packaging, fiber, and film materials with biobased counterparts.* 2021. **23**(22): p. 8795-8820.

37. Youssef, A.M. and S.M.J.C.p. El-Sayed, *Bionanocomposites materials for food packaging applications: Concepts and future outlook.* 2018. **193**: p. 19-27.

38. Das, P. and P.J.T.A. Tiwari, *Thermal degradation study of waste polyethylene terephthalate (PET) under inert and oxidative environments.* 2019. **679**: p. 178340.

39. Li, M. and S.J.A.C. Zhang, *Tandem chemical depolymerization and photoreforming of waste pet plastic to high-value-added chemicals.* 2024. **14**(5): p. 2949-2958.

40. Van Roijen, E. and S.A.J.J.o.C.P. Miller, *Towards the production of net-negative greenhouse gas emission bio-based plastics from 2nd and 3rd generation feedstocks.* 2024. **445**: p. 141203.

41. Kumar, S., *Conversion of waste high-density polyethylene into liquid fuels*. 2014.

42. Cousins, K., *Polymers in building and construction*. 2002: iSmithers Rapra Publishing.

43. Sangam, H.P., *Performance of HDPE geomembrane liners in landfill applications*. 2001.

44. Gandhi, N., et al., *Life cycle assessment of recycling high-density polyethylene plastic waste.* 2021. **9**(8): p. 1463-1483.

45. Gilbert, M. and S.J.B.s.P.M. Patrick, *Poly (vinyl chloride).* 2017: p. 329-388.

46. Mersiowsky, I.J.P.i.p.s., *Long-term fate of PVC products and their additives in landfills.* 2002. **27**(10): p. 2227-2277.

47. Ait-Touchente, Z., et al., *Recent advances in polyvinyl chloride (PVC) recycling.* 2024. **35**(1): p. e6228.

48. Miller, L., et al., *Challenges and alternatives to plastics recycling in the automotive sector.* 2014. **7**(8): p. 5883-5902.

49. Datta, D., G.J.P.S. Halder, and E. Protection, *Enhancing degradability of plastic waste by dispersing starch into low density polyethylene matrix.* 2018. **114**: p. 143-152.

50. Sathish, H.J.P.i.f.p., *PLASTICS BASED PACKAGE FORMS & SPECIALITY PACKAGING FOR FOOD PRODUCTS.*

51. Tahir, F., S. Sbahieh, and S.G.J.M.T.P. Al-Ghamdi, *Environmental impacts of using recycled plastics in concrete.* 2022. **62**: p. 4013-4017.

52. Kausar, A., et al., *Effectiveness of polystyrene/carbon nanotube composite in electromagnetic interference shielding materials: a review.* 2017. **56**(10): p. 1027-1042.

53. Schlummer, M., et al., *Recycling of flame retarded waste polystyrene foams (EPS and XPS) to PS granules free of hexabromocyclododecane (HBCDD).* 2017. **2**(5).

54. Lin, T.A., et al., *Polypropylene/thermoplastic polyurethane blends: Mechanical characterizations, recyclability and sustainable development of thermoplastic materials.* 2020. **9**(3): p. 5304-5312.

55. Maddah, H.A.J.A.J.P.S., *Polypropylene as a promising plastic: A review.* 2016. **6**(1): p. 1-11.

56. Gopinath, K.P., et al., *A critical review on the influence of energy, environmental and economic factors on various processes used to handle and recycle plastic wastes: Development of a comprehensive index.* 2020. **274**: p. 123031.

57. Huang, S., et al., *Plastic waste management strategies and their environmental aspects: A scientometric analysis and comprehensive review.* 2022. **19**(8): p. 4556.

58. Unnisa, S.A., M.J.R. Hassanpour, and s.e. reviews, *Development circumstances of four recycling industries (used motor oil, acidic sludge, plastic wastes and blown bitumen) in the world.* 2017. **72**: p. 605-624.

59. Soong, Y.-H.V., M.J. Sobkowicz, and D.J.B. Xie, *Recent advances in biological recycling of polyethylene terephthalate (PET) plastic wastes.* 2022. **9**(3): p. 98.

60. Fu, Q., et al., *The impact of different low-pressure plasma types on the physical, chemical and biological surface properties of PEEK.* 2021. **37**(1): p. e15-e22.

61. Alao, M.A., O.M. Popoola, and T.R.J.C.E.S. Ayodele, *Waste-to-energy nexus: An overview of technologies and implementation for sustainable development.* 2022. **3**: p. 100034.

62. Pal, S., S.J.R.E.I.B. Pandey, Solar,, and O. Technologies, *Recycling of Plastic Waste into Transportation Fuels and Value-Added Products.* 2024: p. 97-122.

63. Kim, H.-H. and B.-J.J.C.E.J. Kim, *Thermal degradation behavior and decomposition mechanism of thermoset plastic for carbon fiber-reinforced plastic recycling under varied process conditions.* 2024: p. 152407.

64. Suriapparao, D.V., R.J.P.S. Tejasvi, and E. Protection, *A review on role of process parameters on pyrolysis of biomass and plastics: present scope and future opportunities in conventional and microwave-assisted pyrolysis technologies.* 2022. **162**: p. 435-462.

65. Safdari, M.-S., et al., *Heating rate and temperature effects on pyrolysis products from live wildland fuels.* 2019. **242**: p. 295-304.

66. Sakthipriya, N.J.S.o.T.T.E., *Plastic waste management: A road map to achieve circular economy and recent innovations in pyrolysis.* 2022. **809**: p. 151160.

67. Wood, D.A., et al., *Gas-to-liquids (GTL): A review of an industry offering several routes for monetizing natural gas.* 2012. **9**: p. 196-208.

68. Rex, P., L.J.I.J.o.E.S. Miranda, and Technology, *Co-pyrolysis of real-world plastics polystyrene, polypropylene and low-density polyethylene, its thermal behaviour and kinetic studies.* 2024. **21**(4): p. 4279-4294.

69. Pal, S.K., V.S. Prabhudesai, and R.J.J.o.E.M. Vinu, *Catalytic upcycling of post-consumer multilayered plastic packaging wastes for the selective production of monoaromatic hydrocarbons.* 2024. **351**: p. 119630.

70. Clinton, M., R.K.J.G. Rowe, and Geomembranes, *Long-term durability of two HDPE geomembranes formulated with polyethylene of raised temperature resistance (PE-RT).* 2024. **52**(3): p. 304-318.

71. Kumar, S., et al., *Utilization of plastic wastes for sustainable environmental management: a review.* 2021. **14**(19): p. 3985-4006.

72. Demirbas, A.J.J.o.A. and A. Pyrolysis, *Pyrolysis of municipal plastic wastes for recovery of gasoline-range hydrocarbons.* 2004. **72**(1): p. 97-102.

73. Du, S., et al., *Conversion of Polyethylene Terephthalate Based Waste Carpet to Benzene-Rich Oils through Thermal, Catalytic, and Catalytic Steam Pyrolysis.* ACS Sustainable Chemistry & Engineering, 2016. **4**(5): p. 2852-2860.

74. Obuchi, E., M. Suyama, and K. Nakano, *Decomposition of mixed plastics consisting of polypropylene and polyethylene terephthalate into oils over titania/silica catalysts.* Journal of Material Cycles and Waste Management, 2001. **3**(2): p. 88-92.

75. Miandad, R., et al., *Plastic waste to liquid oil through catalytic pyrolysis using natural and synthetic zeolite catalysts.* Waste Management, 2017. **69**: p. 66-78.

76. Cardona, S.C. and A.J.A.C.B.E. Corma, *Tertiary recycling of polypropylene by catalytic cracking in a semibatch stirred reactor: Use of spent equilibrium FCC commercial catalyst.* 2000. **25**(2-3): p. 151-162.

77. Mishra, R., et al., *Recent research advancements in catalytic pyrolysis of plastic waste.* 2023. **11**(6): p. 2033-2049.

78. Vijayakumar, A. and J. Sebastian, *Pyrolysis process to produce fuel from different types of plastic – a review.* IOP Conference Series: Materials Science and Engineering, 2018. **396**(1): p. 012062.

79. Bellussi, G., et al., *Oligomerization of olefins from Light Cracking Naphtha over zeolite-based catalyst for the production of high quality diesel fuel.* 2012. **164**: p. 127-134.

80. Uemichi, Y., et al., *Gas chromatographic determination of the products of degradation of polyethylene over a silica—alumina catalyst.* 1983. **259**: p. 69-77.

81. Uemichi, Y., et al., *Deactivation behaviors of zeolite and silica− alumina catalysts in the degradation of polyethylene.* 1998. **37**(3): p. 867-872.

82. Lin, R. and R.L.J.J.o.a.p.s. White, *Effects of catalyst acidity and HZSM-5 channel volume on the catalytic cracking of poly (ethylene).* 1995. **58**(7): p. 1151-1159.

83. Lin, Y.-H. and M.-H.J.A.C.A.G. Yang, *Catalytic pyrolysis of polyolefin waste into valuable hydrocarbons over reused catalyst from refinery FCC units.* 2007. **328**(2): p. 132-139.

84. Lin, Y.-H., et al., *Catalytic degradation of high density polyethylene over mesoporous and microporous catalysts in a fluidised-bed reactor.* 2004. **86**(1): p. 121-128.

85. Manos, G., et al., *Catalytic degradation of high-density polyethylene over different zeolitic structures.* 2000. **39**(5): p. 1198-1202.

86. Aydemir, B., N. Aslı Sezgi, and T.J.A.j. Doğu, *Synthesis of TPA impregnated SBA-15 catalysts and their performance in polyethylene degradation reaction.* 2012. **58**(8): p. 2466-2472.

87. Lim, S. and Y.-M. Kim, *Catalytic pyrolysis of waste polyethylene terephthalate over waste concrete.* 공업화학, 2019. **30**(6): p. 707-711.

88. López, A., et al., *Catalytic pyrolysis of plastic wastes with two different types of catalysts: ZSM-5 zeolite and Red Mud.* 2011. **104**(3-4): p. 211-219.

89. López, A., et al., *Deactivation and regeneration of ZSM-5 zeolite in catalytic pyrolysis of plastic wastes.* 2011. **31**(8): p. 1852-1858.

90. Akubo, K., M.A. Nahil, and P.T.J.J.o.t.e.i. Williams, *Aromatic fuel oils produced from the pyrolysis-catalysis of polyethylene plastic with metal-impregnated zeolite catalysts.* 2019. **92**(1): p. 195-202.

91. Onwudili, J.A., C. Muhammad, and P.T.J.J.o.t.E.I. Williams, *Influence of catalyst bed temperature and properties of zeolite catalysts on pyrolysis-catalysis of a simulated mixed plastics sample for the production of upgraded fuels and chemicals.* 2019. **92**(5): p. 1337-1347.

92. Kassargy, C., et al., *Gasoline and diesel-like fuel production by continuous catalytic pyrolysis of waste polyethylene and polypropylene mixtures over USY zeolite.* 2018. **224**: p. 764-773.

93. Xu, D., et al., *Performances of syngas production and deposited coke regulation during co-gasification of biomass and plastic wastes over Ni/γ-Al2O3 catalyst: Role of biomass to plastic ratio in feedstock.* 2020. **392**: p. 123728.

94. Yao, D., et al., *Co-production of hydrogen and carbon nanotubes from catalytic pyrolysis of waste plastics on Ni-Fe bimetallic catalyst.* 2017. **148**: p. 692-700.

95. Aboul-Enein, A.A., A.E.J.P.D. Awadallah, and Stability, *Production of nanostructure carbon materials via non-oxidative thermal degradation of real polypropylene waste plastic using La2O3 supported Ni and Ni–Cu catalysts.* 2019. **167**: p. 157-169.

96. Maqsood, T., et al., *Pyrolysis of plastic species: A review of resources and products.* 2021. **159**: p. 105295.

97. Kunwar, B., et al., *Plastics to fuel: a review.* 2016. **54**: p. 421-428.

98. Williams, P.T., E.J.R. Slaney, Conservation, and Recycling, *Analysis of products from the pyrolysis and liquefaction of single plastics and waste plastic mixtures.* 2007. **51**(4): p. 754-769.

99. Ghodke, P. and R.N.J.F. Mandapati, *Investigation of particle level kinetic modeling for babul wood pyrolysis.* 2019. **236**: p. 1008-1017.

100. Mandapati, R.N. and P.K.J.F. Ghodke, *Kinetics of pyrolysis of cotton stalk using model-fitting and model-free methods.* 2021. **303**: p. 121285.

101. Anca-Couce, A.J.P.i.E. and C. Science, *Reaction mechanisms and multi-scale modelling of lignocellulosic biomass pyrolysis.* 2016. **53**: p. 41-79.

102. Vyazovkin, S.J.J.o.C.C., *Modification of the integral isoconversional method to account for variation in the activation energy.* 2001. **22**(2): p. 178-183.

103. Flynn, J.H. and L.A.J.J.o.P.S.P.B.P.L. Wall, *A quick, direct method for the determination of activation energy from thermogravimetric data.* 1966. **4**(5): p. 323-328.

104. Hu, Z., et al., *Characteristics and kinetic studies of Hydrilla verticillata pyrolysis via thermogravimetric analysis.* 2015. **194**: p. 364-372.

105. Coats, A.W. and J.J.N. Redfern, *Kinetic parameters from thermogravimetric data.* 1964. **201**(4914): p. 68-69.

106. Maurya, R., et al., *Non-isothermal pyrolysis of de-oiled microalgal biomass: kinetics and evolved gas analysis.* 2016. **221**: p. 251-261.

107. Ma, Z., et al., *Comparison of the thermal degradation behaviors and kinetics of palm oil waste under nitrogen and air atmosphere in TGA-FTIR with a complementary use of model-free and model-fitting approaches.* 2018. **134**: p. 12-24.

108. Vyazovkin, S., et al., *ICTAC Kinetics Committee recommendations for performing kinetic computations on thermal analysis data.* 2011. **520**(1-2): p. 1-19.

109. Soria-Verdugo, A., et al., *Comparison of wood pyrolysis kinetic data derived from thermogravimetric experiments by model-fitting and model-free methods.* 2020. **212**: p. 112818.

110. Çepelioğullar, Ö., H. Haykırı-Açma, and S.J.W.m. Yaman, *Kinetic modelling of RDF pyrolysis: Model-fitting and model-free approaches.* 2016. **48**: p. 275-284.

111. Tai, H.-S. and C.-Y.J.E.E.S. Chen, *Kinetic study of copyrolysis of waste polyethylene terephthalate, polylactic acid, and rice straw*. 2016. **33**(9): p. 671-680.

112. Aboulkas, A., A.J.E.C. El Bouadili, and Management, *Thermal degradation behaviors of polyethylene and polypropylene. Part I: Pyrolysis kinetics and mechanisms*. 2010. **51**(7): p. 1363-1369.

113. Aboulkas, A., et al., *Pyrolysis kinetics of polypropylene: Morocco oil shale and their mixture*. 2007. **89**: p. 203-209.

114. Saha, B. and A.J.C.E.J. Ghoshal, *Thermal degradation kinetics of poly (ethylene terephthalate) from waste soft drinks bottles*. 2005. **111**(1): p. 39-43.

115. Snegirev, A.Y., et al., *Formal kinetics of polystyrene pyrolysis in non-oxidizing atmosphere*. 2012. **548**: p. 17-26.

116. Encinar, J. and J.J.F.p.t. González, *Pyrolysis of synthetic polymers and plastic wastes. Kinetic study*. 2008. **89**(7): p. 678-686.

117. Mishra, R.K., A. Sahoo, and K.J.B.t. Mohanty, *Pyrolysis kinetics and synergistic effect in co-pyrolysis of Samanea saman seeds and polyethylene terephthalate using thermogravimetric analyser*. 2019. **289**: p. 121608.

118. Eimontas, J., et al., *Catalytic pyrolysis kinetic behavior and TG-FTIR-GC–MS analysis of metallized food packaging plastics with different concentrations of ZSM-5 zeolite catalyst*. 2021. **13**(5): p. 702.

119. Khan, W.U.H., et al., *In depth thermokinetic investigation on Co-pyrolysis of low-rank coal and algae consortium blends over CeO2 loaded hydrotalcite (MgNiAl) catalyst*. Journal of Environmental Chemical Engineering, 2022. **10**(5): p. 108293.

120. Gohar, H., et al., *Investigating the characterisation, kinetic mechanism, and thermodynamic behaviour of coal-biomass blends in co-pyrolysis process*. Process Safety and Environmental Protection, 2022. **163**: p. 645-658.

121. Naeem, N., et al., *Partial oxidation of methane over biomass fly ash (BFA)-supported Ni/CaO catalyst for hydrogen-rich syngas production*. Research on Chemical Intermediates, 2022. **48**(5): p. 2007-2034.

122. Mashouf Roudsari, G., A.K. Mohanty, and M. Misra, *Study of the Curing Kinetics of Epoxy Resins with Biobased Hardener and Epoxidized Soybean Oil*. ACS Sustainable Chemistry & Engineering, 2014. **2**(9): p. 2111-2116.

123. Dubdub, I. and Z. Alhulaybi, *Catalytic Pyrolysis of PET Polymer Using Nonisothermal Thermogravimetric Analysis Data: Kinetics and Artificial Neural Networks Studies*. Polymers, 2023. **15**(1): p. 70.

124. Khan, A., et al., *Investigation of combustion performance of tannery sewage sludge using thermokinetic analysis and prediction by artificial neural network.* Case Studies in Thermal Engineering, 2022. **40**: p. 102586.

125. Chowdhury, T. and Q. Wang, *Study on Thermal Degradation Processes of Polyethylene Terephthalate Microplastics Using the Kinetics and Artificial Neural Networks Models.* Processes, 2023. **11**(2): p. 496.

126. Liu, J., et al., *Pyrolysis treatment of oil sludge and model-free kinetics analysis.* Journal of hazardous materials, 2009. **161**(2-3): p. 1208-1215.

127. Khoja, A.H., et al., *Exploring copyrolysis characteristics and thermokinetics of peach stone and bituminous coal blends.* Energy Science & Engineering, 2023. **11**(11): p. 4302-4323.

128. Friedman, H.L., *Kinetics of thermal degradation of char-forming plastics from thermogravimetry. Application to a phenolic plastic.* Journal of Polymer Science Part C: Polymer Symposia, 1964. **6**(1): p. 183-195.

129. Opfermann, J. and E. Kaisersberger, *An advantageous variant of the Ozawa-Flynn-Wall analysis.* Thermochimica Acta, 1992. **203**: p. 167-175.

130. SP, S.P., G. Swaminathan, and V.V. Joshi, *Thermogravimetric analysis of hazardous waste: Pet-coke, by kinetic models and Artificial neural network modeling.* Fuel, 2021. **287**: p. 119470.

131. Diaz Silvarrey, L.S. and A.N. Phan, *Kinetic study of municipal plastic waste.* International Journal of Hydrogen Energy, 2016. **41**(37): p. 16352-16364.

132. Mishra, R.K., K. Mohanty, and X.J.F. Wang, *Pyrolysis kinetic behavior and Py-GC–MS analysis of waste dahlia flowers into renewable fuel and value-added chemicals.* 2020. **260**: p. 116338.

133. Vinceković, M., et al. *Development and Characterization of a Novel Soil Amendment Based on Biomass Fly Ash Encapsulated in Calcium Alginate Microspheres*. International Journal of Molecular Sciences, 2022. **23**, DOI: 10.3390/ijms23179984.

134. Assad Munawar, M., et al., *Biomass ash characterization, fusion analysis and its application in catalytic decomposition of methane.* Fuel, 2021. **285**: p. 119107.

135. Patel, H., *Environmental valorisation of bagasse fly ash: a review.* RSC Advances, 2020. **10**(52): p. 31611-31621.

136. Venkatachalam, S., et al., *Degradation and recyclability of poly (ethylene terephthalate)*. 2012: InTech Rijeka, Croatia.

137. Costiuc, L., et al., *Investigation on Energy Density of Plastic Waste Materials-ICSW2011 1*. 2013.

138. Strain, I., et al., *Electrospinning of recycled PET to generate tough mesomorphic fibre membranes for smoke filtration.* Journal of Materials Chemistry A, 2015. **3**(4): p. 1632-1640.

139. Gogliettino, M., et al., *Extending the shelf-life of meat and dairy products via PET-modified packaging activated with the antimicrobial peptide MTP1.* Frontiers in Microbiology, 2020. **10**: p. 2963.

140. Pereira, A.P.d.S., et al., *Processing and characterization of PET composites reinforced with geopolymer concrete waste.* Materials Research, 2017. **20**: p. 411-420.

141. Peñalver, R., et al., *Raman spectroscopic strategy for the discrimination of recycled polyethylene terephthalate in water bottles.* Journal of Raman Spectroscopy, 2023. **54**(1): p. 107-112.

142. Rebollar, E., et al., *Physicochemical modifications accompanying UV laser induced surface structures on poly (ethylene terephthalate) and their effect on adhesion of mesenchymal cells.* Physical Chemistry Chemical Physics, 2014. **16**(33): p. 17551-17559.

143. Zhu, C., et al. *Investigation of Raman spectra of polyethylene terephthalate*. in *International Symposium on Photonics and Optoelectronics 2015*. 2015. SPIE.

144. Mohamed, H.H., et al., *ZnO@ porous graphite nanocomposite from waste for superior photocatalytic activity*. Environmental Science and Pollution Research, 2019. **26**(12): p. 12288-12301.

145. Agrawal, S., et al., *Effect of Aqueous HCl with Dissolved Chlorine on Certain Corrosion-Resistant Polymers.* ACS Omega, 2018. **3**(6): p. 6692-6702.

146. Prasad, S.G., A. De, and U. De, *Structural and optical investigations of radiation damage in transparent PET polymer films.* International Journal of Spectroscopy, 2011. **2011**.

147. Stetsiv, Y.A., et al., *Characterization of polyaniline thin films prepared on polyethylene terephthalate substrate.* Polymer Bulletin, 2021. **78**(11): p. 6251-6265.

148. Yousef, S., et al., *Pyrolysis kinetic behavior and thermodynamic analysis of PET nonwoven fabric.* 2023. **16**(18): p. 6079.

149. Alongi, J., G. Camino, and G.J.C.p. Malucelli, *Heating rate effect on char yield from cotton, poly (ethylene terephthalate) and blend fabrics.* 2013. **92**(2): p. 1327-1334.

150. Saha, B., A.K.J.I. Ghoshal, and e.c. research, *Model-fitting methods for evaluation of the kinetics triplet during thermal decomposition of poly (ethylene terephthalate)(PET) soft drink bottles.* 2006. **45**(23): p. 7752-7759.

151. Ganeshan, G., et al., *Degradation kinetic study of pyrolysis and co-pyrolysis of biomass with polyethylene terephthalate (PET) using Coats–Redfern method.* 2018. **131**: p. 1803-1816.

152. Narnaware, S.L. and N.J.B.T.R. Panwar, *Kinetic study on pyrolysis of mustard stalk using thermogravimetric analysis.* 2022. **17**: p. 100942.

153. Gajera, B., et al., *Pyrolysis of cattle manure: Kinetics and thermodynamic analysis using TGA and artificial neural network.* 2023: p. 1-17.

154. Al-Rumaihi, A., et al., *Thermal degradation characteristics and kinetic study of camel manure pyrolysis.* 2021. **9**(5): p. 106071.

155. Khan, A., et al., *Comprehensive investigation of almond shells pyrolysis using advance predictive models.* Renewable Energy, 2024. **227**: p. 120568.

156. Khan, A., et al., *Thermokinetic study of tannery sludge using combustion and pyrolysis process through non-isothermal thermogravimetric analysis.* Sustainable Chemistry and Pharmacy, 2024. **41**: p. 101719.

157. Xu, L., Y. Jiang, and L. Wang, *Thermal decomposition of rape straw: Pyrolysis modeling and kinetic study via particle swarm optimization.* Energy Conversion and Management, 2017. **146**: p. 124-133.

158. Luo, L., et al., *Insight into master plots method for kinetic analysis of lignocellulosic biomass pyrolysis.* Energy, 2021. **233**: p. 121194.

159. Ghetti, P., L. Ricca, and L. Angelini, *Thermal analysis of biomass and corresponding pyrolysis products.* Fuel, 1996. **75**(5): p. 565-573.

160. Munir, S., et al., *Thermal and kinetic performance analysis of corncobs, Falsa sticks, and Chamalang coal under oxidizing and inert atmospheres.* Energy Sources, Part A: Recovery, Utilization, and Environmental Effects, 2017. **39**(8): p. 775-782.

161. Banyhani, Z.M., et al., *Synergistic transformation: Kinetic and thermodynamic evaluation of co-pyrolysis for low-rank bituminous coal and polyurethane foam waste.* Process Safety and Environmental Protection, 2024. **184**: p. 907-921.

APPENDIX A

Title: Thermo-kinetic investigation of polyethylene terephthalate (PET) plastic waste over biomass fly ash (BFA) catalyst using pyrolysis process through non-isothermal thermogravimetric analysis

Journal: Sustainable Chemistry and Pharmacy

Status: Under review